International Journal of Interactive Multimedia and Artificial Intelligence

September 2017, Vol IV, Number 5, ISSN: 1989-1660

it is more important to know
what sort of person has a disease,
than to know what a disease has.
Hippocrates

Special Issue on 3D Medicine and Artificial Intelligence

http://ijimai.unir.net

INTERNATIONAL JOURNAL OF INTERACTIVE MULTIMEDIA AND ARTIFICIAL INTELLIGENCE
ISSN: 1989-1660 –VOL. 4, NUMBER 5

Editor's Note

Although Medicine has always been considered a Health Science, today it is not possible to obviate its relationship with other disciplines as Humanities and Basic Sciences.

Doctors from everywhere and everyday work with the most sophisticated technology are trying to make their profession more accurate and precise, taking in consideration, at the same time, the human part of their daily labour.

In this volume of the Journal, we will try to explore the relation between different medical specialities, basic science and engineering. In fact, modern Medicine requires the participation of these professionals who are involved with doctors in multidisciplinary teams. In this sense, Medical Engineering, is a new degree that is offered in a vast number of Universities along the world.

This relationship between Medicine and Sciences can be found in any medical speciality so that, our aim in this volume, is to show different examples of doctors working together with other scientifics in any area of Medical sciences.

The volume consists on twelve papers. Each paper explores a particular area of this multidisciplinary approach.

The first paper [1] studies the use of Brownian motion based diffusion weighted MRI for head and neck cancer diagnosis. In this field of medical applied images, we have decided to publish three more papers. One of them explores the relationship between tumor´s edge and malignant behaviour in lung nodes [2]. For this purpose they combine CT scan images with fractal segmentation analysis. The same philosophy is found in the following two articles that focus in breast cancer. This type of tumor is the most prevalent in women around the world and early and accurate diagnosis is the key point for a successful treatment. The first article [3] analyzes the usefulness of neural networks and supported vector machines for the study of mammography and MRI (magnetic resonance) lesions. In the second one [4], the authors introduce a mathematical method to analyze radiologic-mammography contour of the lesions to distinguish between benign and malign pathologies. The aim of both articles is to achieve an accurate diagnosis minimizing the errors.

There is also a paper that tries to investigate which is the best method to treat mandibular fractures taking in consideration biomechanical aspects [5]. Neurophysiology and its relationship with neural networks is deeply studied in the following article, trying to find its role in epilepsy [6]. In this area of knowledge, neural sciences, we have chosen three papers. The first one [7], introduces a brain computer interface for microcontroller driven robot based on emotiv sensors, which will be useful for patients who are unable to control or operate their muscular movements. The second one [11], explores the relationships and links between blood markers and personal history of substance abuse with neuropsychological performance. The last article analyzes the value of web-based interventions to promote health and treat mental disorders [9].

Coming back to cancer related disciplines, the last two papers focus on skin and blood malignancies. Melanoma is one of the most malignant tumours of the body. In this paper [8] related to this aggressive tumour, the authors focus again in early detection to allow a curative treatment, throughout digital imaging processing techniques. The other paper [10] is dedicated to Hematology and it analyzes the possibility of using image segmentation in the diagnosis of leukemia, a frequent blood cancer.

Finally, we have included a technical note and reflection about virtual surgery and navigation methods in maxillofacial surgery [12].

We hope you find this volume interesting and you enjoy as much as we did putting it together.

Dr. José Luis Cebrián

References

[1] C. Utrilla Contreras, B. Marín Aguilera, M. Buitrago Sánchez, J. Graessner and PS. García Raya, «Diffusion-Weighted MRI: from Brownian motion to Head&Neck tumor characterization», International Journal of Interactive Multimedia and Artificial Intelligence, vol. 4, no. 5, pp. 6-14, Sep. 2017.

[2] A. A. Rezaie and A. Habiboghli, «Detection of Lung Nodules on Medical Images by the Use of Fractal Segmentation», International Journal of Interactive Multimedia and Artificial Intelligence, vol. 4, no. 5, pp. 15-19, Sep. 2017.

[3] E. Gohariyan, M. Esmaeilpour and M. M. Shirmohammadi, «The Combination of Mammography and MRI for Diagnosing Breast Cancer Using Fuzzy NN and SVM», International Journal of Interactive Multimedia and Artificial Intelligence, vol. 4, no. 5, pp. 20-24, Sep. 2017.

[4] Y. B. Youssef, E. H. Abdelmounim and A. Lamnii, «Contour Detection of mammogram masses using ChanVese Model and B-Spline Approximation», International Journal of Interactive Multimedia and Artificial Intelligence, vol. 4, no. 5, pp. 25-27, Sep. 2017.

[5] J. L. Cebrián Carretero, M. T. Carrascal Morillo and G. Vincent Fraile, «Masticatory System Biomechanical Photoelastic Simulation for the Comparison of the Conventional and Uni-Lock Systems in Mandibular Osteosynthesis», International Journal of Interactive Multimedia and Artificial Intelligence, vol. 4, no. 5, pp. 28-32, Sep. 2017.

[6] R. Abbasi, and M. Esmaeilpour, «Selecting Statistical Characteristics of Brain Signals to Detect Epileptic Seizures using Discrete Wavelet Transform and Perceptron Neural Network», International Journal of Interactive Multimedia and Artificial Intelligence, vol. 4, no. 5, pp. 33-38, Sep. 2017.

[7] P. Gargava and K. Asawa, «Brain Computer Interface for Micro-controller Driven Robot Based on Emotiv Sensors», International Journal of Interactive Multimedia and Artificial Intelligence, vol. 4, no. 5, pp. 39-43, Sep. 2017.

[8] A. H. Hassin Alasadi and B. M. Alsafy, «Diagnosis of Malignant Melanoma of Skin Cancer Types», International Journal of Interactive Multimedia and Artificial Intelligence, vol. 4, no. 5, pp. 44-49, Sep. 2017.

[9] T. Sánchez-Gutiérrez, S. Barbeito and A. Calvo, «A revision of preventive web-based psychotherapies in subjects at risk of mental disorders», International Journal of Interactive Multimedia and Artificial Intelligence, vol. 4, no. 5, pp. 50-54, Sep. 2017.

[10] P. Bagwari, B. Saxena, M. Balodhi and V. Bijalwan, «Comparison of Feedforward Network and Radial Basis Function to Detect Leukemia», International Journal of Interactive Multimedia and Artificial Intelligence, vol. 4, no. 5, pp. 55-57, Sep. 2017.

[11] E. Vázquez-Justo, A. García-Torres and E. Vergara-Moragues, «Influence of lymphocyte T CD4 levels on the neuropsychological performance of population affected by HIV and with a previous history of substance use», International Journal of Interactive Multimedia and Artificial Intelligence, vol. 4, no. 5, pp. 58-64, Sep. 2017.

[12] J. Guiñales, J.L. Cebrian and M. Burgueño, «Virtual Planing And Intraoperative Navigation In Craniomaxillofacial Surgery», International Journal of Interactive Multimedia and Artificial Intelligence, vol. 4, no. 5, pp. 65-67, Sep. 2017.

DOI: 10.9781/ijimai.2017.450

TABLE OF CONTENTS

OPEN ACCESS JOURNAL

ISSN: 1989-1660

Difusion-Weighted MRI: from Brownian Motion to Head&Neck Tumor Characterization

C. Utrilla Contreras[1]*, B. Marín Aguilera[1], M. Buitrago Sánchez[1], J. Graessner[2] *, PS. García Raya[1]

[1]Department of Radiology, La Paz University Hospital, Madrid (Spain)
[2]Collaboration Management MR, Siemens Healthcare GmbH, Hamburg (Deutschland)

Received 17 August 2016 | Accepted 1 November 2016 | Published 23 December 2016

Abstract

This paper describes basic physics as well as clinical applications of diffusion-weighted magnetic resonance imaging. This is a technique that provides complementary information to conventional imaging sequences and it is applied in the field of oncologic imaging. This paper focuses on its specific application in head and neck, mainly in cancer patients, for characterization of primary tumors, and also for monitoring and predicting treatment response after chemotherapy or radiation therapy. Last, although diffusion-weighted imaging is shown to add value in several areas by being part of the multi-parametric magnetic resonance imaging approach, there are some unsolved challenges, which are proposed as future work.

Keywords

Diffusion-weighted Imaging, Magnetic Resonance Imaging, Oncologic Imaging, Tumor Characterization.

DOI: 10.9781/ijimai.2017.451

I. Introduction

Diffusion-weighted (DW) magnetic resonance (MR) imaging is a non-invasive functional MR imaging technique that provides complementary information for classic anatomical imaging sequences.

DW imaging is a form of MR imaging focuses on the micromovements (random, brownian) of the water molecules inside voxels. The relationship between histology and diffusion is complex, however generally densely cellular tissues or those with cellular swelling exhibit lower diffusion coefficients, and thus diffusion is particularly useful in tumor characterization and cerebral ischemia.

The diffusion characteristics of the tissue depend on its internal architecture (cellular packing, nucleus/cytoplasm ratio, intracellular organelles, cell membranes, nature of the extracellular matrix…) and its perfusion (micromotion of molecules in its capillaries) [1].

Molecular diffusion, or brownian motion, was first formally described by Einstein in 1905. Le Bihan *et al*. applied DWI on human brain for the first time in 1986 [2]. DW imaging has been used since the 1990s in central nervous system imaging, but recently the utilization of whole body DWI is becoming a standard application in routine imaging, more specifically, in the field of oncologic imaging.

II. Basics Physics

A. What is Diffusion?

Molecular diffusion is the random movement of molecules – in our case water (H_2O) – within tissues propelled by thermal energy. The motion of water protons in the extracellular compartment, the intravascular compartment, the interaction with cell membranes and intracellular water protons contribute to total diffusion.

The aim of these DW sequences is to obtain images whose contrast is influenced by the differences in water molecule mobility. Stejskal and Tanner [3] introduced the application of symmetric pair of pulsed gradients during the preparatory phase into the basic spin echo sequence that is T2 weighted.

B. How is MR Sensitizing the Tissue for Diffusion Effects?

Within the spin echo preparation period of an EPI sequence, two strong gradient pulses are played out around the 180° pulse. The first pulse dephases the magnetization of moving and static spins and the second pulse will not be able to completely undo the changes induced by the first gradient and rephases only static spins so that the signal experiments almost no changes. In contrast, moving water spins acquire non-zero phase dispersion, resulting in signal attenuation. Free water experiences the strongest signal attenuation at higher b-values (Fig. 1 & 2).

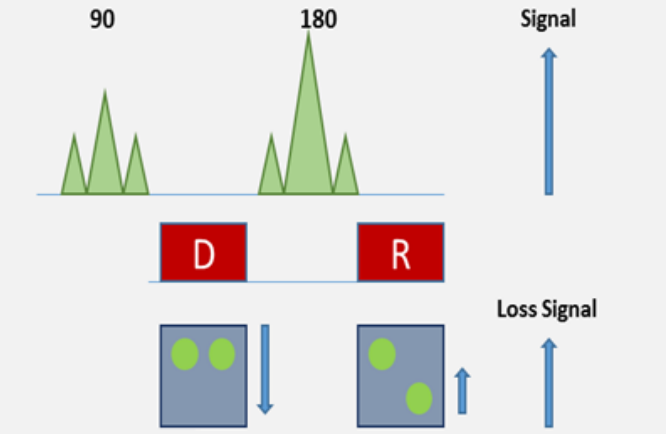

Fig. 1 a. Illustration of physical principles used for EPI diffusion-weighted imaging.

* Corresponding author.
E-mail addresses: cristinautrilla@hotmail.com (C. Utrilla Contreras), joachim.graessner@siemens.com (J. Graessner).

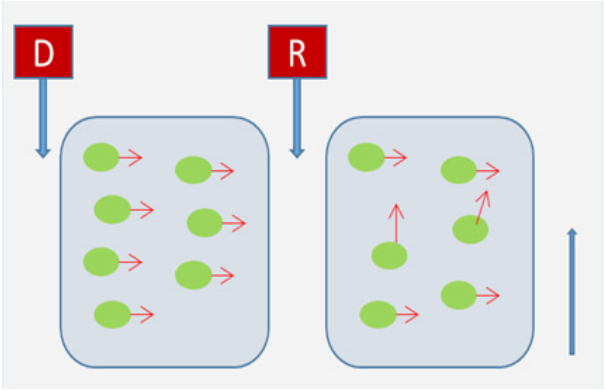

Fig. 1 b. Water molecules displace freely in all spatial directions, travelling long distances between the two gradient applications. These highly mobile molecules acquire phase information after the application of the first gradient, but due to their movement they don´t rephase completely after the application of the second gradient, losing signal.

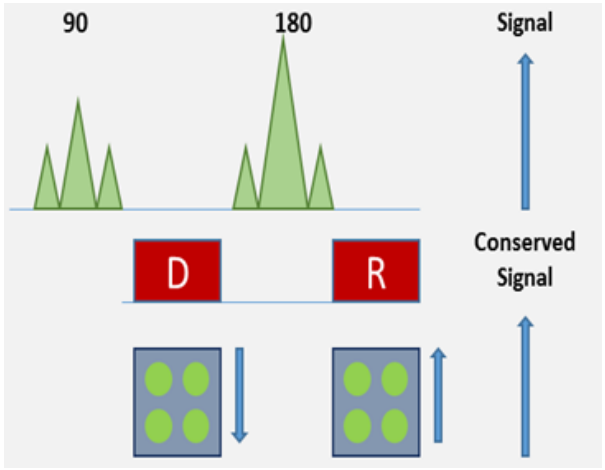

Fig 2. a. Illustration of physical principles used for EPI diffusion-weighted imaging.

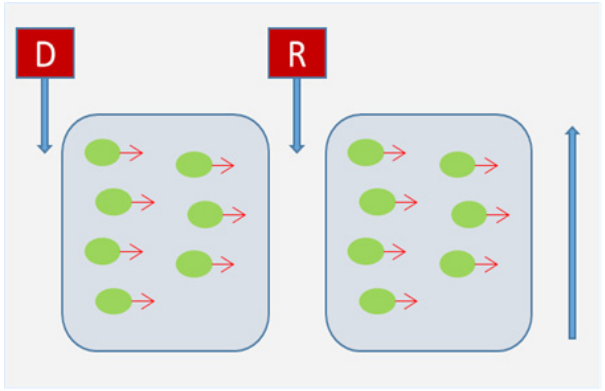

Fig. 2. b. Water molecules which are in a restricted environment don´t travel long distances so phase changes acquired during the application of the first gradient will be canceled by phase changes acquired during the second gradient, without losing signal.

C. What does the b-value Mean?

The degree of diffusion weighting of the sequence, expressed as the b-factor, depends on the characteristics of the diffusion gradients: gradient amplitude, application time and time between the two gradients.

The b-value identifies the measurements sensitivity to diffusion and determines the strength and duration of the diffusion gradients. It combines the following physical factors into b-values and is quantified by the apparent diffusion coefficient (ADC) measured in s/mm² (Fig. 3).

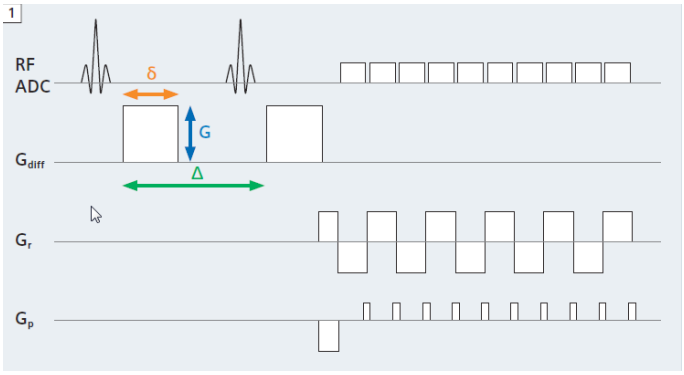

Fig. 3. Diagram of an EPI diffusion-weighted sequence illustrating the physical quantities of the b-values.

$$b = \gamma^2 G^2 \delta^2 (\Delta - \delta/3) \quad (1)$$

The signal ratio diffusion-weighted to non diffusion-weighted signal is:

$$\frac{S}{S_0} = e^{-\gamma^2 G^2 \delta^2 (\Delta - \delta/3) D} = e^{-bD} \quad (2)$$

- S_0 – signal intensity without the diffusion weighting.
- S – diffusion-weighted signal.
- γ – gyromagnetic ratio.
- G – amplitude of the two diffusion gradient pulses.
- δ – duration of the pulses.
- Δ – time between the two pulses.
- D – diffusion coefficient is a measure of the strength (velocity) of diffusion in tissue. The stronger the diffusion, the greater the diffusion coefficient, i.e. the ADC in our in vivo case.

The stronger the gradients, the longer they are applied and the more spread out in time, the greater the b-factor.

D. What is the Optimum b-value?

Images obtained with the lowest b-values (0-100 sec/mm²) provide T2-weighted EPI image with lower signal-to-noise ratio for anatomical reference. However, they included external effects due to perfusion or microvascularization.

In the range of clinically relevant b-values (up to approximately 1000), the greater the b-value, the stronger the diffusion weighting and higher the contrast in pathogenic regions is notice.

Higher b-values may depict even more lesions, at the price of poor SNR due to longer TEs and increased susceptibility. Increasing averages, which result in longer scan times, can compensate this [4]. Changing the b-value immediately influences other parameters like minimal TE, slice thickness and FOV as well as maximum matrix at a given optimal bandwidth. Furthermore anisotropy of tissues, also influences the choice (Fig. 4).

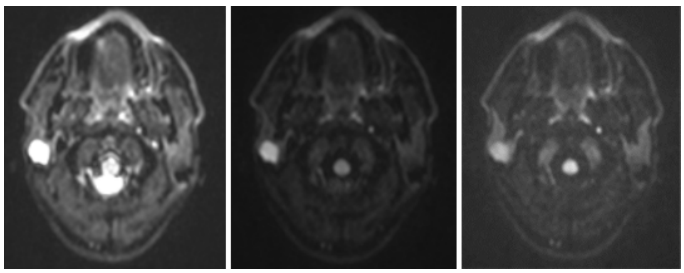

Fig. 4. Values b50 b500 b1000

A. Why do most Head and Neck DWI Protocols Start with b-value 50 s/mm²?

The selection of a low b-value larger than zero provides suppression of large vessels, which makes lesions more conspicuous. The calculation of the tissue ADC can be more accurate when starting with even higher b-values like 100 or 200, to omit the contribution of flow and micro vascular effects.

Low b-values more often serve as anatomical reference. The fact of using b-value 0 in head and neck diffusion is for a shorter period of acquisition or seek greater SNR.

Fig. 4 shows examples of three b-values: b 50, b 500, and b 1000 s/mm².

B. Why is a Minimum of three Directions Measured for each high b-value?

The sensitivity of these sequences is limited to diffusion in the direction of the gradients, so they must be repeated by applying diffusion gradients in at least 3 spatial directions, and diffusion may be different in all three dimensions.

Diffusion magnitude, calculated from the 3 diffusion images thus obtained, minimize the influence of anisotropy, renders the image weighted in global diffusion (trace image). The ADC images are therefore different depending on the sensitizing direction.

The 'trace image' displays the geometric averaging of all three directional measurements, resulting in trace-weighted images. It suppresses to some extent anisotropy information and focuses on differences in signal attenuation. Like the ADC map, the trace-weighted map shows the strength of the diffusion and not its orientation.

Two diffusion sequences with different b-factors can be used to quantitatively measure the degree of molecular mobility, by calculating the ADC, which is represented in the form of a map, whose values (in s/mm²) no longer depend on T2. An ADC hyposignal thus corresponds to a restriction in diffusion.

C. How is the ADC Calculated?

Having measured a set of at least 2 different b-value images (e.g., b 0 and b 1000 s/mm²) the system calculates pixel by pixel the ADC by linear regression.

$$\text{Signal ADC} = -\ln(S/S0)/\ b \qquad (3)$$

The ADC pixel values together form the ADC map. On a half logarithmic scale, the signal decay delivers a straight tilted line whose slope provides the ADC. The faster the signal decay the steeper the slope and the higher the ADC.

The Diffusion image (b 1000) below displays reduced diffusion as hyperintense (brighter pixels); in contrast the ADC map displays it as hypointense (darker pixels).

D. Why should I measure three or more b-values for a DWI protocol when two would be enough for calculating ADC?

While two b-values are sufficient for creating an ADC image, the selection of three b-values (b 50, b 500, b 1000) delivers a more accurate calculation of the ADC values (Fig. 5).

The lower SNR of the b 1000 images introduces a higher standard deviation of the ADC that is partially compensated by the median value of b500.

Here is an example of two ADC images, the first acquired with three b-values and the second with two b-values (Fig. 6).

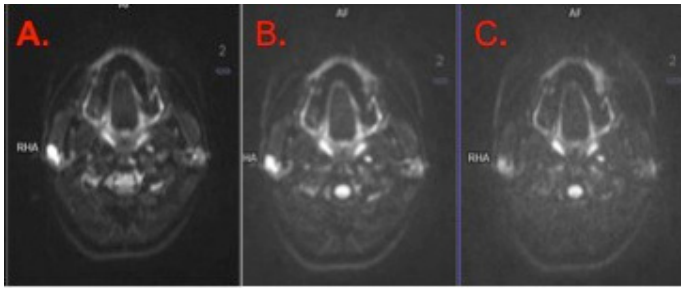

Fig. 5. Values b50 b500 b1000

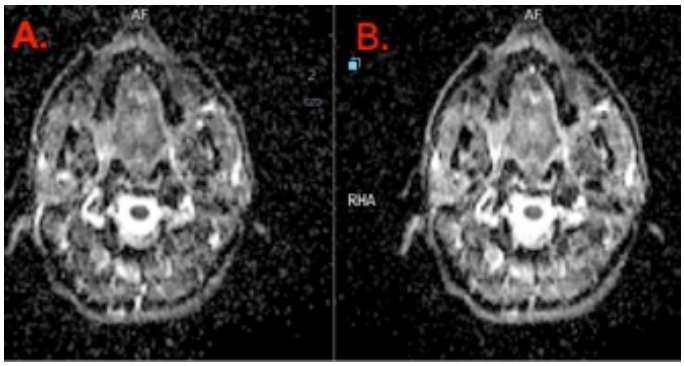

Fig. 6. ADC 3 values de b ADC 2 values b

E. Why do we Need ADC Images, and What does the 'A' in ADC Stand For?

Diffusion sequences are actually T2 weighted sequences, sensitized to diffusion by gradients.

The contrast of the diffusion image will have both diffusion and T2 component, which must be taken into consideration in the interpretation. In areas with long T2, this can simulate reduced diffusion ('T2 Shine-Through' effect). Calculating a pure diffusion coefficient can eliminate these portions of the signal.

The 'A' stands for apparent because we do not measure the pure diffusion coefficient (D or DC). In-vivo tissues, as well as the diffusion processes, have superimposed a capillary pseudo diffusion and gross motion to which the MR measurement is also very sensitive.

F. Why are some Lesions Typically Brighter than the Background Head and Neck Tissue on the Higher b-value Image and Darker on the ADC Map?

Due to the nature of certain lesions and their missing perfusion, the cells swell and hinder a normal diffusion; i.e., the mean free path is shorter. Water molecules cannot move as far in the damaged tissue as in normal tissue [5]. As a result, the ADC is lower and appears darker than the surrounding normal tissue.

G. Which Benefit does the Calculation of an Exponential Map Deliver?

Diffusion imaging cannot distinguish between water molecules motion and different microscopic movements such as those occurring in the microcirculation. Depending on the tissue composition, water molecule movements are different, that is the reason for measuring the apparent diffusion in each voxel.

The exponential map or image is calculated by dividing the maximal b-value diffusion-weighted image by the b0 image. Mathematically the exponential map displays the negative exponential of the ADC; it is a synthetic DW image without T2 'shine-through' effect [6].

The contrast behavior is similar to the high b-value image (Fig. 7).

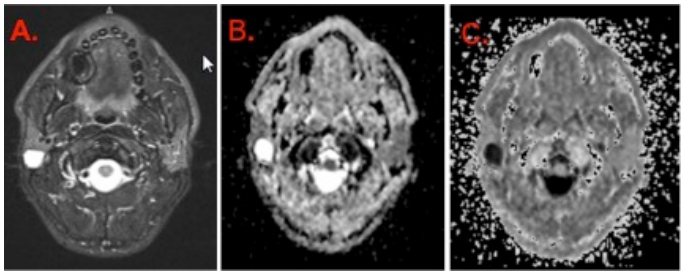

Fig. 7. A. Axial T2 with fat suppression showing a hyperintense lesion in the right parotid gland. B. Notice the high signal intensity of the lesion In the ADC map. C. and the low signal in the exponential map.

H. Why Fat Saturation is Important in Studies of Diffusion?

In most applications the diffusion gradients are integrated in echo planar imaging (EPI) sequences, which exhibit high signal intensity in areas with restricted diffusion as well as in fatty tissue.

Furthermore, the fat signal is displaced in the direction of the chemical shift as compared to the water signal. This makes fat saturation techniques necessary to identify the lesions in the diffusion-weighted images.

There are several techniques to suppress the fat signal in MRI.

For head and neck DWI protocols the fat saturation based on SPAIR technique (SPectral Attenuated Inversion Recovery) is a good compromise between acquisition time, SNR and artifacts homogeneity and STIR (Short Tau Inversion Recovery, another fat saturation technique) provides a more homogeneous fat saturation, free of artifacts.

I. Why DWI in Head and Neck Imaging is so Sensitive to Artifacts?

The most common artifacts are those related with imaging distortion due to the field inhomogeneity and to the differences in magnetic susceptibility from the anatomical tissues that compound this region; besides the presence of air-tissue interfaces, metal implants, dental amalgams or implants common in this area.

Another source of artifacts is related with movements, either voluntary or involuntary, such as breathing or coughing. The collaboration of the patient is mandatory to obtain high quality as well as the short as possible acquisition times.

J. High-resolution DWI, RESOLVE

Single-shot echo-planar imaging (EPI) is well established as the method of choice for clinical, diffusion-weighted imaging with MRI because of its low sensitivity to the motion-induced phase errors that occur during diffusion sensitization of the MR signal.

However, the method is prone to artifacts due to susceptibility changes at tissue interfaces and has a limited spatial resolution.

RESOLVE (multi-shot EPI sequence) is the combination of readout segmented EPI and parallel imaging can be used to address these issues by generating high-resolution, diffusion-weighted images with a significant reduction in susceptibility artifact compared with the single-shot case. The technique uses data from a 2D navigator acquisition to perform a nonlinear phase correction and to control the real-time reacquisition of unusable data that cannot be corrected (Fig. 8).

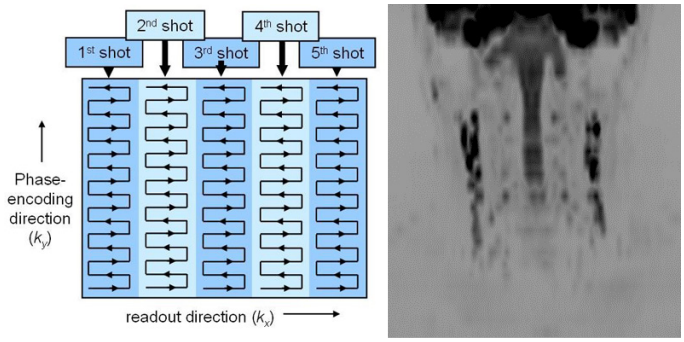

Fig. 8. RESOLVE sequence.

K. Which new DWI Features are Introduced with Software for Siemens?

There is a new 'body diffusion' application card with many new applications [7]:

- diffusion scheme monopolar/bipolar
- start ADC calculation for b > = …
- exponential ADC; no T2 shine-through
- invert gray scale ("PET-like" image) (Fig. 9).
- calculated image of artificial b-values plus (Fig. 9).
- choice of dynamic field correction
- improved fat saturation schemes

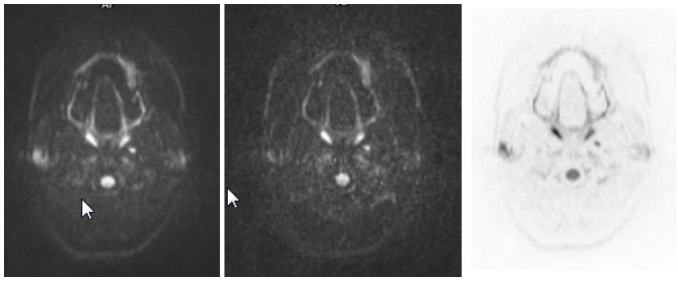

Fig. 9. B1000 Calculated image artificial b1400 Invert gray scale

L. Image Evaluation

DWI analysis is usually qualitative, evaluating the signal intensity of the images obtained with high b-values as well as the correlation with the ADC map. This analysis can also be quantitative calculating the ADC values, placing a ROI (region of interest) on the ADC map sequence and recording the mean value in that ROI. A value of 1000 intensity points is to be interpreted as 1 x 10^{-3} mm^2/s. There are more complex methods such as parametric response maps that allow segmenting a tumor by providing better information about the intratumoral heterogeneity.

I. Clinical Applications

The variation in motion and redistribution of water molecules between tissue compartments that is reflected in DW Imaging and ADC values helps to differentiate disease processes [5] and to characterize tissues, providing complementary information to conventional structural MR imaging [8].

At our institution most of the studies for imaging head and neck pathology are performed in a 1.5 Tesla MR scanner (Avanto Siemens, Erlangen, Germany), using EPI-DW sequences with 3 different b values (0, 500 and 1000 s/mm^2).

It is important not to use a different MR scanner or change the imaging protocol during a patient follow up, as ADC values may differ significantly between MRI systems and sequences. In fact, ADC measurements obtained by one person and in the same MR imaging system, protocol, and sequence are reproducible and independent of time.

In head and neck region, anatomical structures such as the lymph nodes, tonsillar tissue, spinal cord and nerve roots are associated with non-pathological restricted diffusion probably due to their high cellularity or highly packed internal structure [9]. Variable diffusion is usually observed within submandibular and parotid glands. The spinal cord and tonsillar tissue are the structures with the lowest ADC variability and therefore should serve as reference tissue for head and

neck region studies. This is especially relevant evaluating treatment response of a tumor as they can be used for comparison.

DWI in head and neck, mainly in cancer patients, is indicated for tissue characterization of primary tumors and nodal metastases, prediction and monitoring of treatment response after chemotherapy or radiation therapy, and differentiation of radiation changes and residual or recurrent disease [10].

A. Characterization of Primary Tumors

Head and neck cancers account for the sixth most common type of cancer worldwide, causing significant morbidity and mortality, being tobacco and alcohol consumption important risk factors. Differentiation of malignant head and neck tumors from benign lesions and accurate definite diagnosis is essential for treatment planning as well as for prognosis of malignant tumors.

The most relevant reports found that the mean ADC values of benign solid tumors were higher than those observed in malignant tumors, as a result of their histopathological differences.

In general, malignant tumors with hypercellularity, enlarged nuclei, and a reduced extracellular matrix, have a smaller diffusion space of water protons hence reducing ADC values [11]. A threshold ADC value of 1.22 x 10^{-3} mm^2/s provided an accuracy of 86% sensitivity, 84% specificity and 91% for predicting malignancy [12-14].

Furthermore, due to differences in the internal architecture of each lesion, variability in ADC values was reported within each group of tumor (benign or malignant) [12]. (Fig. 10 & 11).

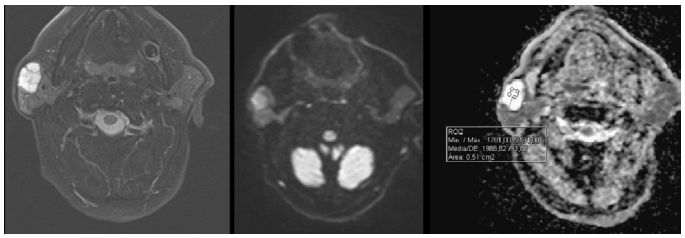

Fig. 10. Benign mixed tumour (BMT) in the superficial lobe of the right parotid gland. A. Axial T2-WI: high-signal round lesion. B. In DW b 1000 is hyperintense. C. On ADC map it does not show restrict diffusion, high signal intensity (1.98 × 10−3 mm^2/sec). The BMT (which contains myxoid tissue) has the highest ADC values of all salivary gland neoplasms, commonly in keeping with benign nature.

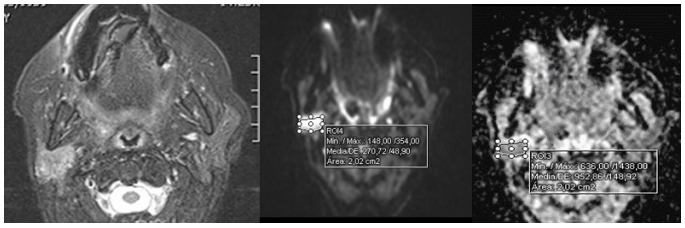

Fig. 11. Malignant tumor of the right parotid gland. A. Axial T2-WI showing a heterogeneous, mostly hyperintense, lesion. B. On DW b1000 is hyperintense. C. On ADC map has low signal intensity (0.952 × 10^{-3} mm2/sec) consistent with restricted diffusion.

In fact, among squamous cell carcinomas (SCC), those showing highly or moderately differentiated histological type present higher ADC values, than poorly differentiated SCC [13-14]. This may be explained by the presence of liquefactive necrosis in the highly differentiated type.

DWI and ADC values can help to discriminate between SCC and non-Hodgkin Lymphoma; pathologic differences between these two tumors, such as the greater cellularity in lymphomas lead to a different behavior in this sequence. Usually lymphomas present greater diffusion restriction and hence lower ADC values [15-16] . The reported mean ADC for lymphoma is fairly consistent, in the range of 0.64 to 0.66 x 10^{-3} mm^2/sec [14, 16]. Distinguishing between SCC and lymphoma is important to optimize the treatment of these patients. Usually SCCs require complex surgeries with extensive resections and reconstructions, alone or combined with radiation therapy and/or chemotherapy, and lymphomas are usually treated with radio-chemotherapy.

Salivary gland tumors are a rare condition, accounting for less than 3% of all head and neck cancers [17]. The salivary gland tumors display a wide spectrum of histologic features tumors are composed of distinctive tissues (tumor cells, myxomatous tissues, lymphoid tissues, necrosis, and cysts). Conventional MRI has limited utility in differentiation of salivary gland tumors [18, 19]; on the other hand DWI is demonstrated to be very sensitive to biophysical abnormalities within the tumor. Preoperative prediction of tumor malignancy is clinically very important, because this information strongly influences the surgical plan. The most common benign salivary gland tumors are pleomorphic adenomas and Warthin tumors. In general, pleomorphic adenomas have highest ADC values due to the cystic or myxomatous component that characterized them, while Warthin tumors have lowest ADC values in keeping with the presence of lymphoid tissue [20] (Fig. 12).

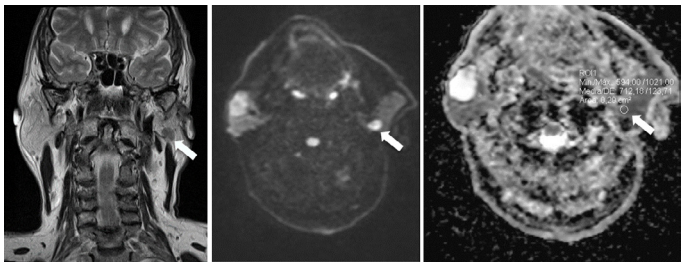

Fig. 12. Warthin tumour (lymphomatous adenoma) in the left parotid gland. A. A smoothly marginated mass, low to intermediate signal in coronal T2-WI MR. B. It is hyperintense on DWI (b 1000 sec/mm^2) (arrow). C. On ADC map it shows low signal intensity (0.71 × 10^{-3} mm^2/sec) (arrow), compatible with restricted diffusion. See the difference with the contralateral tumor in the right parotid gland, which was a benign mixed tumour (BMT).

The ADC maps for malignant salivary gland tumors (such as mucoepidermoid carcinomas) demonstrate relatively homogeneous areas of low ADC values (that represent cell proliferation), in contrast to other salivary gland tumors, for example lymphomas arising in the salivary glands, that are associated to extremely low ADC values (because of the presence of lymphoma cells) [15].

Anyway, in some cases, there is considerable overlap of ADC values, and DWI alone may not be sufficient to discriminate between benign and malignant salivary gland tumors [21, 22].

B. Evaluation of Lymph Nodes

The presence of cervical lymph node metastases is the most important prognostic factor in head and neck squamous cell carcinomas as this worsens the treatment outcome. Pretreatment staging is crucial in the management of head and neck cancer, and it has been considered one of the most important aspects in the selection of treatment options.

Differentiation between inflammatory and metastatic lymphadenopathy is often challenging with conventional imaging [23]. Also, morphologic and size criteria in MRI are not enough for the assessment of lymph node metastases.

DW imaging can help to detect cervical lymph node metastases, and to differentiate between benign and malignant enlarged lymph nodes. The general consensus appears to be that ADCs of malignant lymph nodes are significantly lower than those of normal lymph nodes [13, 23, 24]. Threshold ADC values (1.0-1.38x$10^{-3}$$mm^2$/s) have been reported to differentiate between malignant and benign lymph nodes

[13, 23, 25]. De Bondt et al reported a threshold, when ADC is lower than 1.0×10^{-3} mm²/s this was the strongest independent predictor of presence of metastasis (Fig. 13).

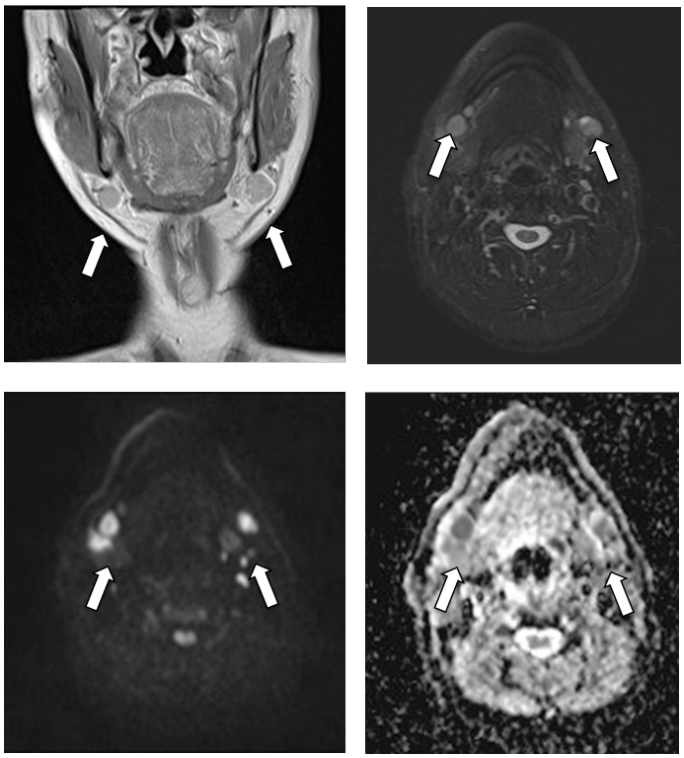

Fig. 13. Metastatic lymph nodes from nasopharyngeal carcinoma. A. Abnormal lymph nodes in bilateral submandibular regions (arrows) show intermediate signal intensity in coronal T1-WI and B. in fat saturations axial T2-WI. C. These nodes are hyperintense on DWI (b value 1000 sec/mm²) (arrows). D. On ADC map they show low signal intensity (from 0.64×10^{-3} mm²/sec to 0.86×10^{-3} mm²/sec) (arrows), compatible with restricted diffusion.

DWI can be better in differentiating between malignant and benign lymph nodes when abnormal lymph nodes show significantly different diffusion characteristics to normal lymph nodes within the same patient, as it is easy to compare. Despite the promising potential of DWI in detection of small malignant lymph nodes, low in-plane resolution of ADC maps and the presence of image artifacts can impact negatively on specificity and reproducibility of findings. For this reason, DWI should always be interpreted in conjunction with other MRI sequences to improve diagnostic accuracy [10]. Nowadays, depicting small metastatic lymph nodes (<4 mm) and lymph nodes with micrometastases that are below the resolution of currently available morphologic MR and DW images, remains challenging.

C. Monitoring and Prediction of Treatment Response after Chemotherapy or Radiation Therapy

The prognosis of patients with SCC of the head and neck remains poor despite aggressive therapeutic regimens and technological advances in surgery [26]. DWI is a noninvasive imaging biomarker to predict tumor response and one of the greatest potential benefits of DW imaging lies in the identification of the group of patients who could respond or fail to respond to therapy. Furthermore this technique could detect disease before clinical signs or symptoms are evident.

As DWI evaluates the motion of water molecules within intracellular and extracellular spaces, it reflects biological changes in tumor microenvironment, and therefore changes in ADC may imply changes in tumor composition.

There are published data that suggest the change in ADC over the course of treatment may indeed be a predictor of outcome [27-29], and could be use in monitoring treatment response. A treatment-induced increase in ADC during therapy for head and neck squamous cell carcinoma has been confirmed in several studies, and results suggest that tumors that show a lower increase or even a decrease in ADC are more likely to fail treatment [24, 28, 30, 31, 32] (Fig. 14 & 15).

Vandencaveye and colleagues reported ADC changes before pretreatment studies and 3 weeks after chemo or radiotherapy allows early assessment of treatment response. This allows early assessment of treatment response. The ADC showed a PPV of 89% and a NPV of 100% for primary lesions and a PPV of 70% and a NPV of 96% for lymph nodes33.

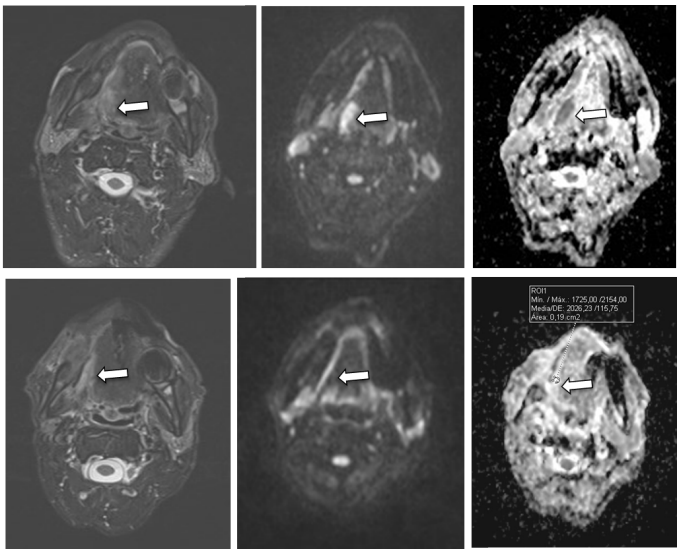

Fig. 14. Oropharyngeal carcinoma. A. A focal area of abnormal signal intensity in the base of the tongue and right tonsil (arrow) in axial T2-WI is seen. B. It is hyperintense onDWI (b value 1000 sec/mm²) (arrow). C. On ADC map it shows low signal intensity (values not shown) (arrow), compatible with restricted diffusion. In this case, the restricted-diffusion lesion most likely corresponds to malignancy.

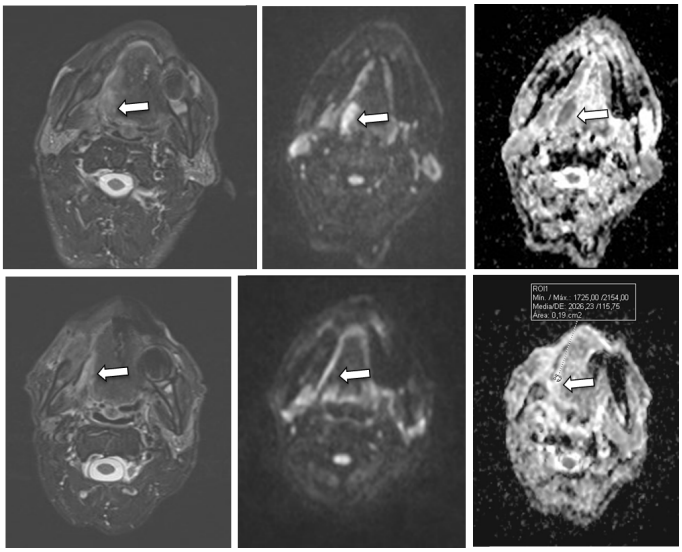

Fig. 15. Oropharyngeal carcinoma. Same patient from Fig. 14, imaging after treatment (chemotherapy and radiation therapy). A. There is a significant decrease in the size of the focal area of abnormal signal intensity in the base of the tongue and right tonsil (arrow) in axial T2-WI. B. This area is no longer hyperintense on DWI B 1000 sec/mm² (arrow). C. On ADC map it shows high signal intensity (2.02×10^{-3} mm²/sec) (arrow), i.e., there is no longer restriction of diffusion. A partial remission (partial response to the treatment) in MRI involves not only morphological improvement (T1-WI, T2-WI) but also complete or partial resolution of restricted diffusion in lesions with this feature.

These findings could lead to stop ineffective treatments and to avoid delays in starting alternative and maybe more effective therapies.

It could also be important to develop prognostic imaging markers that can accurately predict treatment response before therapy. These imaging biomarkers may help in stratifying patients into those who would benefit from chemo-radiation therapy from those who would not. DWI studies of HNSCC have suggested that ADC can be used as a potential marker for prediction of treatment response and long-term survival [28, 32, 34]. These results are consistent with the hypothesis that a high pretreatment ADC value may be indicative of micronecrosis and, consequently, of hypoxia-mediated increased resistance to treatment and poor prognosis in these patients [35].

Kim and cols reported that the mean ADC of responders increases significantly after one week and it increases until the end of treatment. Values were found to be higher in complete responders than in partial responders [30].

This technique potentially could help in the detection of responder or not responder patients.

D. Residual or Recurrent Disease

Chemotherapy or radiation therapy changes and recurrent neck tumor have similar CT and MR appearance and are difficult to differentiate. Anatomical distortion due to surgery and the presence of edema and necrosis after chemo-radiation therapy may difficult the interpretation of the findings [36].

FDG-PET/CT may help to detect recurrent SCC [37], but inflammatory changes within the first 4 months following radiotherapy is an important confounding factor, even biopsies performed after radiotherapy to identify residual/recurrent disease are often equivocal [38].

Qualitative DW imaging analysis after treatment may be helpful and is most of the times is performed by means of visual assessment of signal intensity on DW images [39].

Post-therapeutic changes induced by radio or chemotherapy can be visualized as high, or sometimes also low, signal intensity on high-b-value images but generally show high signal intensity on the corresponding ADC map, as compared with tumors [10].

Recurrent head and neck SCCs are seen as soft-tissue masses with high FDG uptake in PET-CT, moderately high T2 signal intensity, and moderate to high contrast enhancement. At DW imaging, recurrent tumor shows restricted diffusion with low ADCs (most often $<1.3 \times 10^{-3}$ mm^2/sec) [28, 33, 39], which allows differentiation from benign radiation therapy–induced changes (ADC $>1.6–1.8 \times 10^{-3}$ mm^2/sec) [13, 40].

Although ADCs often allow differentiation between tumor and inflammation, reported ADC thresholds differ from one series to another because of variable technical parameters used by various investigators [33, 39, 41]. For example, Vandecaveye et al [33] reported a high sensitivity (94.6%), specificity (95.9%) and accuracy (95.5%) for DWI to distinguish between tumoral and nontumoral tissue. The ΔADC showed a PPV of 89% and an NPV of 100% for primary lesions and a PPV of 70% and an NPV of 96% for lymph nodes. They also found that DWI yielded fewer false positives in comparison with CT or PET for both residual primary tumor and lymph node metastases.

As there may be some overlap between ADCs measured in recurrent tumors and those in radiation therapy–induced inflammatory tissue, DW imaging findings must be correlated with morphologic MR imaging findings.

II. What About the Future?

DWI has been shown to add value in several areas by being part of the multi-parametric MRI approach, even though quantitative values tend to overlap.

Investigations into the clinical applications are still at an early stage. A challenge that DWI faces is standardization of imaging protocols allowing for better comparisons across studies, getting higher spatial resolution for better tumor delineation, to depict smaller lesions, to reduce susceptibility artifacts and acquisition times.

The improvement of other (nonEPI) techniques, less sensitive to artifacts, such as halfFourier single-shot turbo spin-echo (HASTE), the split acquisition of fast spin-echo signals (SPLICE), PROLLELER, or BLADE could lead into a better approach to this difficult area. To achieve field homogeneity, both 1.5 Tesla and 3 Tesla, allowing better fat suppression could also be helpful.

There are new applications in this field: diffusion scheme monopolar/bipolar, start ADC calculation for b >, exponential ADC; no T2 shine-through, invert gray scale (“PET-like” image) calculated image of artificial b-values plus, choice of dynamic field correction, improved fat saturation scheme.

Moreover, to develop methods to analyze ADC maps more accurately will be essential as well as the standardization of the technique acquisition and post processing methods that would allow setting thresholds and integrating them in clinical settings.

Finally, it will be crucial to correlate DWI with morphology on MRI and other functional techniques, such as Perfusion MRI, Dynamic Contrast Enhanced (DCE) Imaging and PET to reach a better clinical approach.

References

[1] Ozgen B, Oguz KK, Cila A. Diffusion MR Imaging Features of Skull Base Osteomyelitis Compared with Skull Base Malignancy. Am J Neuroradiol [Internet]. 2011 Jan 1;32 (1):179–84. Available from: http://www.ajnr.org/content/32/1/179.abstract

[2] Le Bihan D, Breton E, Lallemand D, Grenier P, Cabanis E, Laval-Jeantet M. MR imaging of intravoxel incoherent motions: application to diffusion and perfusion in neurologic disorders. Radiology. UNITED STATES; 1986 Nov;161(2):401–7.

[3] Stejskal EO, Tanner JE. Spin Diffusion Measurements: Spin Echoes in the Presence of a Time Dependent Field Gradient. J Chem Phys. 1965;42(1).

[4] Kingsley PB, Monahan WG. Selection of the optimum b factor for diffusion-weighted magnetic resonance imaging assessment of ischemic stroke. Magn Reson Med. United States; 2004 May;51(5):996–1001.

[5] Padhani AR, Liu G, Koh DM, Chenevert TL, Thoeny HC, Takahara T, et al. Diffusion-weighted magnetic resonance imaging as a cancer biomarker: consensus and recommendations. Neoplasia. Canada; 2009 Feb;11(2):102–25.

[6] Provenzale JM, Engelter ST, Petrella JR, Smith JS, MacFall JR. Use of MR exponential diffusion-weighted images to eradicate T2 “shine-through” effect. Am J Roentgenol [Internet]. American Roentgen Ray Society; 1999 Feb 1;172(2):537–9. Available from: http://dx.doi.org/10.2214/ajr.172.2.9930819

[7] Hagmann P, Jonasson L, Maeder P, Thiran J-P, Wedeen VJ, Meuli R. Understanding diffusion MR imaging techniques: from scalar diffusion-weighted imaging to diffusion tensor imaging and beyond. RadioGraphics. United States; 2006 Oct;26 Suppl 1:S205–23.

[8] Schafer J, Srinivasan A, Mukherji S. Diffusion magnetic resonance imaging in the head and neck. Magn Reson Imaging Clin N Am. United States; 2011 Feb;19(1):55–67.

[9] Kolff-Gart AS, Pouwels PJW, Noij DP, Ljumanovic R, Vandecaveye V, de Keyzer F, et al. Diffusion-Weighted Imaging of the Head and Neck in Healthy Subjects: Reproducibility of ADC Values in Different MRI Systems and Repeat Sessions. Am J Neuroradiol [Internet]. 2015 Feb 1;36 (2):384–90. Available from: http://www.ajnr.org/content/36/2/384.abstract

[10] Thoeny HC, Keyzer F De, King AD. Diffusion-weighted MR Imaging in the Head and Neck 1. Radiology. 2012;263(1):19–32.

[11] Guo AC, Cummings TJ, Dash RC, Provenzale JM. Lymphomas and high-grade astrocytomas: comparison of water diffusibility and histologic characteristics. Radiology. United States; 2002 Jul;224(1):177–83.

[12] Srinivasan A, Dvorak R, Perni K, Rohrer S, Mukherji SK. Differentiation of Benign and Malignant Pathology in the Head and Neck Using 3T Apparent Diffusion Coefficient Values: Early Experience. Am J Neuroradiol [Internet]. 2008 Jan 1;29 (1):40–4. Available from: http://www.ajnr.org/content/29/1/40.abstract

[13] Abdel Razek AAK, Soliman NY, Elkhamary S, Alsharaway MK, Tawfik A. Role of diffusion-weighted MR imaging in cervical lymphadenopathy. Eur Radiol. Germany; 2006 Jul;16(7):1468–77.

[14] Wang J, Takashima S, Takayama F, Kawakami S, Saito A, Matsushita T, et al. Head and neck lesions: characterization with diffusion-weighted echo-planar MR imaging. Radiology. United States; 2001 Sep;220(3):621–30.

[15] Sumi M, Ichikawa Y, Nakamura T. Diagnostic ability of apparent diffusion coefficients for lymphomas and carcinomas in the pharynx. Eur Radiol. Germany; 2007 Oct;17(10):2631–7.

[16] Maeda M, Kato H, Sakuma H, Maier SE, Takeda K. Usefulness of the apparent diffusion coefficient in line scan diffusion-weighted imaging for distinguishing between squamous cell carcinomas and malignant lymphomas of the head and neck. AJNR Am J Neuroradiol. United States; 2005 May;26(5):1186–92.

[17] Harnsberger, H.R., Wiggins, R.H., Hudgins, P.A., Michel, M.A., Swartz, J., Davidson HC et al. Diagnostic imaging: head and neck. Salt Lake City, UT; Amirsys; 2004.

[18] Freling NJ, Molenaar WM, Vermey A, Mooyaart EL, Panders AK, Annyas AA, et al. Malignant parotid tumors: clinical use of MR imaging and histologic correlation. Radiology. UNITED STATES; 1992 Dec;185(3):691–6.

[19] Joe VQ, Westesson PL. Tumors of the parotid gland: MR imaging characteristics of various histologic types. AJR Am J Roentgenol. UNITED STATES; 1994 Aug;163(2):433–8.

[20] Eida S, Sumi M, Sakihama N, Takahashi H, Nakamura T. Apparent diffusion coefficient mapping of salivary gland tumors: prediction of the benignancy and malignancy. AJNR Am J Neuroradiol. United States; 2007 Jan;28(1):116–21.

[21] Matsushima N, Maeda M, Takamura M, Takeda K. Apparent diffusion coefficients of benign and malignant salivary gland tumors. Comparison to histopathological findings. J Neuroradiol. France; 2007 Jul;34(3):183–9.

[22] Habermann CR, Arndt C, Graessner J, Diestel L, Petersen KU, Reitmeier F, et al. Diffusion-weighted echo-planar MR imaging of primary parotid gland tumors: is a prediction of different histologic subtypes possible? AJNR Am J Neuroradiol. United States; 2009 Mar;30(3):591–6.

[23] de Bondt RBJ, Nelemans PJ, Hofman PAM, Casselman JW, Kremer B, van Engelshoven JMA, et al. Detection of lymph node metastases in head and neck cancer: a meta-analysis comparing US, USgFNAC, CT and MR imaging. Eur J Radiol. Ireland; 2007 Nov;64(2):266–72.

[24] Galbán CJ, Mukherji SK, Chenevert TL, Meyer CR, Hamstra DA, Bland PH, et al. A Feasibility Study of Parametric Response Map Analysis of Diffusion-Weighted Magnetic Resonance Imaging Scans of Head and Neck Cancer Patients for Providing Early Detection of Therapeutic Efficacy. Transl Oncol [Internet]. Neoplasia Press Inc.; 2009 Aug 18;2(3):184-90. Available from: http://www.ncbi.nlm.nih.gov/pmc/articles/PMC2730136/

[25] Vandecaveye V, De Keyzer F, Vander Poorten V, Dirix P, Verbeken E, Nuyts S, et al. Head and neck squamous cell carcinoma: value of diffusion-weighted MR imaging for nodal staging. Radiology. United States; 2009 Apr;251(1):134–46.

[26] Zorat PL, Paccagnella A, Cavaniglia G, Loreggian L, Gava A, Mione CA, et al. Randomized phase III trial of neoadjuvant chemotherapy in head and neck cancer: 10-year follow-up. J Natl Cancer Inst. United States; 2004 Nov;96(22):1714–7.

[27] Hatakenaka M, Nakamura K, Yabuuchi H, Shioyama Y, Matsuo Y, Ohnishi K, et al. Pretreatment apparent diffusion coefficient of the primary lesion correlates with local failure in head-and-neck cancer treated with chemoradiotherapy or radiotherapy. Int J Radiat Oncol Biol Phys. United States; 2011 Oct;81(2):339–45.

[28] King AD, Mo FKF, Yu K-H, Yeung DKW, Zhou H, Bhatia KS, et al. Squamous cell carcinoma of the head and neck: diffusion-weighted MR imaging for prediction and monitoring of treatment response. Eur Radiol. Germany; 2010 Sep;20(9):2213–20.

[29] Hamstra DA, Lee KC, Moffat BA, Chenevert TL, Rehemtulla A, Ross BD. Diffusion magnetic resonance imaging: an imaging treatment response biomarker to chemoradiotherapy in a mouse model of squamous cell cancer of the head and neck. Transl Oncol. United States; 2008 Dec;1(4):187–94.

[30] Kim S, Loevner L, Quon H, Sherman E, Weinstein G, Kilger A, et al. Diffusion-weighted magnetic resonance imaging for predicting and detecting early response to chemoradiation therapy of squamous cell carcinomas of the head and neck. Clin Cancer Res. United States; 2009 Feb;15(3):986–94.

[31] Berrak S, Chawla S, Kim S, Quon H, Sherman E, Loevner LA, et al. Diffusion weighted imaging in predicting progression free survival in patients with squamous cell carcinomas of the head and neck treated with induction chemotherapy. Acad Radiol. United States; 2011 Oct;18(10):1225–32.

[32] Vandecaveye V, Dirix P, De Keyzer F, de Beeck KO, Vander Poorten V, Roebben I, et al. Predictive value of diffusion-weighted magnetic resonance imaging during chemoradiotherapy for head and neck squamous cell carcinoma. Eur Radiol. Germany; 2010 Jul;20(7):1703–14.

[33] Vandecaveye V, Dirix P, De Keyzer F, Op de Beeck K, Vander Poorten V, Hauben E, et al. Diffusion-weighted magnetic resonance imaging early after chemoradiotherapy to monitor treatment response in head-and-neck squamous cell carcinoma. Int J Radiat Oncol Biol Phys. United States; 2012 Mar;82(3):1098–107.

[34] Whitcher B, Schmid VJ, Collins DJ, Orton MR, Koh D-M, Diaz de Corcuera I, et al. A Bayesian hierarchical model for DCE-MRI to evaluate treatment response in a phase II study in advanced squamous cell carcinoma of the head and neck. MAGMA. Germany; 2011 Apr;24(2):85–96.

[35] Chawla S, Kim S, Dougherty L, Wang S, Loevner LA, Quon H, et al. Pretreatment Diffusion-Weighted and Dynamic Contrast-Enhanced MRI for Prediction of Local Treatment Response in Squamous Cell Carcinomas of the Head and Neck. Am J Roentgenol [Internet]. American Roentgen Ray Society; 2013 Jan 1;200(1):35–43. Available from: http://dx.doi.org/10.2214/AJR.12.9432

[36] Tartaglino LM, Rao VM, Markiewicz DA. Imaging of radiation changes in the head and neck. Semin Roentgenol. UNITED STATES; 1994 Jan;29(1):81–91.

[37] Terhaard CH, Bongers V, van Rijk PP, Hordijk GJ. F-18-fluoro-deoxy-glucose positron-emission tomography scanning in detection of local recurrence after radiotherapy for laryngeal/ pharyngeal cancer. Head Neck. United States; 2001 Nov;23(11):933–41.

[38] Bar-Ad V, Mishra M, Ohri N, Intenzo C. Positron Emission Tomography for Neck Evaluation Following Definitive Treatment with Chemoradiotherapy for Locoregionally Advanced Head and Neck Squamous Cell Carcinoma. Rev Recent Clin Trials [Internet]. 2012 Feb;7(1):36–41. Available from: http://www.ncbi.nlm.nih.gov/pmc/articles/PMC3809074/

[39] Varoquaux A, Rager O, Dulguerov P, Burkhardt K, Ailianou A, Becker M. Diffusion-weighted and PET/MR Imaging after Radiation Therapy for Malignant Head and Neck Tumors. RadioGraphics [Internet]. Radiological Society of North America; 2015 Aug 7;35(5):1502–27. Available from: http://dx.doi.org/10.1148/rg.2015140029

[40] Tshering Vogel DW, Zbaeren P, Geretschlaeger A, Vermathen P, De Keyzer F, Thoeny HC. Diffusion-weighted MR imaging including bi-exponential fitting for the detection of recurrent or residual tumour after (chemo) radiotherapy for laryngeal and hypopharyngeal cancers. Eur Radiol. Germany; 2013 Feb;23(2):562–9.

[41] Sadick M, Schoenberg SO, Hoermann K, Sadick H. Current oncologic concepts and emerging techniques for imaging of head and neck squamous cell cancer. GMS Curr Top Otorhinolaryngol Head Neck Surg. Germany; 2012;11:Doc08.

Cristina Utrilla Contreras

Cristina Utrilla Contreras is neuroradiologist in University Hospital La Paz, in Madrid, Spain. After finishing the studies in Complutense University in Madrid in 2006, she completed the residency program in Radiology in University Hospital La Paz in 2011. She participated in the European School of Radiology Exchange Programme for Neuroradiology Fellowship during 2013 in University Hospital Freiburg. She has published several papers in international journals and presented communications in national and international meetings. Doctor Utrilla presented her PhD work entitled: “The value of volumetric computed tomography in the study of the Chronic Obstructive Pulmonary Disease” in April 2016.

Begoña Marin Aguilera

Graduate of Medicine and Surgery in 2001. Medical specialist in Radiology in 2007. Neuroradiology specialist in La Paz University Hospital (from May 2008 to present) with training and experience to perform Vascular and Interventional Neuroradiology. Author of several publications in the field of specialization and collaborator in investigation projects. Participation as speaker in courses of medical specialization. Tutor specialty (2011-2015).

Nelson Mauricio Buitrago Sánchez

Radiology and Internal Medicine specialist. Currently practicing in the neuroradiology area, La Paz University Hospital, Madrid (Spain).

Joachim Graessner

Siemens Healthcare GmbH
Collaboration Management MR
HC CEMEA GER SV ES&DS CM
Lindenplatz 2
20099 Hamburg, Deutschland

Pilar García Raya

Neuroradiologist since 1993 to present in University Hospital La Paz, Madrid, Spain. Residency in Radiology in La Paz University Hospital 1989-1992. Graduate/ Medical School in Madrid Autonoma University 1982-1988. Membership of Spanish Society of Neuroradiology and European Society of Neuroradiology. Member of La Paz University Hospital Head and Neck Cancer multidisciplinary Committee with several collaborations in specialiced meetings and courses.

Detection of Lung Nodules on Medical Images by the Use of Fractal Segmentation

Afsaneh Abdollahzadeh Rezaie, Ali Habiboghli*

Department of Computer Science and Engineering, Khoy Branch, Islamic Azad University, Khoy (Iran)

Received 2 September 2016 | Accepted 1 November 2016 | Published 23 December 2016

Abstract

In the present paper, a method for the detection of malignant and benign tumors on the CT scan images has been proposed. In the proposed method, firstly the area of interest in which the tumor may exist is selected on the original image and by the use of image segmentation and determination of the image's threshold limit, the tumor's area is specified and then edge detection filters are used for detection of the tumor's edge. After detection of area and by calculating the fractal dimensions with less percent of errors and better resolution, the areas where contain the tumor are determined. The images used in the proposed method have been extracted from cancer imaging archive database that is made available for public. Compared to other methods, our proposed method recognizes successfully benign and malignant tumors in all cases that have been clinically approved and belong to the database.

Keywords

Segmentation, Lung Cancer, CT Scan Images, Fractal Dimensions, Benign and Malignant Tumors.

DOI: 10.9781/ijimai.2017.452

I. Introduction

More than 9 million people die annually around the world as the result of the chest diseases. Lung cancer is the second leading reason of death caused by cancer in the world [1]. More than 85% of all lung cancer cases have been attributed directly to smoking [2]. The reduction in mortality of lung cancer can be achieved by doing successfully the three strategies of quitting smoking, early detection and development of treatment methods [3]. At present, it is impossible to detect signs of lung cancer in the early stages, because they are similar to other diseases. Therefore, patients with lung cancer are usually detected in advanced stages of disease in which the treatment options are limited and this leads to a very low chance to survive. If patients are diagnosed in the earliest stages, the survival rate will be nearly 70%.When patients are diagnosed at the stages of two and three, the survival rate drops dramatically to 34% and 13%.The initial symptoms of the cancer can be coughing and hemoptysis which turn into chronic and recurrent infection of the chest [4].

Today, some of the common methods of biochemistry and pathology and graphic methods, including sputum cytology, chest radiography, fluorescence bronchoscope, polymerase chain reaction (PCR), computerized tomography (CT), low-dose computed CT scan and bronchial sampling are used widely to diagnose lung cancer [4]. For early detection of lung cancer, screening programs are applied to asymptomatic high-risk groups by several technologies such as sputum sampling, circulation of tumor biomarkers, serum proteome patterns, chest CT scan, nuclear magnetic resonance (NMR), or a combination of them (e.g., Chest X-rays by low-dose computed tomography (CT)), and other methods that have been the subject of study and debate over the past few decades [5].

CT imaging techniques are advanced and more sensitive in the detection of lung cancer and have a high quality contrast. They are one of the best techniques for imaging soft tissue behind the bone structure. Modern CT machines enable fast acquisition of an accurate collection of successive images with very high resolution and support reliable detection. It been has proved that screening by CT scan has a strong potential to improve the likelihood of detecting lung cancer in its early and curable stages [6]. Computer-aided diagnosis (CAD) has been examined for the detection of nodules, because the computer can improve diagnostic accuracy [1, 7]. For quantitative evaluation of results obtained from the analysis by computer systems, the physical measure of fractal dimension (FD) is used. The ability to determine ripples causes that the analysis of FD is especially useful in applications related to the tissues. Various amounts of FD show the structure of different tissues in the image.When the structure of the tissue is more complex, the amount of its FD will usually be higher [8].

Following section of this paper has been organized as follows: section 2 involves a literature review and an overview of the diagnosis of lung cancer by different methods. Section 3 describes the proposed method including both CAD systems and fractals. The results of the tests have been represented in section 4 and finally, this paper ends with the conclusions in section 5.

II. Literature Review

For lung cancer screening, Hidetaka Arimura et al (2004) and Heidi Roberts et al (2005) used computerized scheme and computer-aided detection (CAD) to detect automatically lung nodules in low-dose computed tomography images. The first study was based on the subtraction of the image to improve the detection of lung nodules and to eliminate the majority of normal background structures [9]. Using low-dose CT scans in the program of lung cancer screening,

* Corresponding author.

E-mail addresses: afsaneh.abdollahzadeh@yahoo.com (Afsaneh Abdollahzadeh Rezaie), habiboghli@iaukhoy.ac.ir (Ali Habiboghli).

Samuel Armato et al (2004) studied the detection of lung nodules. In this method, the detection of lung nodules was done automatically in two phases: gray-level thresholding for the early detection of nodule candidates, followed by the application of a rule-based classifier and linear discriminant analysis to distinguish between candidates that correspond to the actual lung nodules and those that correspond to non-nodules [10].

Using PET scan, Wardwell Jr. et al (2005) tried to detect lung nodules. PET scans attempt to diagnose cancer based on glucose metabolism by measuring the absorption of 18FFDG and provide biochemical information about the lesions in the image [2]. To detect and classify lung cancer in the chest radiography, JunjiShiraishiet al (2006) used computer-aided diagnosis. By using a database of the chest images, this method combined the independent CAD scheme for detection and the classification of lung nodules as a new CAD scheme which can improve the accuracy of radiologists in the detection of lung cancer [11]. Using fractal-feature distance in digital chest radiography to detect subtle lung nodules, Kuniharu Imai et al (2008) assessed quantitatively the influence of anatomic noise. They conducted a fractal analysis of the square chest images using the virtual volume method. The fractal-feature distances between the considered and the reference images were calculated using the pseudo-fractal dimension and complexity, and the square images without the simulated nodule were employed as the reference images [12].

De Boo et al (2009) detected lung nodules and small tumors in chest radiographs using computer aided diagnosis (CAD).They show that CAD with its detection sensitivity detects nodules better than a first reader, in other words, it is as a second reader [13].Using a two-step approach for feature selection and classifier ensemble construction, Michael Lee et al (2010) detected pulmonary nodules with the help of the computer. In this method, ensemble classifierswere constructed using RSM or GA-based feature selection and were tested via leave-one-out validation with feature selection and classifier training executed within each iteration. They further tested a two-step approach using a GA ensemble to first assess the relevance of the features, andthen using this information to control feature selection during a subsequent RSM step. The base classification was performed using linear discriminant analysis (LDA) [14].

By ensemble-based computer-aided diagnosis, Hui Chen et al (2010) differentiated lung nodules on CT images. In 2012, they differentiated lung nodes by comparing the performance of artificial neural network and logistic regression model in CT scans. In this study, morphological characteristics (size, margins, and internal characteristics) in the CT images and the patient's age, gender and history of hemoptysis were registered for each nodule, and then main operation was performed based on differentiation [15].

Elisa Ventura et al (2010) detected nodal metastatic disease in patients with non-small cell lung cancer and compared positron emission tomography (PET), contrast-enhanced computed tomography (CT), and combined PET-CT [16].

By means of virtual dual-energy radiography, Sheng Chen, Kenji Suzuki (2013) detected lung nodules in a computerized system. They aimed to develop a CADe scheme with improved sensitivity and specificity by the use of virtual dual-energy (VDE) CXRs where ribs and clavicles are suppressed with massive-training artificial neural networks (MTANNs) [17]. Christe et al (2013) used different computer-aided detection software (CAD) at different dose levels to detect lung nodules in lung cancer screening. In this method, anthropomorphic lung phantom and artificial lung nodules were used and studied to simulate screening CT-examination at standard dose and 8 different low dose levels. Two radiologists and 3 different computer aided detection software (CAD) were paired to find the highest sensitivity [18]. Qingzhu Wang et al (2013) detected lung nodules using computer-aided detection by SVM based on 3D matrix patterns. By the proposed support vector machine based on three dimensional matrix patterns (SVM3Dmatrix) which improves the classifier of SVM, 3D volume of interest of suspected lung nodules can be used directly as the training samples [19].

III. Methodology

A. CAD System

There are two main computing systems to help radiologists; they are CADe (computer-aided detection system) and CADx (computer-aided diagnosis system). CADe systems detect lesions through medical images, while CADx systems aim to measure the characteristics of the lesion. CADe systems have the following objectives [20]:

- Improvement of accuracy in detection.
- Cooperation in early detection of cancer.
- Reduction of the time spent by radiologists in evaluating the test.

CADe systems for the diagnosis of lung nodules are usually composed of five subsystems: acquisition (acquiring medical images), pre-processing (with the aim of improving the quality of the images to increase accuracy), segmentation, nodule detection and elimination of false positive.

CAD techniques are used to increase productivity and to observe the effect of methods that help the radiologist to detect suspected cases in CT scan by a computerized system as a second reader. The next aim of using CAD is the extraction and analysis of the characteristics of benign or malignant lesions to help radiologists to reduce the number of FP malignant cancer diagnoses. In summary, it can be said that computers play three roles: detection, diagnosis and noise cancellation [21]. Fig. 1 shows the general principles of computer-aided detection systems.

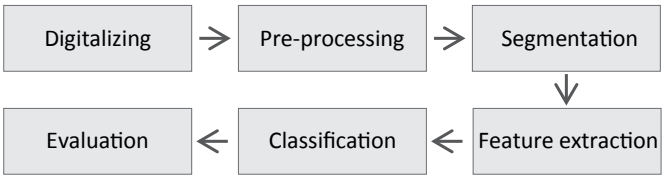

Fig. 1. General principles of computer-aided detection system (CAD).

B. Fractal

Fractal is a geometric structure consisting of components, in which the same initial structure is obtained by enlarging each component with a certain proportion. In other words, a fractal is a structure in which each component is similar to the whole [22]. There are many methods to calculate the fractal dimensions and each of these methods has its own theoretical basis. Although the algorithms used to calculate the fractal dimensions are different from each other, but they follow the same bases that are briefly described in three stages:

- Quantification of objects using different sizes of steps and stages
- Quantities measured against the size of steps and adjustment of least squares regression line through the data points
- Estimation of fractal dimension as the slope of the regression line

The methods for calculating the fractal dimensions are: box counting method (box- counting dimension), difference box-counting method (DBCM), extended configuration management (XCM), correlation dimension, generalized box-counting dimension and its relationship with the generalized correlation, fractional Brownian motion (FBM), the methods of calculating perimeter.

C. Box Counting Method (Box- Counting Dimension)

The box counting method has been used in the present paper for calculating the fractal dimension. In this method, signals are provided on limited-scale grids and the effects of grid with the fractal dimensions interact with each other. This method was used for the first time in 1985 by Kolmogorov in the field of dynamic systems. Fig. 2 shows a sample of the implementation of the box-counting method; empty boxes are not counted. The calculation method is so that a box of radius R is considered and the minimum number of boxes that are required to cover all parts of the geometric object, N (R), is counted. In the study of dynamic systems, the studied set is commonly a set of points in the state-space of the dynamic system. In this case, the empty boxes should not be included in the calculation. The amount of N (R) will be increased with the decrease of R.Box-counting dimension, D_b, is defined by a number which applies in equation 1:

$$\mathrm{N(R)}=\lim_{\mathrm{R}\to 0} KR^{-D_b} \tag{1}$$

Where K is the proportionality constant. In practice, to find the amount of the dimension by taking the algorithm on both sides of the above mentioned equation, before taking the limit, the equation 2 is obtained:

$$D_b = \lim_{R\to 0}\{\frac{-lo\,\mathrm{g}(N(R))}{lo\,\mathrm{g}(R)}+\frac{lo\,\mathrm{g}(K)}{lo\,\mathrm{g}(R)}\} \tag{2}$$

And by taking the limit on the above equation, the amount of box-counting dimension is obtained from the equation 3

$$D_b = \frac{\log(\mathrm{N(R)})}{\log(R)} \tag{3}$$

The chart of log (N (R)) in terms of log (R) is plotted and in the region where linear behavior can be seen, the slope of the line is calculated and Minkowski dimension is obtained. The topological dimension is always less than or equal to the box-counting dimension and in general the following relationship is available [23].

$$D_b \geq D_F$$

That, D_F is fractal dimension.

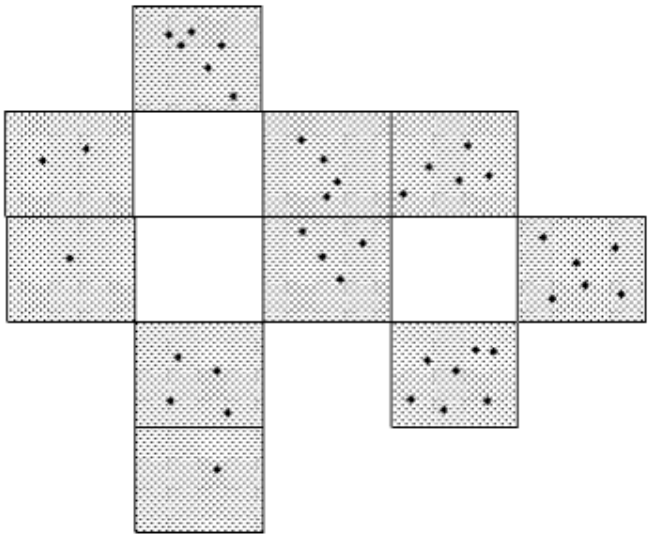

Fig.2. A sample of the implementation of the box-counting method; empty boxes are not counted.

IV. Experimental Results

In this method, our idea is the use of image analysis and fractal dimension and their combination to detect benign and malignant tumors in lung CT scan images with high contrast, better resolution and less rate of error than other methods.

The proposed method has been tested by using the images obtained from the database of the community of cancer images analysis. 43 images of lung CT scan with the sizes of 128×128 and the depth of 24 were selected, of which 29 cases were malignant and 14 cases were benign. In other words, the level of gray ranged from 0 (black) to 255 (white). The images were read by an operator of CT scan images and the existing abnormalities were identified and marked. Each image consisted of a set of information: the type and location of anomalies. We selected people who were suffering from the cancer tumor. The images were divided into two groups of benign and malignant. The separation of the images was done based on the Help file in the given web site. To better detect, only a portion of the images which involved regions with cancer tumor were examined. All images were shown with maximum improved contrast so that the full normalized range was from 0 (black) to 1 (white). Fig. 3 shows block diagram of the proposed method.

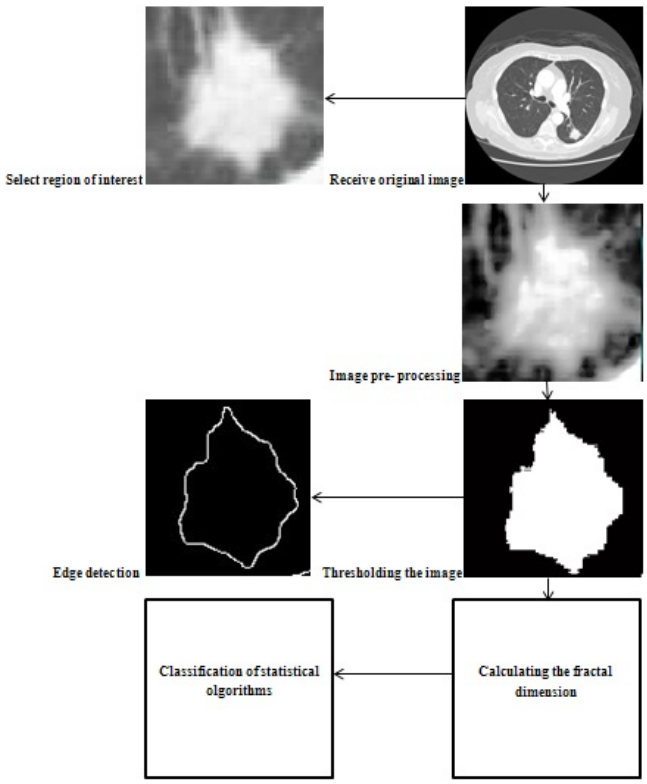

Fig.3. Block diagram of the proposed method.

In the first stage (the selection of the interested area), the regions where were suspected to have cancer tumor were cut from the input images. This process is done manually and the coordinates of the cut location were stored. To pre-process the image, the contrast of the cut images was improved by converting the values in the image intensity using the histogram equalization to increase the accuracy of the tumor diagnosis. Then, the image noise was reduced by the use of the median filtering. The median filter aims to reduce noise and maintain the edge simultaneously. Then segmentation was used to specify a particular area of the image. Segmentation of an image indicates segregation of the image into areas so that the pixels of each area share in a special feature (that can belong to an object).The easiest method for segmenting of an

image is the thresholding. Thresholding was performed by the use of FCM method which is the fuzzy c-means clustering. FCMTHRESH thresholding was done by 3-class fuzzy c-means clustering. Then edge detection was carried out in MATLAB using the edge function; this function performs the thresholding operation by the partial derivation of the adjacent pixel data and the points in which derivation is maximal are known as edge. In this method, the pixels are searched that are specific to the edge of the object and edge detection is performed in the Fig. using the filters. There are many filters for edge detection. The filter of Canny edge detector has been used in this method. Then, the fractal dimension was calculated for images by the use of box-counting dimension that is show in Fig. 4.

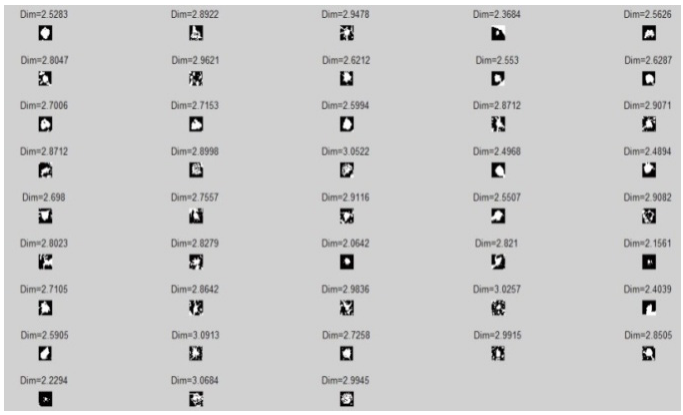

Fig.4. Calculation of fractal dimension by BoxDim.

The fractal dimension is calculated by coding in MATLAB software. Some examples of output images have been shown in Fig. 5.

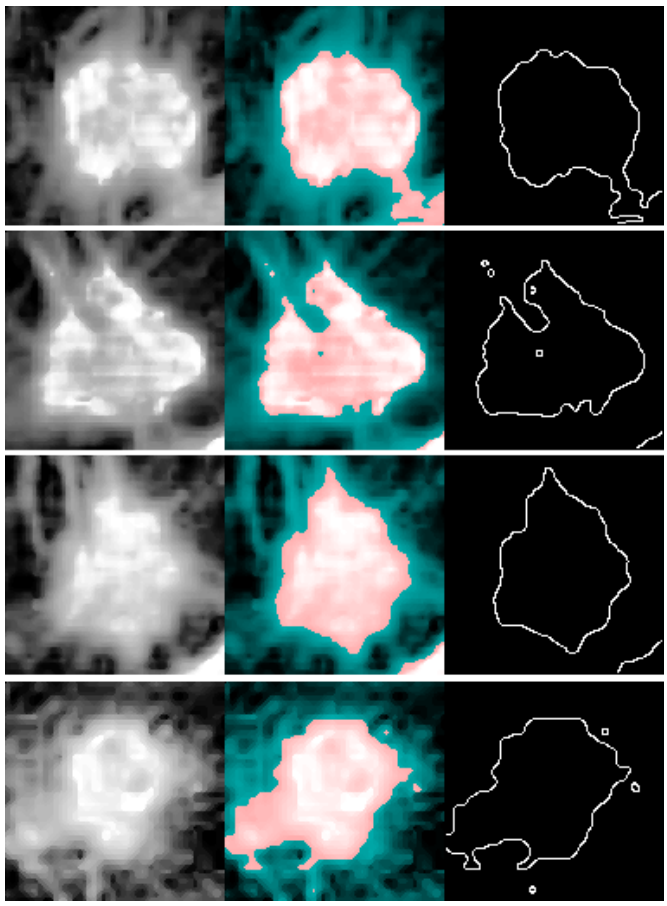

Fig.5. The final results derived from the software for detection of lung nodules based on fractal segmentation.

In this method, box- counting fractal dimension has been calculated. An example of the output data stored in the Data file after deriving MATLAB results has been shown in table 1.

TABLE I
FINAL RESULTS OF DATA

Input data No.	Tumor (benign: 1, malignant: 0)	BoxDim
18	0	2.5283
19	0	2.8921
22	0	2.9478
24	0	2.3683
30	0	2.5626
32	0	2.8047
34	0	2.9620
38	1	2.6211
47	0	2.8712
48	1	2.9070
51	0	2.8712
52	1	2.8998
54	1	3.0522

Finally, by the use of Weka software, the results obtained from the fractal dimension were compared with the results of statistical methods such as entropy, mean, standard deviation, Skewness and Kurtosis which have been obtained from coding in MATLAB and applying on input images and then finding output stored in Out Data (in MATLAB). The output of some data stored in Out Data has been shown in table 2. Evaluation has been done based on correlation coefficient (R), mean absolute error (MAE) and root mean square error (RMSE) which has been summarized in table 3.

TABLE II
RESULTS SAVED FROM MATLAB IN OUT DATA FILE

Data No.	Class	BoxDim	Kurtosis	Skewnesss	STD	Average	Entropy
18	0	2.5283	6.4956	0.1847	24.5	132.27	6.4550
19	0	2.8921	19.7273	0.6678	20.41	72.4323	6.0815
22	0	2.9478	4.4962	0.0250	24.05	99.2346	5.9721
24	0	2.3683	1.7701	0.0889	9.234	134.8543	6.7318
30	0	2.5626	3.7067	0.8463	19.70	28.8060	4.4824
32	0	2.8047	3.5349	0.3733	11.77	99.6131	5.4047
34	0	2.9620	2.0430	-0.5647	19.51	102.6989	5.6951
38	1	2.6211	2.4763	-0.4398	13.76	123.7399	6.7962
47	0	2.8712	5.3510	-0.0953	14.96	91.7998	5.6488
48	1	2.9070	3.5091	1.2990	18.76	92.8455	6.4508
51	0	2.8712	3.7755	-0.2651	15.17	93.7937	5.0410
52	1	2.8998	1.7232	0.1099	19.8	142.1170	7.0741
54	1	3.0522	6.4988	-0.2526	11.08	151.6860	7.3466

TABLE III
COMPARISON OF THE RESULTS OF STATISTICAL ALGORITHMS AND FRACTALS

Algorithm evalution	Box Dim	Kurtosis	Skewness	STD	Average	Entropy
R	0.90	0.63	0.58	0.32	0.88	0.87
MAE	0.14	3.40	0.35	3.82	5.36	0.25
RMSE	0.17	3.92	0.46	4.61	7.21	0.30

As can be seen in table 3, the results obtained from fractal dimension have better performance and provide more acceptable responses than statistical algorithms. According to this study and the obtained results, the fractal dimension algorithm can be selected as a preferred method.

V. Conclusions

Interpretation and analysis of the medical images constitute the important and major part of the detection field of a machine. Computer-aided detection systems are used for all cancers, which cannot be detected by radiologists or CT scan operators. In other words, CAD is used to increase productivity and see the impact of the methods that as the second reader by the computerized system help the operators to diagnose cases which are suspected to lung cancer. In short, it can be said computers play three roles in the analysis of lung cancer: detection, diagnosis and noise cancellation. Then there is a tendency for computer-aided detection systems aimed at helping the medical community to achieve high accuracy and efficiency.

The present study aimed to detect lung nodules on medical images via computerized calculations to help pathologists along with other pathologic methods. Several computerized methods for processing the images of lung cancer have been developed to detect the possible existence of tumors. As it can be seen in the present paper, the use of fractal dimension in the classification of cancer tumors has better results than previous methods.

References

[1] Kenji Suzuki, Hiroyuki Abe, Heber MacMahon, KunioDoi, Image-Processing Technique for Suppressing Ribs in Chest Radiographs by Means of Massive Training Artificial Neural Network)MTANN(.IEEE TRANSACTIONS ON MEDICAL IMAGING, VOL. 25, NO. 4, APRIL 2006.

[2] Noel R. Wardwell Jr, Pierre P. Massion. Novel Strategies for the Early Detection and Prevention of Lung Cancer. National Center for Biotechnology Information 32(3):259-68, (2005).

[3] Luis M. Montuenga, Ruben Pio. Current challenges in lung cancer early detection biomarkers. Eur J Cancer. 2009 Sep;45Suppl 1:377-8. doi: 10.1016/S0959-8049(09)70055-3.

[4] Jingwei Ma, Qishi Fan, Lianhui Wang, NengqinJia, ZhidongGu, Hebai Shen. Synthesis of magnetic and fluorescent bifunctional nanocomposites and their applications in detection of lung cancer cells in humans. Talanta. (2010) Jun 15;81(4-5):1162-9. doi: 10.1016/j.talanta.2010.01.042.

[5] M.D. Luque de Castro, M.A. Ferna´ndez-Peralbo. Analytical methods based on exhaled breath for early detection of lung cancer. Trends in Analytical Chemistry Volume 38, September 2012, Pages 13–20.

[6] Hui Chen, Jing Zhang, Yan Xu, Budong Chen, Kuan Zhang. Performance comparison of artificial neural network and logistic regression model for differentiating lung nodules on CT scans. Expert Systems with Applications, Volume 39, Issue 13, 1 October 2012, Pages 11503–11509.

[7] Shoji Kido, Chikazumi Kuroda, Shinichi Tamura: Quantification of Interstitial Lung Abnormalities with Chest Radiography: Comparison of Radiographic Index and Fractal Dimension. AcadRadiol (1998).

[8] Khan M. Iftekharuddin, Jing Zheng, Mohammad A. Islam, Robert J. Ogg. Fractal-based brain tumor detection in multimodal MRI. Applied Mathematics and Computation, Volume 207, Issue 1, 1 January 2009, Pages 23–41.

[9] Hidetaka Arimura, ShigehikoKatsuragawa, Kenji Suzuki, Feng Li, JunjiShiraishi, Shusuke Sone, KunioDoi. Computerized Scheme for Automated Detection of Lung Nodules in Low-Dose Computed Tomography Images for Lung Cancer Screening. AcadRadiol. 2004 Jun;11(6):617-29.

[10] Samuel G. Armato, Arunabha S. Roy, Heber MacMahon, Feng Li, KunioDoi, Shusuke Sone, Michael B. Altman. Evaluation of Automated Lung Nodule Detection on Low-dose Computed Tomography Scans From a Lung Cancer Screening Program. AcadRadiol. 2005 Mar;12(3):337-46.

[11] JunjiShiraishi, Hiroyuki Abe, PhD, Feng Li, Roger Engelmann, Heber MacMahon, KunioDoi: Computer-aided Diagnosis for the Detection and Classification of Lung Cancers on Chest Radiographs: ROC Analysis of Radiologists' Performance. AcadRadiol. 2006 Aug;13(8):995-1003.

[12] Kuniharu Imai, Mitsuru Ikeda, Yukihiro Enchi, TakanagaNiimi. Quantitative assessment of the influence of anatomic noise on the detection of subtle lung nodule in digital chest radiography using fractal-feature distance, Eur J Radiol. 2008 Nov;68(2):353-7.

[13] D.W. De Boo, M. Prokop, M. Uffmann, B. van Ginneken, C.M. Schaefer-Prokop. Computer-aided detection [CAD] of lung nodules and small tumours on chest radiographs. Eur J Radiol. 2009 Nov;72(2):218-25. doi: 10.1016/j.ejrad.2009.05.062.

[14] Michael C. Lee, Lilla Boroczky, KivilcimSungur-Stasik, Aaron D. Cann, Alain C. Borczuk,Steven M. Kawut, Charles A. Powell. Computer-aided diagnosis of pulmonary nodules using a two step approach for feature selection and classifier ensemble construction. Artificial Intelligence in Medicine Volume 50, Issue 1, September 2010, Pages 43–53.

[15] Hui Chen, Yan Xu, Yujing, Binrong. Neural Network Ensemble-Based Computer-Aided Diagnosis for Differentiation of Lung Nodules on CT Images. Academic Radiology, Volume 17, Issue 5, May 2010, Pages 595–602.

[16] Elisa Ventura, Tina Islam, Michael S. Gee, Umar Mahmood,MartaBraschi, Mukesh G. Harisinghan.: Detection of nodal metastatic disease in patients with non-small cell lung cancer: comparison of positron emission tomography (PET), contrast-enhanced computed tomography (CT), and combined PET-CT. Clinical Imaging, 2010 Jan-Feb;34(1):20-8. doi: 10.1016/j.clinimag.2009.03.012.

[17] Sheng Chen, Kenji Suzuki. Computerized Detection of Lung Nodules by Means of "Virtual Dual-Energy" Radiography. IEEE Trans Biomed Eng. 2013 Feb;60(2):369-78. doi: 10.1109/TBME.2012.2226583.

[18] A. Christe, L. Leidolt, A. Huber, P. Steiger, Z. Szucs-Farkas, J.E. Roos,J.T. Heverhagen, L. Ebner. Lung cancer screening with CT: Evaluation of radiologistsanddifferent computer assisted detection software (CAD) as first andsecond readers for lung nodule detection at different dose levels. European Journal of Radiology, Volume 82, Issue 12, December 2013, Pages e873–e878.

[19] Qingzhu Wang, Wenwei Kang, Chunming Wu, Bin Wang. Computer-aided detection of lung nodules by SVM based on 3D matrix patterns. Clin Imaging. 2013 Jan-Feb;37(1):62-9. doi: 10.1016/j.clinimag.2012.02.003.

[20] Qiang Li. Recent progress in computer-aided diagnosis oflung nodules on thin-section CT. Comput Med Imaging Graph. 2007 Jun-Jul;31(4-5):248-57.

[21] Allahverdi.F. Analysis and Control of Operating System Error of mammography machine, master›s thesis, Electrical Engineering, Tehran Azad University, Science and Research branch, 2007.

[22] H. Von Koch, «Sur unecourbe continue sans tangente, obtenue par une construction géométriqueélémentaire,» ArkivförMatematik, vol. 1, pp. 681-704, 1904.

[23] M. Schroeder. Fractals, Chaos, Power Laws. Minutes from an Infinite Paradis. W. H. FreemanAnd Company, 1991.

Afsaneh Abdollahzadehrezaie

Afsaneh Abdollahzadehrezaie received the B.S. degree from department of engineering of Islamic Azad University Khoy Branch in 2011. He received the M.Sc. degree in computer science-intelligent system from Islamic Azad University, Khoy Branch, Iran in 2015. His research focuses on medical image processing.

Ali Habiboghli

Ali Habiboghli received the B.S. degree from department of engineering of Islamic Azad University, KHOY Branch in 2004. He received the M.Sc. degrees from electronic, computer engineering and information technology from Islamic Azad University of Qazvin Branch, Iran in 2007. From 2007 to already is with the Islamic Azad University of KHOY Branch. His research focuses on artificial intelligence, algorithms, biometric and image processing.

The Combination of Mammography and MRI for Diagnosing Breast Cancer Using Fuzzy NN and SVM

Elham Gohariyan[1], Mansour Esmaeilpour[2] *, Mohammad Mehdi Shirmohammadi[2]

[1]Department of Computer Engineering, Buin-Zahra Branch, Islamic Azad University, Buin-Zahra (Iran)
[2]Department of Computer Engineering, Hamedan Branch, Islamic Azad University, Hamedan (Iran)

Received 2 September 2016 | Accepted 1 November 2016 | Published 23 December 2016

Abstract

Breast cancer is one of the common cancers among women so that early diagnosing of it can effectively help its treatment in this study, considering combination of Mammography and MRI pictures, we will try to recognize glands in existing pictures which identify all around of gland complete and precisely and separate it completely. In this method using artificial intelligence algorithm such as Affine transformation, Gabor filter, neural network, and support vector machine, image analysis will be carried out. The accuracy of proposed method is 98.14. In this work a special framework is presented which simplifies cancer diagnosis. The algorithm of proposed method is tested on z16 images. High speed and lack of human error are the most important factors in proposed intelligent system.

Keywords

Breast Cancer, Mammography and MRI Pictures, Improved Neural Network, Support Vector Machine, Affine Transformation.

DOI: 10.9781/ijimai.2017.453

I. Introduction

Reast cancer is one of the common illnesses [2]. According to calculations of the national cancer institute of America, from each 8 women one is suffering of breast cancer. Breast cancer is the most common cancer among women and includes 32 percent of all women – related cancer and 19 percent of death reason of women with cancer, in other hand. It is the second reason of death with cancer [3]. If this cancer be diagnosed in time, it can be cured easily. Cancers are the third reason of death in our country and among 101 to 105 persons die due to it every day [3]. Gynecologist's emphasis that if women with breast cancer take action early, possibility of their treatment is more and their costs will be less [1]. In accordance with survey of Breast cancer research Centre (SID). The majority of patients (about 57 percent) are in second step of illness when they are in initial step [4]. The incidence of this cancer in Iran is z6 cases per 100/000 population of women over 30 years and in western countries it is 130 cases per 100/000, however, age of Iranian women who are infected with cancer is at least a decade less than women in developed countries [1]. Statistics show that incidence of cancer is increasing percent in the world annually. Despite of increments of it death amount caused by it has been decreased which indicates the development of notification methods thereby early detection of it becomes possible.

In past articles different methods of cancer detection are used. Technique using a new hybrid approach based on cuckoo algorithm and support vector machine classifier advantages of which are increasing computation performance and accuracy of SVM parameters that for improving it we have applied combination of fuzzy neural network and SVM. In another article namely the combination, decision tree and support vector machine have been used for breast cancer detection advantages of which are high accuracy and sensitivity and disadvantage of which is that its accuracy is relevance to the size of the training set [4]. However in this work we have attempted to train input data with evolutionary algorithm and then give its output to support machine that can be categorized easily. Fig. 1 indicates complete framework of this study.

* Corresponding author.
E-mail address: esmaeilpour@iauh.ac.ir

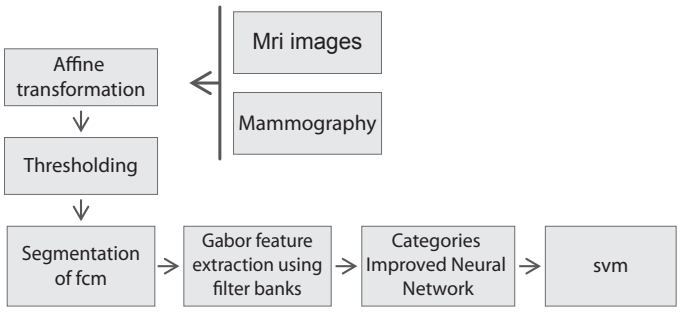

Fig. 1. The proposed method.

II. Affine Transformation and Fencing and Threshold Images

Affine transformation leaps either linearly (all points on a line will stay on a line after transformation) or the distances. In affine transformation straight lines stay straight and parallel lines will stay parallel [10].

Contractions, expansions, congruence, reflections, rotations and shear of similarity transformations, transfer and their combinations are all affine transformation keeps ratios on the line however it doesn't need to keep angles and length too. In Fig. 2 a sample of MRI and mammography pictures are shown.

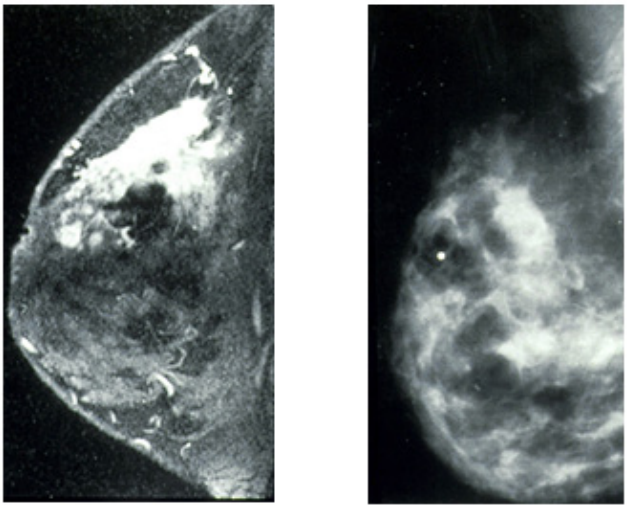

Fig. 2. Mamo right image and the left image is an MRI image.

In Fig. 3 these pictures are combined and in Fig. 4 an affine transformation has been applies to Fig. 3.

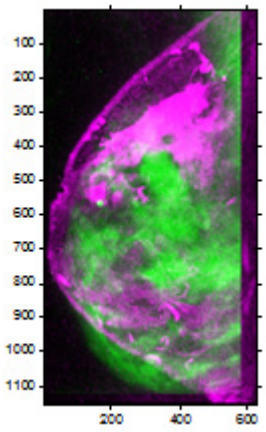

Fig. 3. Combined mammography and MRI.

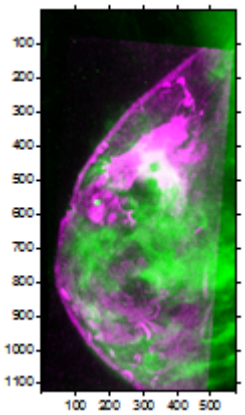

Fig. 4. Affine transformation conversions on images.

The main objective of fencing medical images is dividing it to different anatomy structures such as blood useless and tumors from background. For fencing first we use threshold for making dork points to light points in order to increase accuracy. Using threshold method in to transform images with gray scale to black and white images, these methods are accompanied with errors. In cases with threshold that pixels of background will became pixels of image will cause that object becomes thicker or thinner. For solving this problem we will use fuzzy logic. FCM classification method is based on fuzzy theory [2]. In Fig. 5 threshold method is used for improving injured points.

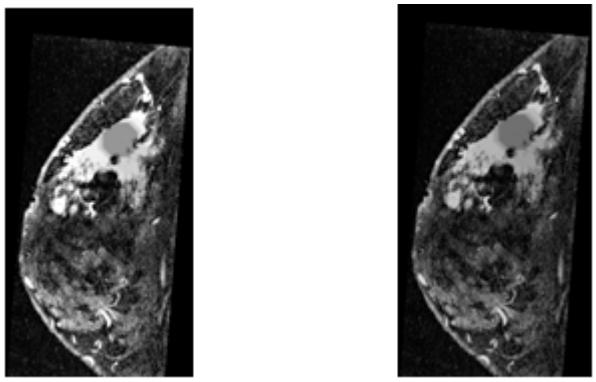

Fig. 5. Image segmentation with FCM.

In Fig. 5 is an example of image segmentation with FCM method is shown. To improve the image and isolation of cancer using noise removal methods can be performed better Isolated a sample of the image we have shown in Fig. 6.

Fig. 6. Image isolated tumor with FDM after noise.

III. Feature Extraction with Gabor Filter Banks

While working on texture of image, features such as local spatial frequency and in formations related to pixel directions will be addressed. A certain approach for determining these features is calculating the power spectrum of image however Fourier transformation of an image calculates just a total estimation of image frequency in formation. A Gabor filter can be considered as a sinusoidal part with certain directions and frequencies that have been modeled by a Gaussian cover.

Gabor filter can be formulated as below

$$\varphi(x,y)=exp\left(i\left(f_x x+f_y y\right)\right)\times exp\left(-\frac{\left(f^2\right)\left(x^2+y^2\right)}{2\sigma^2}\right) \quad (1)$$

IV. Feature Extraction with Gabor Filter Banks

The classification of improved neural network Fig. 7 indicates a total structure of RFNN model where N is input. And the classifier algorithm of support vector machine.

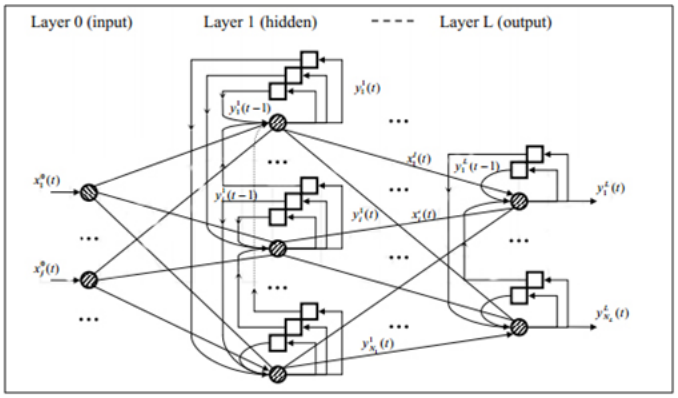

Fig. 7. Image isolated tumor with FDM after noise.

M is tern for each variable and p is output variable. Considering to Fig. 7 it is obvious that RFNN method has 6 layers. Each date function has a return relations ship with its structure. Kith rule with M inputs and N outputs in RFNN method is defined as below

$$Rule\ K:\ If\ x_1\ is\ A_1^K\ and\ x_2\ is\ A_2^K\ and\ \ldots x_N\ is\ A_N^K\ then$$
$$y_j^K = a_{j0}^K + a_{j1}^K x_1 + \ldots + a_{jN}^K x_N \quad j = 1,\ldots,M \tag{2}$$

A. RFNN Network Training Based on Descending Gradient

RFNN network training is based on descending Gradient the cost function used in RFNN method training is de fined as below in formula

$$E(k) = \frac{1}{2}\sum_j (T(k) - O^5(k))^2 \tag{3}$$

T(k) is target vector of K_{th} sample in RFNN method rules of linear combination consists of inputs in addition a constant. The derivative of w_{st} function considering to parameters of date function is so important. When normalization comes in every output of 4^{th} layer entails a function of all rules in RFNN method that this issue will complicate calculations.

B. Network Training Based on Learning by Combinatorial Optimization Algorithm

RFNN network training is based on learning by combinatorial optimization algorithms. In this part RFNN network training based on learning by combinatorial optimization algorithms will be addressed. Since cost function with parameters of first part is complex, we use 4 optimization algorithms for optimizing these parameters.

C. Discussion

Technique using a new hybrid approach based on cuckoo algorithm and support vector machine classifier advantages of which are increasing computation performance and accuracy of SVM parameters that for improving it we have applied combination of fuzzy neural network and SVM.

The main advantage of it is to avoid over training and if it occurs, model will be able to predict similar data, which are used in learning step, be applied, system will have improper operation. Each data function in first part from RFNN model has 3 parameters for training. The centers of Fuzzy data functions are shown with m and standard deviation is determined by Q. O weight provides mobility for Fuzzy data functions should be trained. Parameters of teleport are trained with training algorithm of descending gradient. Every components of each part, includes fuzzy return data function, m, q, o, in this algorithm and in every stage of combinatorial optimization algorithm parameters are completed in the first interaction and mean square error is calculated. Semi code [1] indicates steps of training of RFNN network based on learning by combinatorial optimization algorithms.

Assume that we have data point sets and we want to segregate them pair wise. Every vector is consists of real numbers that are variables of software behavior. Linear classification methods try to segregate data with super surface [5]. Support vector machine classifier method that is the best linear classification, will find this super surface [4].

```
BIGIN
    DEFINE the structure of RFNN
    CONSTRUCT template parameter vector X for holding RFNN weights and biases;
    DEFINE the cost function as function of error function of RFNN parameters;
        a. INITIALISE population with random candidate solutions
        b. COMPUTE_FITNESS of each candidate
        c. while not STOP_CRITERION do
            i. SELECT parents
            ii. RECOMBINE pairs of parents
            iii. MUTATE the resultant offspring
            iv. EVALUATE of new candidates
            v. SELECT individuals for the next generation;
    SELECT the parameter vector (RFNN parameter set) with best cost (training error)
    function from population and defining weights and thresholds for RFNN;
END
```

Fig. 8. RFN algorithm pseudo-code training.

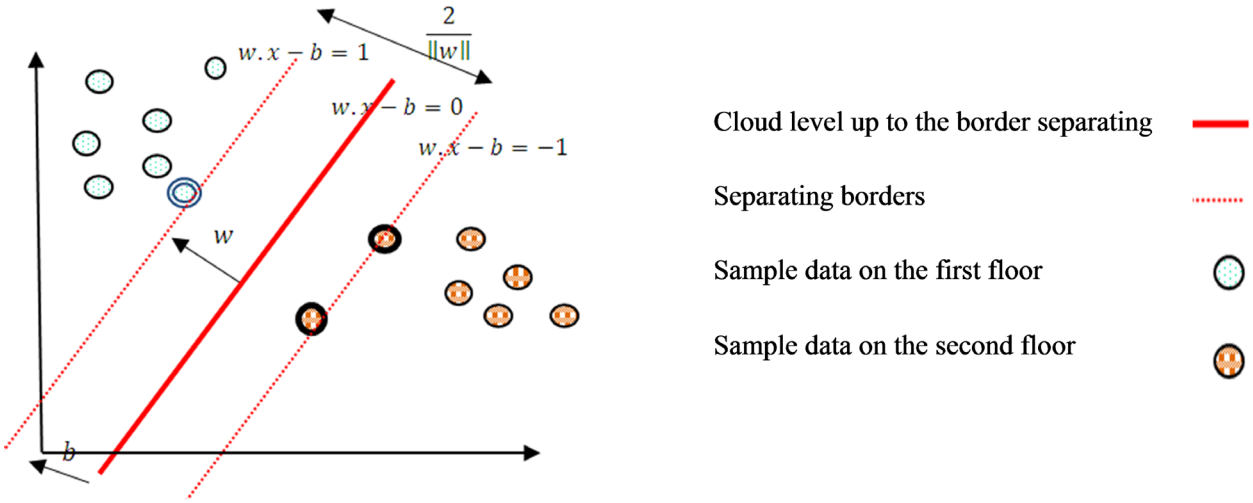

Fig. 9. How it classifies the SVM.

Goal of these classifications understand if a gland is benign or malignant. A common criterion for rating used is information gain 9 criterions defined as below.

$$IG(t_j) = \sum_{c=1}^{r} p(L_c)\ log_r \frac{1}{p(L_c)} - \sum_{m=1}^{1} p(t_j = m) \sum_{c=1}^{r} p(L_c|t_j = m) log_r \frac{1}{p(L_c|t_j=m)} \quad (4)$$

Where P(lc) is fractions of documents that has class LC. P(tj=1) and P(tj=0) means number of documents that have term tj or don't have it. IG(ti=0) is calculated for all terms and terms with vary law IG will be skipped.

V. Evaluation Criteria and Proposed Method Evaluation

Compare to digital and normal radiographies, digital radiographies are more a accurate [10]. Level of accuracy or measurement is determined by accurate. Goal of this study is to verify if this proposed method will increase accuracy in breast cancer detection or not.

$$Accuracy = \frac{(TP + TN)}{TP + TN + FP + FN}$$

$$Sensitivity = \frac{TP}{(TP + FN)}$$

$$Specificity = \frac{TN}{(TN + FP)} \quad (5)$$

In this section we compare our proposed method with other methods. In table we can conclude that results from Fuzzy C-Mean are better than network neural so this algorithm will be chosen as basic algorithm in other steps.

TABLE I.
Compare Image Segmentation Error

RMSE	Testing Error	RMSE	Learning Error	
0.30	0.14	0.17	4.12*e-5	NN
0.29	0.15	0.19	-1.08*e-7	FCM

Also for input and output variables training we will use particle swarm optimization Algorithm (PSO), Genetic Algorithm (GA), Imperialist competitive Algorithm (ICA) and simulated annealing Algorithm (SA). In accordance with results of performance, simulation and evaluation and also comparing classification errors we can conclude that PSD method is better.

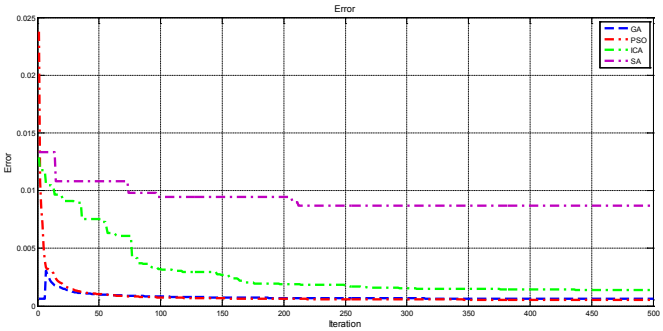

Fig. 10. Compare simulated fault.

TABLE II.
Compare Classification Error

	Train			Test		
	MSE	RMSE	R	MSE	RMSE	R
RFNN+PSO	3.316e-04	0.0251	0.9988	0.0024	0.0498	0.9647
RFNN+GA	5.414e04	0.0233	0.9989	0.0018	0.0427	0.9739
RFNN+ICA	0.0624	0.2498	0.8868	0.0289	0.1700	0.8201
RFNN+SA	0.2109	0.4593	0.2530	0.1323	0.3637	0.2321

Table II indicates that error caused by combination of RFNN and PSO is less than other methods. Since verifying it we use confusion matrix.

TABLE III.
Confusion Matrix before Evaluating SVM

Non- Cancerous	Cancerous	TrueForecast
2	23	Cancerous
29	0	Non- Cancerous

Values of accuracy, sensitivity a features are formulated as below.

$$Accuracy = \frac{23+29}{23+29+0+2} \times 100 = 96.30$$

$$Sensitivity = \frac{23}{23+2} = 0.92$$

$$Specificity = \frac{29}{29+0} = 1$$

It is obvious that step of algorithm accuracy is 97%.

TABLE IV.
Confusion Matrix after Evaluating SVM

Non-Cancerous	Cancerous	True Forecast
1	23	Cancerous
30	0	Non- Cancerous

In accordance with values in table IV we have.

$$Accuracy = \frac{23+30}{23+30+0+1} \times 100 = 98.14$$

$$Sensitivity = \frac{23}{23+1} = 0.95$$

$$Specificity = \frac{30}{30+0} = 1$$

You can see that after applying SVM final result has been improved and is 98.14.

VI. Conclusion and Future works

Breast cancer is a common cancer among women. In this study in order to early breast cancer detection we have proposed a method based on processing mammography and MRI images presented here. This method uses classification methods and different so that detection and determine the exact place of lump. This method effectively decease human errors. Proposed algorithms applied to 216 cases of images and all results verified efficiency of it. According to results and comparing them, ability of Gabor bank fitter in producing feature vector has been proved. Tests and performance evaluations are done on images such as MRI and mammography. A sample image which had cancer lumps gotten from processing images and can be seen as segregated parts. Then inputs entered into improved neural network and results calculate precisely. In order to comparing proposed method evaluation with other methods, results shown in table V.

TABLE V.
COMPARE CLASSIFICATION ERROR

Proposed (RFNN+SVM)	Proposed (RFNN)	PSOWNN (22)	DEOWNN (21)	SONN (20)	
95	92	94.167	93.333	90.984	Sensitivity%
100	100	92.105	89.474	86.111	Specificity%
98.14	96.3	93.671	92.405	89.873	Accuracy%

This study is a unique work in breast cancer detection realm. So results of which can be expanded. For this purpose suggestions are told. Multi – objective evolutionary algorithms and classification technology so that achieving better results are proposed.

REFERENCES

[1] Amin R., "Categorizing normal and cancer patterns in mammography to detect breast cancer", Eighth conference on vision machine and image processing, 2013.

[2] Daroogar M., "Detection of breast cancer using an integrative approach new feature selection algorithm based on Cuckoo algorithm and support vector machine", fifth national conference of electrical and electronic engineering of Iran, 2012.

[3] Falahnejad M., "Mammography images segmentation using Fuzzy Nero for automatic detection of breast cancer", second national conference on new ideas in electrical engineering, 2012.

[4] Kazemi A., "Combination of decision trees and support vector machine for detecting breast cancer", First national conference on intelligent systems applications in science and technology, 2013.

[5] Abbasa, Q., Celebic, M.E. and Garcíad, I.F., "Reast mass segmentation using region-based and edge-based methods in a 4-stage multiscale system",Biomedical Signal Processing and Control, 8(2): 204–214,March 2013.

[6] Al-Shamlan and El-Zaart," Feature Extraction Values for Breast Cancer Mammography Images", Bioinformatics and Biomedical Technology (ICBBT). IEEE, Chengdu, pp. 335-340, 2010.

[7] Dom´Ænguez, A.R. and Nandi, A.K., "Enhanced Multi-Level Thresholding Segmentation and Rank Based Region Selection for Detection of Masses in Mammograms", Acoustics, Speech and Signal Processing. IEEE, pp. I-449- I-452, 2007.

[8] Kimori, Y.,"Morphological image processing for quantitative shape analysis of biomedical structures",effective contrast enhancement. NCBI, 1(1): 848–853, 2013.

[9] Li, L., Qian, W., Clarke, L.P., Clark, R.A. and Thomas, J.A., "Improving mass detection by adaptive and multiscale processing in digitized mammograms", SPIE--The International Society for Optical Engineering. Proceedings of the SPIE, pp. 490-498, 1999.

[10] Paramkusham, S., Kunda.M.M.Rao and Rao, B.V.V.S.N.P.," Early stage detection of breast cancer using novel image processing techniques, Matlab and Labview implementation", Advanced Computing Technologies (ICACT). IEEE, pp. 1-5, 2013.

[11] Rizzi, M., D'Aloia, M. and Castagnolo, B., "Computer aided detection of microcalcifications in digital mammograms adopting a wavelet decomposition", Integrated Computer-Aided Engineering, 16(2): 91-103, 2009.

[12] Aboul Ella Hassaniena, Hossam M. Moftahb, "Ahmad Taher Azar, Mahmoud Shoman, MRI breast cancer diagnosis hybrid approach using adaptive ant-basedsegmentation and multilayer perceptron neuralnetworks classifier", Applied Soft Computing 14 62–71, 2014.

[13] Dheeba J, Tamil Selvi S. "A swarm optimized neural network system forclassification of microcalcification in mammograms". J Med Syst;36(5):3051–61,2012.

[14] Dheeba J, Tamil Selvi S. "An improved decision support system for detection oflesions in mammograms using differential evolution optimized wavelet neuralnetwork". J Med Syst;36(5):3223–32,2012. approach", Journal of Biomedical Informatics 49 45–52,2014.

[15] Dheeba J, N. Albert Singh, S. Tamil Selvi, "Computer-aided detection of breast cancer on mammograms: Aswarm intelligence optimized wavelet neural network.

Elham Gohariyan

Elham Gohariyan received her B.S in Computer Engineering- Software and M.S in Computer Engineering-Artificial intelligent at Department of Computer Engineering, Islamic Azad University, Buin-Zahra Branch, Iran. He is currently lecturer in Department of Computer Engineering, Islamic Azad University, Hamedan Branch, Hamedan, Iran. His research interests are Learning Systems and Medical Image Processing.

Mansour Esmaeilpour

Mansour Esmaeilpour, received the B.S. and M.S. degrees in Computer Engineering-Software Engineering in Iran, in 2002 and 2004, respectively. He also received the Ph.D. degree in Computer Engineering from The National University of Malaysia, in 2012. Currently, he is an assistant professor in Computer Engineering Department at Islamic Azad University, Hamedan Branch, Hamedan, Iran. As well as, he worked from 2013 to 2014 as Postdoctoral Researcher at National University of Malaysia. His research interests include Data mining, Process Mining, Learning Systems and Machine Learning.

Mohammad Mehdi Shirmohammadi

Mohammad Mehdi Shirmohammadi received his B.S in Computer Engineering- Software and M.S in Information Technology from Islamic Azad University, Qazvin Branch, Qazvin, Iran and he is PhD student in Computer Engineering-Software systems in Islamic Azad University, Arak Branch, Arak, Iran. He is currently lecturer at Department of Computer Engineering, Islamic Azad University, Hamedan Branch, Hamedan, Iran. His main research interest is Sensor networks and decision systems.

Contour Detection of Mammogram Masses Using ChanVese Model and B-Spline Approximation

Youssef Ben Youssef[1], El hassane Abdelmounim[1], and Abdellah Lamnii[2] *

[1]ASTI Laboratory, [2]MISI Laboratory. Hassan First University. 26000 Settat (Morocco)

Received 11 January 2016 | Accepted 1 November 2016 | Published 23 December 2016

Abstract

ChanVese model segmentation has been applied for contour detection of mass region in mammogram in our previous work. Available information of the desired object contour is used, in this paper, for B-spline approximation. The mass region boundary (contour) is thereafter approximated by a B-spline curve. This approach allows synthesizing the shape of the suspected mass appearing in the mammogram. Experimental results show the accurateness of mass region contour in mammograms using B-spline approximation.

Keywords

B-spline, ChanVese model, Mammogram, Segmentation.

DOI: 10.9781/ijimai.2017.454

I. Introduction

Breast cancer is one of the leading causes of cancer deaths among women in the world. Early detection is a key of the reduction of women mortality. Although breast cancer incidence has increased over the last decade, breast cancer mortality has declined among women of all ages. People have the highest chance of survival if cancer could be detected at the early stages and thanks to the development of both breast cancer treatment and mammography screening. Some studies have demonstrated that mammography may be particularly beneficial for women who are 80 years of age and older [1, 2]. According to the American Cancer society the death rate from breast cancer was increasing until 1990 when the advent of widespread screening began to have an effect on the population [3]. An abnormality detected on a mammogram is the early sign of cancer. It can appear as an abnormal area of density mass or calcification. The preferred screening examination for breast cancer is mammography. Digital mammography, and other imaging modalities such as magnetic resonance imaging (MRI), X-ray computed tomography (CT), and ultrasound provide an effective means for non invasively mapping the anatomy of a breast. Medical images in their raw form are represented by arrays of numbers in the computer, with the numbers indicating the values of relevant physical quantities that show contrast between different types of body tissue.

Segmentation plays a significant role not only in image processing but also in pattern recognition. Medical images with high resolution and fine details are always needed and required in many visual tasks.

Image segmentation is defined as the subdividing of an image into non overlapping component regions which are homogeneous with respect to some characteristic such as intensity, color or texture [4, 5, 6].

In digital mammography, segmentation is typically performed for detection or localization of tumors [7], micro calcification clusters [8], or other indicators of pathology [9]. In delineating suspicious masses for mammography, segmentation methods are typically employed in one of two ways. In the first way, the mammogram is initially segmented into candidate regions which are then labeled as being suspicious or normal [10]. In the second way, the image is first processed to detect for the presence of pathology and segmentation is performed as a final step to determine its precise location [11, 12].

Contour or shape extraction is a very important feature in medical image processing. Many medical image analysis applications, like the measurement of anatomical structures, require prior extraction of the organ from the surrounding tissue.

In this paper, our special interest is the contour extraction of the mammogram that contains masses or tumors. The mass can be benign or malignant. The contour points extracted with Chan Vese model are used as control points for B-spline curve for getting a better contour result. The structure of this paper is arranged as follows. Section 2, briefly introduces ChanVese model for segmentation. In Section 3, a background of B-spline curve is presented. The simulation results and discussion are shown in Section 4. This paper is concluded in Section 5.

II. Chan Vese Model Segmentation

Analysis and processing of medical images are useful in transforming raw images into a quantifiable symbolic form for ease of searching and mining, in extracting meaningful quantitative information to aid diagnosis and make decision. One fundamental problem in medical image analysis is image segmentation, which identifies the boundaries of objects.

Classical approaches to solve segmentation are divided into different models: discontinuity approach, similarity approach, and variational methods [4]. In medical images, active contour or snakes are used heavily for boundary delineation or shape detection. Snake is defined as an energy minimization whose energy depends on its shape and location within the image. Shape of the snake is controlled by the internal forces and external forces. The external force guides the snake towards the features in the image, and internal force acts as smoothing constraint for the snake. The deformable model or snake offers several options for medical image analysis, especially mammographic images, delineation of suspect region and assist radiologists in locating potentially cancerous cases [13].

When object contour is not clearly defined as mass region in mammographic image region based model is more suitable such as Chan Vese model. CV model is a based on global and statistical

* Corresponding author.

E-mail addresses: youssefbenyoussef12@gmail.com (Youssef Ben Youssef), hassan.abdelmounim@hotmail.fr (El hassane Abdelmounim), abdellah.lamnii@uhp.ac.ma (Abdellah Lamnii).

information to overcome the inhomogeneous intensity distribution, and thus, to drive the evolving curve towards the true boundaries. Initially, Chan Vese model aims to divide image into two parts inside Ω_{int} and outside Ω_{ext} of contour Γ. The goal of the segmentation algorithm will be to minimize this energy function for a given image defined [14].

$$E(\Gamma, c_1, c_2) = \lambda_1 \int_{\Omega_{int}} |I_0(x,y) - c_1|^2 \, dxdy + \lambda_2 \int_{\Omega_{ext}} |I_0(x,y) - c_2|^2 \, dxdy + \nu |\Gamma| \quad (1)$$

where $\lambda_1 \geq 0$, $\lambda_2 \geq 0$, and $\nu \geq 0$, are fixed weight parameters, Γ is the evolving contour, $|\Gamma|$ is its length, and c_1 and c_2 are two constants that approximate the image intensity in inside Γ and outside Γ. This model is not based on the gradient of the image $I_0(x,y)$ for the stopping process. In our previous work, we have used CV model for mass delineation contour and extracted some shape descriptors [15]. In this work, we are interested to segment a single part (mass) from the whole image or background tissue.

III. B-Spline Curve Representation and Approximation

A. Motivation

B-splines descend from a larger family of functions named piecewise polynomial interpolation functions. In reference [16], authors study the use of continuous B-spline representation for signal processing applications such as interpolation, differentiation, filtering, noise reduction, and data compression. Among other polynomial interpolators, B-splines have the capacity to give an approximated representation of the signal [17]. Splines are useful in computer vision because they allow accurate, manipulable internal models of complex shapes [18].

The B-spline has the following important properties: i) it is a piecewise polynomial curve with a given degree. This property makes with lower degree polynomials to design a complex curve using multiple segments joined with certain continuity constraints, ii) The B-spline curve is contained in the convex hull of its control polyline defined by the B-spline control points and it can be used to represent the shape of the curve, iii) Changing of the position of the control points only locally affects the curve, this property allows to B-spline curve the flexible controllability, 4i) No straight line intersects the B-spline curve more times than it intersects the curve's control polyline, 5i) affine transformation such as rotation, translation, and scaling can be applied to the B-spline control points quite easily instead of to the curve itself. This results in the affine invariance property [19-20].

In this work, we are interested to B-spline curves which play a central role and are widely used in computer aided design. All those properties hold for the B-spline curves and play an integral part in image shape modeling for our work.

B. Basic Theory

In this section, we briefly give an explicit representation of B-spline curve. The B-spline curve C(u) of order k, ($1 < k \leq n+1$), is defined by

$$C(u) = \sum_{i=0}^{n} P_i B_i^k(u) \qquad u \in [u_{k-1}, u_{n+1}] \quad (2)$$

where :

- P_i, i=0,…, n are called control points or de Boor points.
- k is the order of the polynomial segments of the B-spline curve. Order k means that the curve is made up of piecewise polynomial segments of degree k – 1.
- The $B_i^k(u)$ are the "normalized B-spline basis functions". They are described by the order k and by a non-decreasing sequence of real numbers $u_0, u_i, \ldots, u_{n+k}$ called the "knot sequence". The $B_i^k(u)$ is defined recursively as follows:

$$B_i^0(u) = \begin{cases} = 1 \, if & u_i \leq u \leq u_{i+1} \\ = 0 & otherwis \end{cases} \quad (3)$$

$$B_i^k(u) = \frac{u - u_i}{u_{i+k} - u_i} B_i^{k-1}(u) + \frac{u_{i+k+1} - u}{u_{i+p+1} - u_{i+1}} B_{i+1}^{k-1}(u) \quad (4)$$

The curve C(u) possess the following properties analogous to those of the Bézier curves:

- Endpoint interpolation property
- Convex hull property: the basis functions have the properties of non-negativity and partition of unity, as a consequence, the entire B-splines curve segment must lie inside the control polygon spanned by $P_0, \ldots, P_n$.
- Variation diminishing property : no straight line intersects a B-splines curve more times than it intersects its control polygon.
- Convexity-preserving property: the variation diminishing property means the convexity preserving property holds.

IV. Results and Discussion

A. Methodology

In order to evaluate our method, we have used image mammogram extracted from MIAS database [22]. The Mammographic Image Analysis Society (MIAS) MIAS is an organization of research groups on mammograms of the United Kingdom (UK). The mammogram, in original MIAS database, is digitized at 50 micron pixel edge and has been reduced to 200 micron pixel edge padded so that every image is 1024 x1024 pixels. All images are held as 8-bit gray level scale images with 256 different gray levels (0-255) and physically in portable gray map (pgm) format. For each abnormal case (benign and malign), MIAS database gives the coordinates of abnormality center and the approximate radius of a circle enclosing this abnormality; it contains 322 images, where 207 images represent normal, while 64 and 51 images referred as benign and malignant cases respectively. The MIAS database is limited on single view mediolateral oblique.

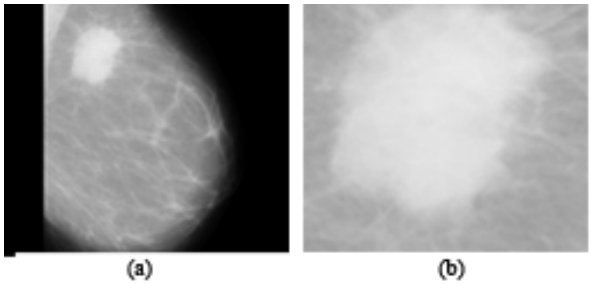

Fig. 1. (a) Original image, (b) image cropped and resized.

Original image from mammogram data is depicted in Fig.1(a), and image obtained after cropping and resizing preprocessing is shown in Fig.1(b) which contains a mass called region of interest (ROI). This technique is needed for reducing cost computing and removing the unnecessary data.

B. Contour Extraction using CV Model and B-Spline Curve Approximation

After cropping and resizing mammographic image where mass is isolated, we use ChanVese model for segmentation. Mass contour points are used as control points. Then B-splines curve is used for contour fitting. The results obtained are shown in Fig. 2.

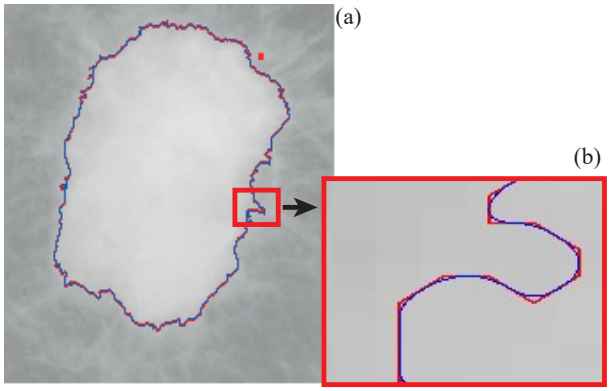

Fig 2. (a) Mass region segmented. (b) Zoom-in view of the region inside the square.

Fig. 2(a) presents a mammogram (mdb184) where a circumscribed mass is segmented with CV model (red curve). While the B-spline curve used to fit the contour is represented in blue. Fig. 2(b) shows the B-spline approximation of a given 10 control points.

It can be seen from Fig.2(b) the difference betwen contour obtained with ChanVese model and B- spline curve approximation. As shown in the zooming part of the contour, it is noted that the contour provided by B-spline is a complementary processing of the contour detection provided by CV model which give a realistic contour rather than a curve line represented by a series of juxtaposed segments presented as In the approximation, the B-spline curve does not have to pass through all data points except the first and the last data points.

V. Conclusion

In this work, we have used the ChanVese model for mammogram segmentation, in which the local image information is incorporated. CV model is an efficient and accurate method to isolate and extract masses in mammograms, and is better adapted to perform segmentation of regions with weak boundaries and noise. The data points used in this work are obtained from contours of the segmented regions after performing mammogram segmentation. These contour points extracted are used as control points for B-spline curve to give a realistic contour of the ROI.

References

[1] MA. Schonberg , RA. Ramanan , EP..McCarthy, ER.Marcantonio "Decision making and counseling around mammography screening for women aged 80 or older". *J Gen Intern Med*. 21 (9), pp. 979-85, September 2006.

[2] B.D.Badgwell, S.H.Giordano, Z.Z.Duan, S.Fang,I.Bedrosian, H.M.Kuerer, "Mammography Before Diagnosis Among Women Age 80 Years and Older With Breast Cancer" *J Clin Oncol*. April 2008.

[3] American Cancer Society. Breast Cancer Facts & Figures 2013-2014. American Cancer Society. Available at http://www.cancer.org/acs/groups/content/@research/documents/document/acspc-042725.pdf. Accessed: May 6, 2015.

[4] R.C. Gonzalez and R.E. Woods, Digital Image Processing. Addison-Wesley, 1992.

[5] R.M. Haralick and L.G. Shapiro. "Image segmentation techniques. Comput". Vis. Graph. Im. Proc.,29, pp. 100–132, 1985.

[6] R.J. Schalkoff. Pattern recognition: statistical, structural and neural approaches. John Wiley and Sons, 1992.

[7] S. Pohlman, K.A. Powell, N.A. Obuchowski, W.A. Chilcote, and S. Grund fest-Broniatowski. "Quantitative classification of breast tumores in digitzed mammograms" Med. Phys., 2, pp.1337–1345, 1996.

[8] H. Cheng, Y.M. Lui, and R.I. Freimanis, "A novel approach to microcalcification detection using fuzzy logic technique", IEEE Tran. Med. Imag., 17, pp.442–450, 1998.

[9] M. Kallergi, K. Woods, L.P. Clarke, W. Qian, and R.A. Clark,"Image segmentation in digital mammography: comparison of local thresholding and region growing algorithms", Comput. Med. Im. Graph., 16, pp.323–331, 1992.

[10] H.D. Li,M. Kallergi, L.P. Clarke, V.K. Jain, and R.A. Clark, "Markov random field for tumor detection in digital mammography". IEEE Trans. Med. Imag., 14, pp.565–576, 1995.

[11] R. Gupta and P.E. Undrill,"The use of texture analysis to delineate suspicious masses in mammography", Phys. Med. Biol., 40, pp.835–855, 1995.

[12] C.H. Chen and G.G. Lee,"On digital mammogram segmentation and microcalcification detection using multiresolution wavelet analysis" Graph. Mod. Im. Proc., 59, pp. 349–364, 1997.

[13] Y.BenYoussef, E.H.Abdelmounim, J. Zbitou. and A, Belaguid, "Segmentation of mass region in abnormal mammogram using deformable Model" .International Journal of Emerging Technology and Advanced Engineering.vol 4 (7), pp.578-582, 2014.

[14] T.F.Chan, and L.A. Vese, "Active contours without edges".IEEE transaction on image processing, (10), pp. 266-277. 2001.

[15] Y. BenYoussef, E. Abelmounim, J. Zbitou and A.Belaguid," Global and Local Descriptors Comparison for Classification into Malignant and Benign Mammograms using Support Vector Machine", Mediteranean Conference on Information & Communication Technologies'2015 May 7-9, 2015 Saïdia Morocco.

[16] M, Unser,A. Aldroubi,and M.Edden,"B-Spline signal processing:Part I-Theory", IEEE Trans. Sign. Proces., Vo41,2,February, 1993.

[17] C. Ciulla," Improved Signal and Image Interpolation in Biomedical Applications: The Case of Magnetic Resonance Imaging (MRI)", Medical Information science reference, Hershy New York, 2009.

[18] A.Blake and M.Isard, "Active Contours". Springer Verlag. 1998.

[19] F.Mokhtarian, and A.K.Mackworth, "A theory of multiscale, curvature-based shape representation for planar curves", Pattern Analysis and Machine Intelligence, IEEE Transactions on, Vol. 14, Issue 8, pp. 789-805, Aug. 1992.

[20] D.H. Ballard, C.M, Brown, "Computer Vision",Prentice Hall,1982.

[21] P. Saint-Marc, H. Rom, and G. Medioni, "B-spline contour representation and symmetry detection," in Pattern Analysis and Machine Intelligence, IEEE Transactions on , vol.15, no.11, pp.1191-1197, Nov 1993.

[22] J.Suckling, J,D.Parker, S.Dance, I,Astley, I.Hutt, and C. Boggis."The mammographic image Analysis society digital mammogram database", exerpta medica. International congress seriesvol(1069),375-378,1994.

Youssef Benyoussef

Youssef Benyoussef is currently pursuing his PhD Degree in System Analysis and Information Technology Laboratory "ATSI" in science and technology faculty Hassan 1st, University Settat Morocco. He holds a Bachelor in electronic at Mohammed 1st university Oujda in 1993, and Master of Science and Technology in electrical engineering at Hassan 1st university in 2011. His research interests are on computer vision, image processing, machine learning, and artificial intelligence. In 1995, he graduated from the aggregation in physics from Higher Normal School. Currently, he is professor of physics in preparatory class for high schools, Settat, Morocco.

Elhassane Abdelmounim

Elhassane Abdelmounim was born in Oued-Zem Morocco in 1965, he received his PhD in Spectral analysis from Limoges University at Science and Technology Faculty, France in 1994. In 1996, he joined, as Professor, applied physics department of Science and Technology faculty, Hassan 1st University, Settat, Morocco. His current research interests include digital signal processing and machine learning. He is currently coordinator of a Bachelor of Science in electrical engineering and he is researcher at System Analysis and Information Technology Laboratory at Hassan 1st University, Settat, Morocco.

Abdellah Lamnii

Abdellah Lamnii was born in Ain Beni Mathar Morocco in 1978. PhD in applied mathematics from Mohammed 1st university Oujda-Morocco, cotutelle with the University of Pau Et pays de l'adour in 2009. 2010 as Professor, applied mathematics Department of Mathematics and Informatics, Hassan 1st University, Settat, Morocco. His current research interests include applied mathematics and digital signal.

Masticatory System Biomechanical Photoelastic Simulation fot the Comparison of the Conventional and Uni-Lock Systems in Mandibular Osteosynthesis

José Luis Cebrián Carretero[1] *, María Teresa Carrascal Morillo[2], Germán Vincent Fraile[3]

[1]Servicio de Cirugía Oral y Maxilofacial, Hospital Universitario La Paz, Madrid (Spain)
[2]Departamento de Mecánica, E.T.S Ingenieros Industriales, UNED, Madrid (Spain)
[3]Laboratorio de Prótesis Dental Vincent Dental, Madrid (Spain)

Received 31 August 2016 | Accepted 1 November 2016 | Published 23 December 2016

Abstract

The biomechanical consequences of the interaction between titanium trauma plates and screws and the fractured mandible are still a matter of investigation. The mathematical and biomechanical models that have been developed show limitations and the experimental studies are not able to reproduce muscle forces and internal stress distributions in the bone-implant interface and mandibular structure. In the present article we show a static simulator of the masticatory system to demonstrate in epoxy resin mandibular models, by means of 3D (three-dimensional) photoelasticity, the stress distribution using different osteosynthesis methods in the mandibular angle fractures. The results showed that the simulator and 3D photoelasticity were a useful method to study interactions between bone and osteosynthesis materials. The "Lock" systems can be considered the most favourable method due to their stress distribution in the epoxy resin mandible. 3D photoelasticity in epoxy resin models is a useful method to evaluate stress distribution for biomechanical studies. Regarding to mandibular osteosynthesis, "lock" plates offer the most favourable stress distribution due to being less aggressive to the bone.

Keywords

3D Photoelasticity, Biomechanical Simulator, Masticatory System Simulator, Mandibular Biomechanics, Mandibular Osteosynthesis.

DOI: 10.9781/ijimai.2017.455

I. Introduction

Although cranio-maxillo-facial osteosynthesis principles were developed during the '60's and 70's, their universal application was delayed until the 80's. In this situation, the first retrospective studies with an acceptable follow-up did not appear until 1990. In these papers osteosynthesis showed its superiority over any other traditional method for fracture treatment [1, 2, 3].

In the field of mandibular osteosynthesis, research continues to focus on the size, shape, number, and biomechanics of plate/screw systems to improve surgical outcome.

In conventional bone plating stability is achieved systems when the head of the screw compresses the fixation plate to the bone as the screw is tightened (Fig. 1). Morbidity with these systems is commonly related to: 1) mobility and hardware failure; 2) alterations in the alignment of the segments that cause changes in the occlusal relationship; 3) resorption of the bone cortex adjacent to the plate. In some cases, if the plate is not contoured precisely and is not in intimate contact with the bone or if the host is compromised (medically or nutritionally), the "race" between fracture healing and cortex resorption will be lost and will result in unstable fixation [4].

* Corresponding author.
E-mail address: josel.cebrian@salud.madrid.org

The Locking plate/screw systems have certain advantages over conventional plates and screws. They achieve stability through a device that "locks" the screw to the plate while the screw shaft secures the bone. Theoretically, they offer the advantages of: 1) less screw loosening; 2) greater stability across the fracture site; 3) less precision required in plate adaptation because of the "internal/external fixator"; and 4), less alteration in osseous or occlusal relationships when the screw is tightened [5, 6].

The lock between the plate and screw obviates the requirement for compression between the plate and mandible as is required in a conventional screw plate system (3) and fewer screws might be needed to achieve maximal load resistance [7, 8].

Although some biomechanical studies have focused on the higher stability of these "locking" systems in comparison to non-locking systems (Gutwald, Haug), the theoretical advantage of avoiding bone compression and cortical plate resorption has not yet been biomechanically proven.

There are two requirements to prove this:

1. First, it is necessary to create a simulator of the studied biomechanical system that accounts for the variability of the in vivo interaction between human and non-human tissues. [9-11]
2. It is also necessary to develop a technique that allows us to analyze the interphase between the implant and bone. [11, 12]

Numerous in vitro models of fracture fixation have been described in the literature. These include cadaveric mandible models: freshly harvested ovine/sheep mandibles; porcine/sheep mandibles and bovine/cow ribs. Although different simulators have been developed, they have never actually been employed to explore the biomechanical interaction between implant and bone [12].

The purpose of the present investigation is to develop a biomechanical simulator of the masticatory system so as to evaluate and compare the mechanical behavior of locking and conventional plate and screw systems placed under ideal conditions employing the photoelastic techniques.

II. Methods

A. Photoelasticity and Tension Freezing Method

Photoelasticity is based on an optic phenomenon called occasional birrefringency. It takes place when a transparent material, with specific characteristics, is put under mechanical stress and then observed in a polarized light field; under this light, a constant isochromatic band, that are directly related with the tensional force in each area. Polarized light reveals a constant pattern of isochromatic bands in the transparent material that are directly related with the stress level in each area.

The stress freezing procedure takes advantage of resin epoxy photoelasticity. This type of resin has two molecular phases, and when baked/heated for 2 hours at 70ºC one of the phases becomes viscous, while the other, which is crystalline remains solid. The model is heated and exposed to a stress load, the solid phase of the material is deformed, with the resulting internal stress loads being revealed by the isochromatic lines revealed by polarized light. The difference in tension/stress between the two bands is given by the following formula:

$$\text{Stress/Tension Differential} = N \times F / h \quad (1)$$

Where, N is an a-dimensional constant for each band whose value rises with the stress in the area.

"F" is constant that is related with the kind of material and "h" is thickness (Fig 1).

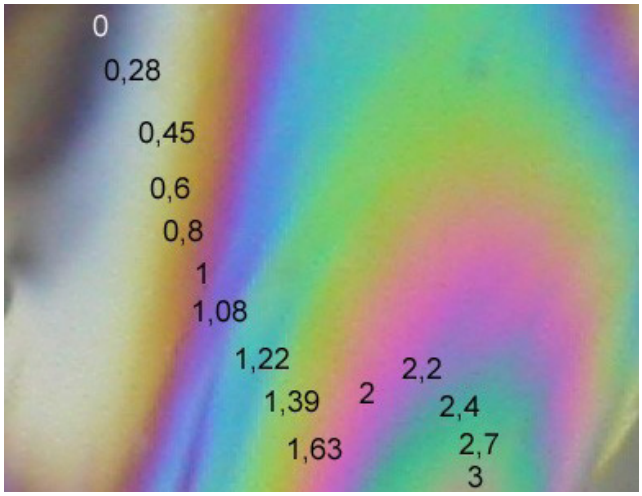

Fig. 1. Isocromatics spectrum where each number represent "n" value in different frames.

III. Biomechanical Simulator

1:1 scale dentate mandibles made of epoxy resin, which is an acceptable substitute for bone in studies of mandibular fixation, were used to simulate the intact mandible. The mandibular model was mounted on a polyurethane cranium. The mastication musculature (Fig. 2) was mounted placing screws in the points at which muscles are inserted to hold elastic bands that create forces like those applied by the masticary muscles. The following muscles were simulated: maseteri, lateral and medial pterigoid, temporal and depressor muscles. So as to reproduce the mechanics of the system, stresses proportional to those calculated by Meyer [13] for healthy individuals in maximum intercuspidation were applied.

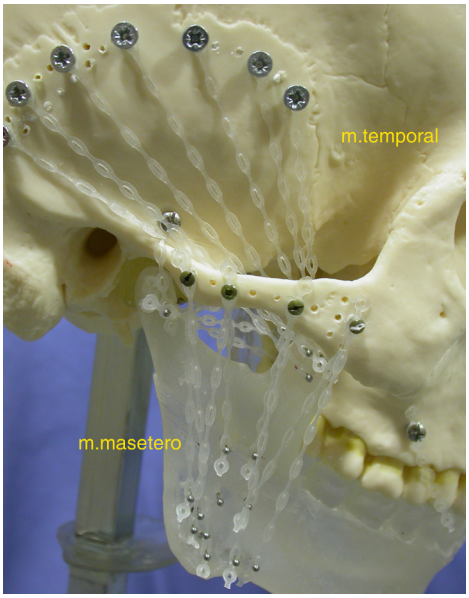

Fig. 2. Mastication musculature.

IV. Assays

Angle fractures were caused/provoked in the right mandibular angle of two mandibles. They were fixed using two different osteosynthesis methods:

1. Conventional miniplates: 2.0 miniplates.
2. "Locking" plates: 2.4 locking plates. (Fig. 3)

To study the interface between bone and screw osteosynthesis material was removed after applying the freezing tension method and the mandible was cut into 5 mm slices from angle to angle.

These mandibular slices were polished until they were smooth/transparent and before being observed under the polaroscope.

Applying the stress differential formula and considering "f" and "h" as constants, we can see that semiquantitatively, the greater the N, the higher the stress.

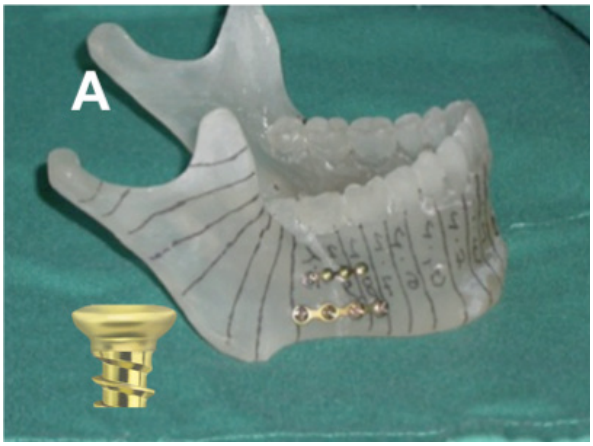

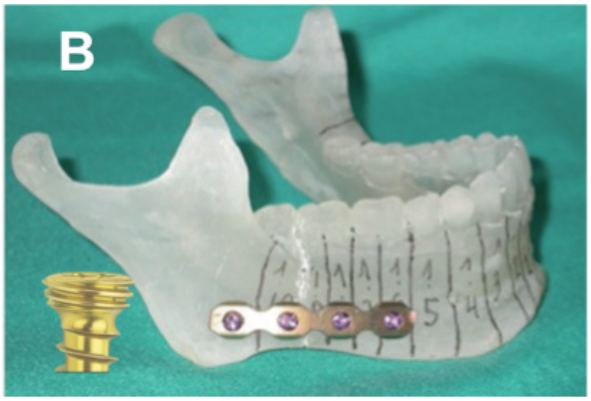

Fig. 3. Epoxi resin mandibular prototype. A. Ostheosinthesis with 2.0 miniplates. B. Ostheosynthesis with "lock" type plate.

V. Results

When the screw tightened the plate directly onto the mandible, the stresses related with the compression forces were concentrated in the external cortical bone, in the area in which the plate was apposed to the plate. These stress lines were very intense along the length of the screw, reaching the basilar area and alveolar bone, with an important reaction in the opposite cortical bone (Fig 4. A and B).

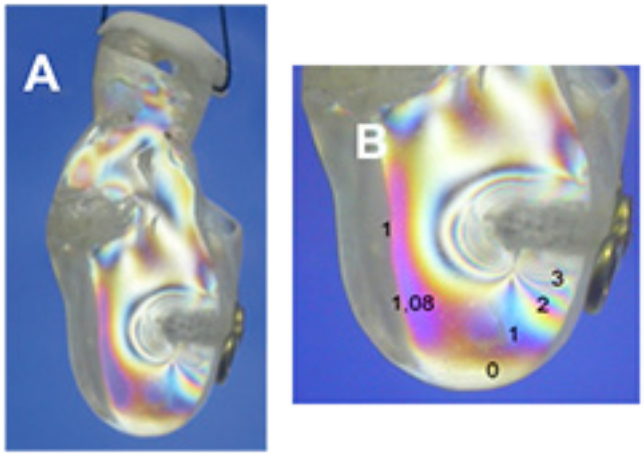

Fig. 4. A. Ostheosynthesis with 2.0 conventional plates. B. Notice the high tension concentration related with compresive strenghts surrounding the screw and both bony corticals.

On the contrary, when a locking plate/screw system was used, the compression force lines on the mandible/in the mandible were much less. Fig. 5.A and B show how the concentration of stresses was less than with the conventional plate system, and, in addition, stress lines were limited to the tip of the screw without extending to the proximal part of the screw. In the same way, there was no compression over the cortical bone in contact with the plate, or even less stress reaction in the contralateral cortex.

Observation of the stress lines along the cortical slices shows that both the maximum intensity and the maximum density were less than with the previous model.

In cases in which 2 conventional 2.0 mm miniplates (Fig 6) were used, the concentration of stress lines along the length of the implant, independently of implant length, and along the external cortical bone, was high. The isochromatic bands surrounding the two screws expanded into each other, creating an area of concentrated high stresses between the two screws.

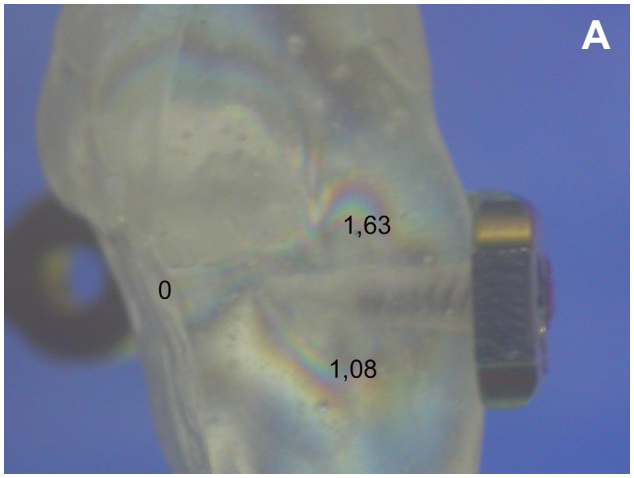

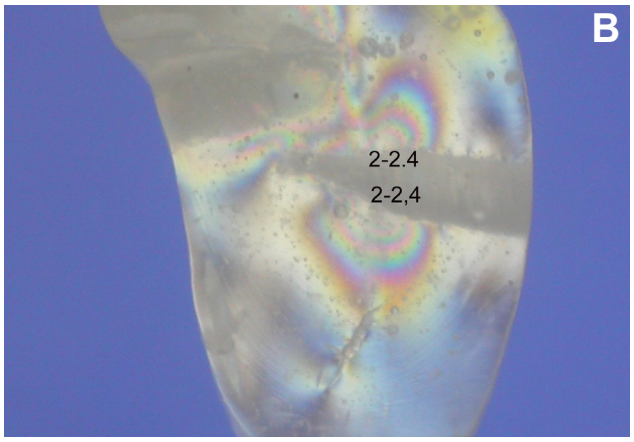

Fig. 5. A and B.–«Lock» system. Notice the low tensión along the screw, with only higher tensions in the tip area.

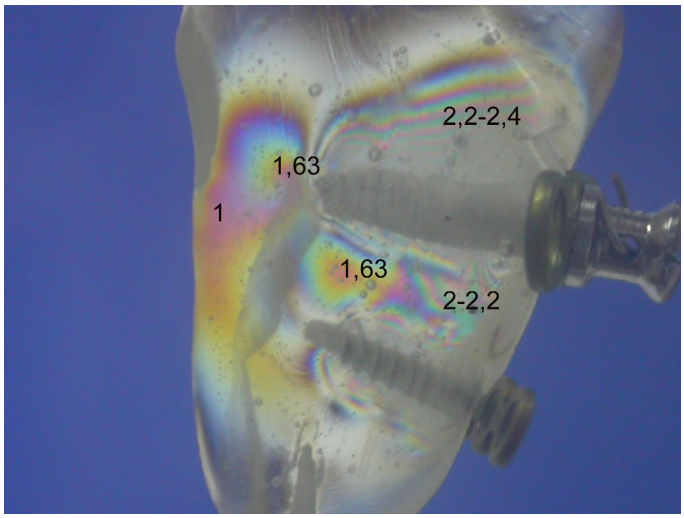

Fig. 6. Tension spectrum surrounding two 2.0 conventional screws. Notice the high tension´s concentration along the hole screw body, over both cortical areas and in the cancellous bone between both screws.

VI. Discussion

During the past thirty years, research into osteosynthesis has focused on the achievement of the most biocompatible material in terms of composition, shape and size. Nevertheless, only a few biomechanical studies have analyzed what is the ideal osteosynthesis. It makes sense that this osteosynthesis should function without interrupting, at all, or

as little as possible, the normal tension-sress pattern in the mandible [14, 15].

Conventional bone plate/screw systems require precise adaptation of the plate to the underlying bone and screw compression to maintain the occlusal relationship and fracture stabilization. This system ensures primary healing, but a long-term side effect could be screw loosening and external cortical bon resorption resulting from plate compression [7, 8].

The most significant advantage of locking systems may be that they make it unnecessary for the plate to have intimate contact with the underlying bone in all areas. As the screws are tightened, they "lock" to the plate, thus stabilizing the segments without the need to compress the bone to the plate. This obviates the risk that screw insertion will alter the reduction. This theoretical advantage is certainly more important when using large bone plates like reconstruction plates, which can be very difficult to adapt perfectly. The other problem is pressure from the screw. The amount of stability provided across the fracture osteotomy gap is greater than when standard non-locking screws are used.

In an attempt to explore the relationship between bone, plates and screws, the present study employed photoelasticity and freezing tension method to analyze the interphase between bone and plates and screws.

Photoelasticity has been widely employed to evaluate osteosynthesis methods. Perhaps the most influential studies are those of Champy et al, which, between 1970-1980, subjected photoelastic resin blocks to stress in order to draft the basic fundamentals of osteosynthesis [12, 13, 14]. At this point, several studies employing photoelasticity to evaluate osteosynthesis options for traumatology, orthodontics ad mandibular reconstruction after a hemimandibulectomy have been done [16, 17, 18].

All these studies employed systems that subjected a mandibular model to a bidimensional study of the surface.

The advantages of tension freezing methods in mandibular slices are double:

1. They allow the study of the interphase between bone and screws.
2. They allow tridimensional studies if the mandibular slices are analyzed sequentially.

The novelty of the present experimental design is that it applies a stress-freezing technique to interpret the *stress* forces created by the insertion of the osteosynthesis materials, since, even though the component or implant is removed, the stress lines are "memorized".

The experiments in our study have shown how the compression of the plate by the screw in the non-locking systems is directly transmited to the bone into the cortical bone. In this situation, experimental studies have shown a disruption of cortical blood supply directly beneath the bone plate, favoring bone resorption [19, 20].

This is very important in the body of the mandible and in compromised patients in which vascularization is impaired.

This over pressure is avoided when locking systems are used

Although reports of the use of locking plate and screw systems for maxillofacial reconstruction have existed for more than three decades, their clinical use has not become popular until the last decade [21] Herford and Ellis concluded that "the use of a locking plate/screw system was found to be simple and it offers advantages over conventional bone plates by not requiring the plate to be compressed to the bone to provide stability [6, 22].

The first biomechanical comparison of locking and non-locking plates to appear in the maxillofacial surgical literature was made by Gutwald in 1999 [5]. That investigation was performed using 16 cadaver mandibles. They concluded that a higher stability was achieved with locking plates. If we add this advantage to the fact of the decreased potential bone damage we have demonstrated here, we can conclude that the use of locking plates and screws is clinically advisable.

Recent studies involving the use of miniplates have questioned the role of biomechanical testing because of conflicting data when in vivo and in vitro models are compared. Biomechanics is only one factor to be considered in the treatment of mandibular fractures and many others may also be involved.

The main disadvantage of the locking system is cost.

Therefore functional overloading of regions that need not undergo compressive *forces* is much greater in the conventional systems. Although it is yet to be proven "in vivo", it can be supposed that this system will avoid compromising external cortical bone during healing.

We used the 2.4 mm locking system in this study because at the time of the experimental work the single 2.0mm lock plate was still controversial for treating body angle fractures [21, 22], but since then, similar fixation rates have been reported with the 2. mm plate, which offers a similar, or even better stability than conventional osteosynthesis systems [23, 24].

It is true thah biomechanicals aspects are only one side of the problema when we are facing mandibular fractures, but it is also clear that the bone and tissue care that is ensure by "lock" systems has been clinically proven. In fact, this systems are heavily recommended for savage in those case in which ostheosynthesis has failed [25, 26, 27].

VII. Conclusion

In the present study we propose a reliable and predictable model to explore biomechanichal characteristics of muscle-skeletal masticatory system.. The system is particularlly useful to study ostheosynthesis in case of mandibular fractures offering a semi-cuantitative assesment about stress and tensions that are working in the fractured system. In this sense it has allowed us to conclude how "locked" systems are the less harmful for the bone and also those who are more respectful with mandibular forces and tensions. This study shows hoe photoelasticity and freezing tensions methods are very useful systems to study mandibular biomechanics as it has been shown in preliminary reports [25, 26].

Acknowledgements

We appreciate the cooperation of Dr. Rodríguez Avial director of the Laboratory of Materials of the ETSII of the UNED where this study was developed. The authors declare no interest conflict.

References

[1] Thaller SR, Reavie D, Daniller A. Rigid internal fixation with miniplates and screws: a cost-effective technique for treating mandible fractures? Ann Plast Surg. 1990;24:469–74.

[2] Hoffman WY, Barton RM, Price M, Mathes SJ. Rigid internal fixation vs. Traditional techniques for the treatment of mandible fractures. J Trauma. 1990;30:1032–5.

[3] Moreno JC, Fernández A, Ortiz JA, Montalvo JJ. Complication rates associated with different treatment for mandibular fractures. J Oral Maxillofac Surg. 2000;58:273–80.

[4] Klotch DW, Gal TJ, Gal RL. Assessment of plate usemandibular reconstruction: Has changing technology made a difference? Otolaryngol Head Neck Surg. 1999;121:388–92.5.

[5] Gutwald R. Biomechanical stability of an internal mini fixation system in maxillofacial osteosynthesis. J Med Biol Eng Comp. 1999;37:S280.

[6] Hertford AS, Ellis E. Use of a locking reconstruction bone plate/screw system for mandibular surgery. J Oral Maxillofac Surg. 1998;56:1261–5.

[7] Haug RH, Street CC, Goltz M. Does plate adaptation affect stability? A biomechanical comparison of locking and nonlocking plates. J Oral

Maxillofac Surg. 2002;60:1319–26.
[8] Haug RH, Fattahi TT, Goltz M. A biomechanical evaluation of mandibular angle fracture plating techniques. J Oral Maxillofac Surg. 2001;59:1199–210.
[9] Bredbenner TL, Haug RH. Substitutes for human cadaveric bone in maxillofacial rigid fixation research. Oral Surg Oral Med Oral Pathol Oral Radiol Endod. 2000;90:574–80.
[10] Pacey MN, Haake SJ, Paterson EA. A novel instrument for automated principal stress separation in reflection photoelasticity. J Test Eval. 2000;28:229–35.
[11] Champy M, Lodde JP, Jaeger J, Wilk A. Ostéosynthéses. Mandibulaires selon la technique de Michelet. Bases biomécaniques. Rev Stomatol Chir Maxillofac. 1976;77:569–76.
[12] Gross MD, Nissan J, Samuel R. Stress distribution around maxillary implants in anatomic photoelastic models of varying geometry. Part I. J Prosth Dentistry. 2001;85:442–9.
[13] Meyer U, Vollmer D, Benthaus S, Felczegi E, Joos U, Piffko F. Experimentelle un finite element analysie der biomechanik des unterfiekersunter belastung. Mund KieferGesichtschir. 2000; 4: 14- 20.
[14] Kim YK, Nam KW. Treatment of mandible fractures using low profile titanium miniplates: preliminary study. Plast Reconstruc Surg. 2001;108:38–43.
[15] Rudman RA, Roshental SC, Shen C, Ruskin JD, Ifju PG. Photoelastic analysis of miniplate osteosynthesis for mandibular angle fracture. Oral Surg Oral Med Oral Pathol Oral Radiol Endod. 1997;84:129–36
[16] Shetty V, Caputo AA. Biomechanical validation of the solitary lag screw technique for reducing mandibular angle fractures. J Oral Maxillofac Surg. 1992;50:603–7.
[17] Yi Z, Jian-Guo Z, Guang-Yan Y. Reconstruction plates to bridge mandibular defects: a clinical and experimental investigation in biomechanical aspects. Int J Oral Maxillofac Surg. 1999;28:445–50.
[18] Champy M, Lodde JP. Synthéses mandibulaires. Localisation de synthése en fonction des contraintes mandibulaires. Rev Stomatol Chir Maxillofac. 1976;77:971–6.
[19] Weinans H, Huiskes R, Grootenboer HJ. Quantitative analysis of bone reactions to relative motions at implant-be interfases. J Biomechanics. 1993;26:369–82.
[20] Rietbergen B, Huiskes R, Weinam H, Sumner DR, Turner TM, Galante JO. The mechanics of bone remodeling and resorption around prefitted systems. J Biomechaics. 1993;26: 369–82.
[21] Alpert B, Gutwald R, Schmelzeisen R. New innovations in craniomaxillofacial fixation: the 2.0 lock system. Keio J Med. 2003;52:120–7.American Cancer Society. Breast Cancer
[22] Ellis E, Graham J. Use of a 2.0 mm locking reconstruction bone plate/ screw system for mandibular fracture surgery. J Oral Maxillofac Surg. 2002;60:642.
[23] Cebrián JL. Desarrollo de un simulador estático para estudios biomecánicos foto-elásticos del sistema músculo-esquelético masticatorio. Tesis.
[24] Gbara A, Heiland M, Schmelzle R, Blake F. Mechanical aspects of a multidirectional, angular stable osteosynthesis system and comparison with four conventional systems. J Craniomaxillofac Surg. 2008;36:152–6.
[25] Navarro I, Cebrián JL, Demaría G, Chamorro M, López-Arcas JM, Mún˜ oz JM, et al. Fracaso de la osteosíntesis mandibular. Consideraciones biomecánicas y tratamiento. A propósito de dos casos clínicos. Rev Esp Cir Oral y Maxilofac. 2009;31:122–7.
[26] Cebrián JL, Carrascal MT, Vincent G, Ortiz de Artinano F. Estudio biomecánico experimental del sistema musculo-esquelético masticatorio Aplicaciones para el estudio de la osteosíntesis. Rev Esp Cirug Oral y Maxilofac.2009;31:39–45 at.
[27] Cebrián-Carretero JL, Sánchez Burgos R, Carrascal-Morillo MT, Vincent-Fraile G, Ortiz de Artiñano F, Burgueño García MAComparación biomecánica entre los sistemas convencionales y uni-lock en osteosíntesis del ángulo mandibular. Estudio fotoelástico. Rev Esp Cir Oral y Maxilofac. 2012;34:1-7.

José Luis Cebrián Carretero

José Luis Cebrián Carretero got his Medical Degree Universidad Autónoma de Madrid (UAM) in 1993. He is PhD by the same university in 2005. He also studied Oral and Maxillofacial training H.U. La Paz from 1995 to 2000. He got is Dental Degree in the Universidad Europea de Madrid (UEM) in 2009. He is fellow of the European Board of Oral and Maxillofacial Surgery, Specialist in Oral and Maxillofacial Surgery, La Paz University Hospital, Madrid and Chief of Division in Oral and Maxillofacial Surgery, La Paz University Hospital, Madrid, and Director of Oral and Maxillofacial Surgery Departments at Quironsalud Hospital Sur de Madrid y Clínica La Luz. Finally he is Vice-President of the SECOM (Spanish Society of Oral and Maxillofacial Surgery). He is author of 2 books, 15 chapters and more than 50 scientific articles. His main research areas are Implantology, Head and Neck Oncologic Surgery and Orthognatic and Oral Surgery.

María Teresa Carrascal Morillo

Associate Professor within the Department of Mechanics at the Higher Technical School of Industrial Engineering of the National University of Distance Education (UNED). Director of Biomechanics Laboratory tests in which biological and synthetic materials are made.

German Vincent

German Vincent is dental prosthesis technician, specialist surgical splints for orthognathic surgery. He works in his own laboratory called Vincentdental in Madrid. He is a national speaker at numerous courses of orthodontics and facial deformities related pathology and Tempero-mandibular joint.

Selecting Statistical Characteristics of Brain Signals to Detect Epileptic Seizures using Discrete Wavelet Transform and Perceptron Neural Network

Rezvan Abbasi[1], and Mansour Esmaeilpour[2]*

[1]Department of Computer System Architecture, Arak Branch, Islamic Azad University, Arak (Iran)
[2]Department of Computer Engineering, Hamedan Branch , Islamic Azad University, Hamedan (Iran)

Received 26 June 2016 | Accepted 1 November 2016 | Published 23 December 2016

unir
LA UNIVERSIDAD EN INTERNET

Abstract

Electroencephalogram signals (EEG) have always been used in medical diagnosis. Evaluation of the statistical characteristics of EEG signals is actually the foundation of all brain signal processing methods. Since the correct prediction of disease status is of utmost importance, the goal is to use those models that have minimum error and maximum reliability. In anautomatic epileptic seizure detection system, we should be able to distinguish between EEG signals before, during and after seizure. Extracting useful characteristics from EEG data can greatly increase the classification accuracy. In this new approach, we first parse EEG signals to sub-bands in different categories with the help of discrete wavelet transform(DWT) and then we derive statistical characteristics such as maximum, minimum, average and standard deviation for each sub-band. A multilayer perceptron (MLP)neural network was used to assess the different scenarios of healthy and seizure among the collected signal sets. In order to assess the success and effectiveness of the proposed method, the confusion matrix was used and its accuracy was achieved98.33 percent. Due to the limitations and obstacles in analyzing EEG signals, the proposed method can greatly help professionals experimentally and visually in the classification and diagnosis of epileptic seizures.

Keywords

Discrete Wavelet Transforms (DWT), Accuracy, Electroencephalogram Signals (EEG), Multilayer Perceptron (MLP), Epileptic Seizure.

DOI: 10.9781/ijimai.2017.456

I. Introduction

Epilepsy is one of the most prevalent neurological disorders among people[1]. It is estimated that 5 people are afflicted with epilepsy among each 1000 people. Epilepsy could be defined as a sudden change in the intracellular and extracellular potential difference. This definition implies that the type of neuron determines clinical demonstrations[2]. The automatic diagnosis of epileptic convulsions has attracted the attention of clinicians and engineers since 1970. The automatic prediction of seizures is useful in drug delivery systems and neural stimulation simulation devices [3, 4]. An important issue in predicting epileptic convulsions is that they are predictable through analyzing the changes in the features of EEG signals that happen before the occurrence of seizures [5]. Epileptic seizures prediction needs further analysis due to the following reasons [6]:

1. Generally, their results are not repeatable. In other words, their confidence rate is not certain.
2. The dependence of the result on sensitivity and inaccurate prediction rate is not taken into account.
3. Their efficiency is not mostly acceptable and has a high acceptance and rejection rate.

* Corresponding author.
E-mail address: esmaeilpour@iauh.ac.ir

II. Materials and Methods

In an automatic epileptic convulsion detection system, a distinction should be made between the pre-convulsion, during convulsion, and post-convulsion EEG signals. Then, they should be analyzed [7]. Some studies focused on single-channel EEG signals, while some others focused on multi-channel recorded EEG signals [8]. This paper studied the epileptic and healthy signals of R. G. Andrzejak database from the University of Bonn [9]. The data relate to three different categories:normal situation of the patient, pre-seizure and seizure. The collected EEG signals include 5 categories which, respectively, are called (A,B,C,D,E).Each of these categories includes 100 single-channel signals with a length of 26.3 seconds.

Category A: Surface EEG signal recorded from 5 healthy volunteers in a relaxed awake state with eyes open.

Category B: EEG signal recorded from 5 healthy volunteers in a relaxed state with eyes closed.

Category C: Deep signals recorded from epileptic patients during the interval between seizures from inside the area that caused the seizure. (focal signals)

Category D: Deep recorded signals from epileptic patients during the intervals between seizures from outside the area that caused the seizure. (non-focal signals)

Category E: Signals recorded from epileptic seizures.

All EEG signals were recorded with the 128-channel system with

common average voltage. Sampling frequency in this database is 173.61 Hz. According to the Nyquist Theorem ,the maximum useful sampling frequency is half of the sampling frequency. Here we have:

$$\frac{173.61}{2} = 86.6\ Hz \quad (1)$$

The placement design of surface electrodes is related to the 20-10 global system,is shown in Fig. 1. Therefore, the electrodes were named as follows [10, 11]:

FP1,FP2,F3,F4,C3,C4,P3,P4,F7,F8,T1,T2,T3,T5,T6,O1,O2,F2,P2

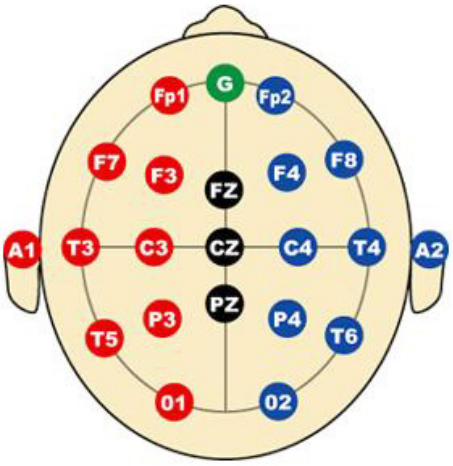

Fig. 1. The pattern of surface electrodes placement following that of the universal system 20-10.

The frontal lobe, temporal lobe, parietal lobe, central lobe, and occipital lobe were named F, T, P, C, and O, respectively [12].The Fig. 2 describes the anatomy of the brain with different regions[10].

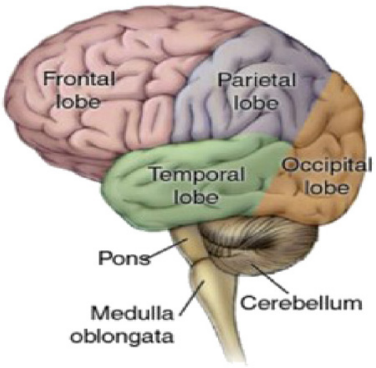

Fig. 2.Human brain structure.

Fig. 3, 4 and 5 show healthy,convulsive and epileptic signals. The signal overlap healthy and epileptic shown in Fig. 6. In processing medical signals, it is vitally important to minimize existing noises and artifacts in order that they have the minimum effect on the feature extraction stage. In a wide-spreading spectrum, recorded EEG signals may contain technical and physiological noises [13]. By taking into account the physiological aspects, such as the artifacts caused by electrooculography (EOG), electromyography (EMG), and electrocardiography (ECG), and by applying an appropriate pre-processing, frequencies higher than 60 Hz were considered as noises and filtered.

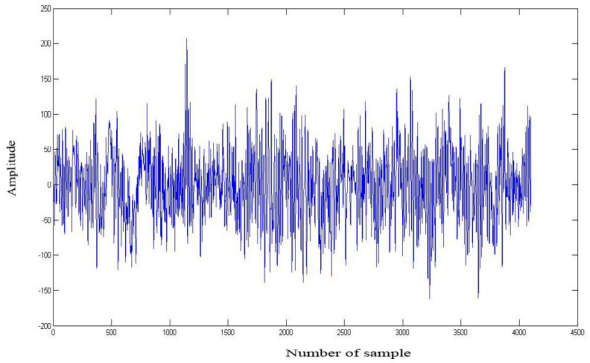

Fig. 3. An example of healthy signals.

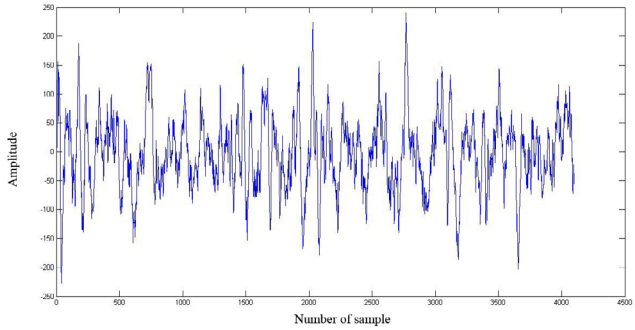

Fig. 4. An example of convulsive signals.

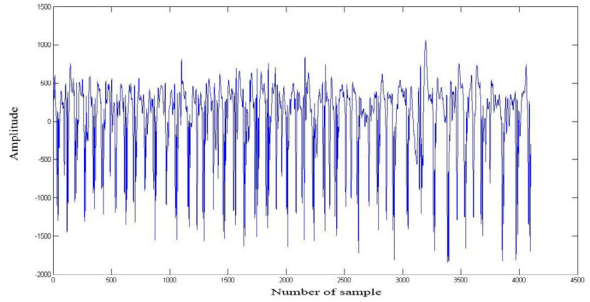

Fig. 5. An example of epileptic signals..

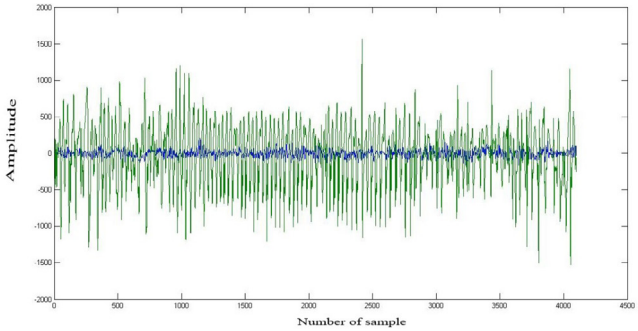

Fig. 6. Healthy and epileptic signals overlap rate.

A. Features Extraction by DWT

It is vitally important to select features which can best describe EEG signals for diagnosing convulsion and categorization. Since EEG signals are non-stationary waves [11], wavelet transform was used in their estimation. This frequency processing tool extracts a set of transient and local signals in space and frequency domains [14-16] . Wavelet transform decomposes signals into a set of basic functions called wavelet. These functions are obtained by applying delays, contractions, and transfer them on a unique function called wavelet pattern. Continuous wavelets are the functions resulted from an odd

function using delays and transfers. They are dependent on transfer parameter. In order to remove noises and generate a signal appropriate for decomposition, EEG signals were limited by a low-pass filter and impulse response. Compared to EEG signals, sub-bands have more accurate information about neurons activities. They may not be evident in the original signals due to specific changes. Therefore, decomposition is carried out. The discrete wavelet signal is analyzed in the form of different frequency value bands and different magnifications. Using signal decomposition, the discrete wavelet signal is decomposed into coarse approximations and detailed information. In fact, discrete wave transform (DWT) employs a set of functions called measurement functions and wavelet functions. They are dependent on low-pass and high-pass filters. Decomposing signals into various frequency bands is simply achievable through successive applications of high-pass filters (HPFs) and low-pass filters (LPFs) [17, 18]. This decomposition method is known as multi-resolution decomposition. This type of analysis is illustrated in detail is shown in Fig. 7. The number of decomposition levels is selected based on dominant frequency components of the signal [17]. Selected levels maintain signal parts that highly correlate to the frequency related to signal classification in the wavelet.

The proposed method involves 4 layers and 5 frequency bands. It is due to the fact that higher order filters have fluctuations and lower order filters are rougher. Therefore, the signal was decomposed into D1-D4 details and the last estimation A4. Frequency sub-band values are shown in Table 1. Figures 8, 9, and 10 show the sub-bands resulted from the decomposition of healthy, convulsive, and epileptic signals using wavelet function Db4 in 4 levels. First, signals are decomposed into 5 levels. Then, level 5 approximation signal is removed. It has the lowest frequency band. It does not contain epileptic information, but contains noise information. Finally, the signal is reconstructed.

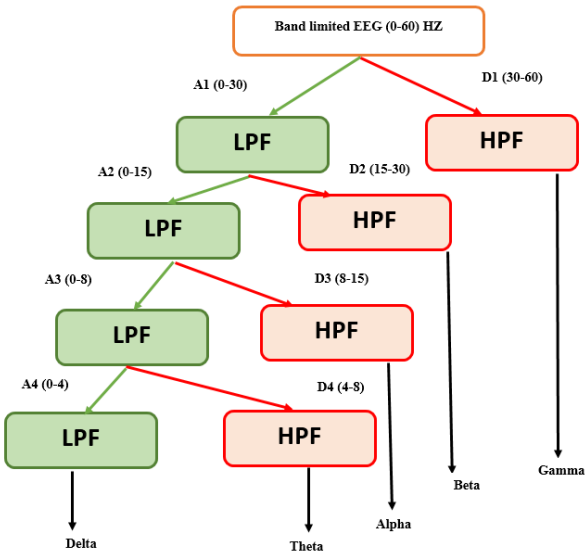

Fig. 7. Original signal decomposition level using daubechies wavelet transform.

TABLE I
WAVELET-DECOMPOSITION LEVEL AND EEG SUB-BANDS RELATIONSHIP.

Band-limited EEG	Decomposition level	Freqency band	Frequency bandwidth(Hz)
(0-4)	A4	Delta	4
(4-8)	D4	Theta	4
(8-15)	D3	Alpha	8
(15-30)	D2	Beta	15
(30-60)	D1	Gamma	30

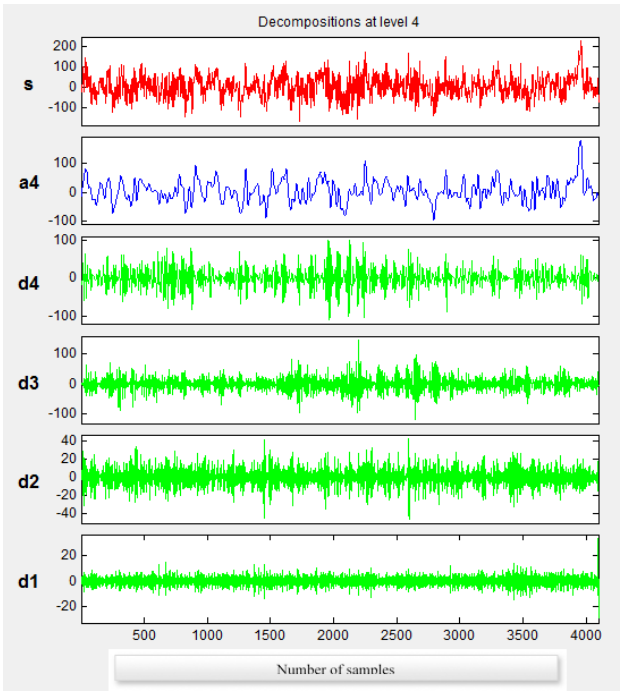

Fig. 8. A healthy signal with Daubechies 4 at level 4.

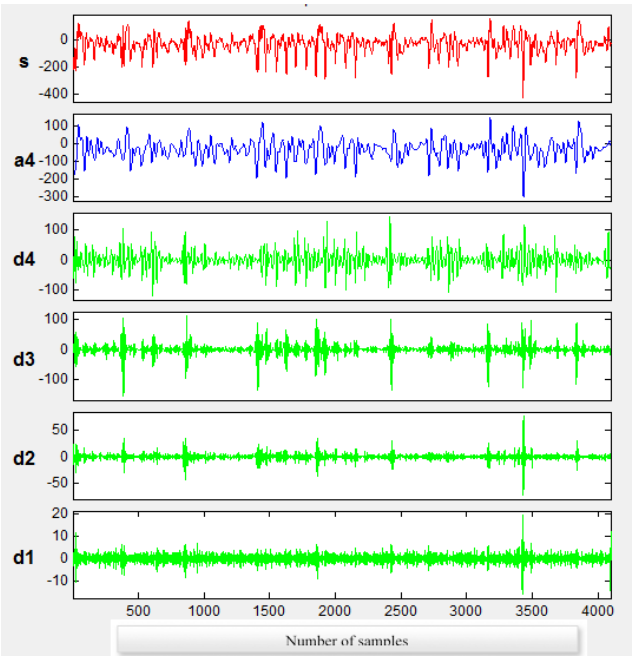

Fig. 9. A convulsive signal with Daubechies 4 at level 4.

Having applied pre-processing and carried out required processes, the desired feature vector was obtained. Statistical features, such as the maximum, minimum average, and standard deviation of each sub-band were used. Feature extracted are shown in Table 2.

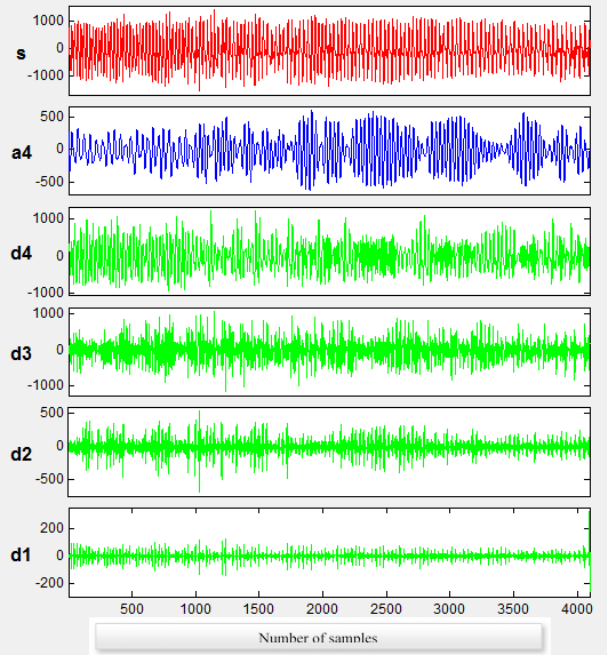

Fig. 10. Epileptic signals with Daubechies 4 at level 4.

B. Classification by Neural Network

Several statistical models have been proposed for classification and prediction. Classifying and predicting disorders based on risk factors is one of the applications of artificial neural networks [19, 20]. Artificial neural networks are simply applicable to problems with no algorithmic solution, a complex algorithmic solution, and problems that are simple for people but difficult for computers [21]. They are also useful as an alternative solution for problems that generally have statistical solutions, such as regression modeling, predicting time series, cluster analysis, discriminate analysis, statistical decision-making problems, process control, and estimating the conditional distribution [19, 20]. An artificial perceptron multi-layer neural network [22] with error back propagation algorithm was used for evaluating different states of EEG signals, such as healthy, convulsive, and epileptic states. Structure of Multilayer perceptron shown in Fig. 11.

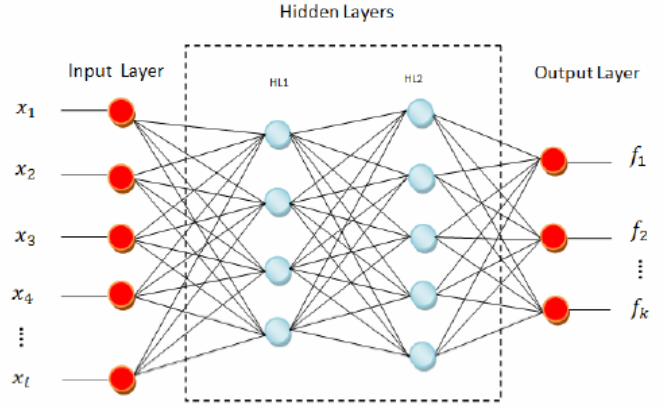

Fig. 11. Multilayer perceptron.

Having extracted desired statistical features using DWT, artificial neural network was used for classification. An artificial neural network with (12-15-3) structure and with sigmoid transfer function was designed and trained based on 80% of the available data. In the training phase, 80% of the collected data were used for training the artificial neural network. Having implemented the multi-layered perceptron (MLP) neural network using error back propagation learning (EBPL), having tested multiple layers and neurons, and having observed the errors, the most appropriate structure was selected. The most appropriate structure was (12-15-3), that is the network had four input variables for each category. The variables are the extracted statistical features, three output variables, and 15 neurons for maintaining the hidden layer. The output variable was defined based on three states, such as healthy, convulsive, and epileptic stages. Then, 20% of the available data were used for testing the neural network. In this phase, MLP with EBPL and (12-15-3) structure was used. For a more appropriate evaluation of results, feature and sensitivity were also calculated.

C. Analyzing System Performance using Confusion Matrix

Generally, in classification systems and disorder diagnosis systems, confusion matrix and receiving operating characteristic (ROC) curves are used for evaluating efficiency [23]. For analyzing the confusion matrix of classification and disorder diagnosis, four states are defined: true positive (TP), true negative (TN), false positive (FP), and false

TABLE II
FEATURE EXTRACTED OF SUBBANDS

Set	Feature	Subbands				
		D1	D2	D3	D4	A4
A	Max	12.039	31.306	75.769	120.014	192.677
	Min	-12.014	-42.073	-92.374	-105.366	-172.499
	Mean	-0.261	0.177	1.602	2.170	34.4130
	Std	4.968	14.841	41.186	60.346	96.4623
B	Max	14.144	46.928	102.260	242.521	302.978
	Min	-14.757	-51.484	-139.186	-157.733	-208.899
	Mean	0.472	0.089	-7.327	-2.741	24.0453
	Std	6.048	17.938	60.054	88.495	146.456
C	Max	6.4079	17.195	49.523	142.374	231.600
	Min	-7.373	-21.110	-42.639	-182.481	-269.463
	Mean	0.066	-0.135	2.264	-12.340	-39.066
	Std	2.800	9.514	25.913	95.077	153.392
D	Max	26.029	117.964	32.348	88.246	320.445
	Min	-20.682	-82.160	-61.542	-89.151	-175.767
	Mean	-0.193	0.112	-2.211	-2.636	94.158
	Std	4.387	19.245	20.175	43.635	126.357
E	Max	258.080	644.365	1524.400	1420.100	1639.200
	Min	-325.450	-1074.600	-1508.900	-1107.000	-1917.600
	Mean	-0.133	0.105	65.561	-77.229	281.401
	Std	75.144	303.674	716.087	614.261	1138.500

negative (FN) [24]. Each variable has a specific meaning in confusion matrix. TP is the number of patients suffering from epilepsy who are correctly diagnosed by the computer system. FP is the number of patients with epilepsy who are incorrectly diagnosed as healthy by the computer system. TN is the number of convulsive patients and healthy people correctly diagnosed as healthy by the computer system. FN is the number of convulsive patients or healthy people incorrectly diagnosed as epileptic by the computer system. P is the number of patients correctly classified by the system. In other words, it is the number of epileptic patients who are diagnosed correctly. It is also the number of healthy, convulsive, or non-epileptic people correctly classified. N is the number of the people who are incorrectly classified. In other words, it is the number of epileptic patients who are incorrectly diagnosed as healthy, or the number of healthy or convulsive people incorrectly diagnosed as epileptic or convulsive. Using the defined concepts, the efficiency of the proposed method was analyzed and they were named as sensitivity, specificity, classification, and precision, respectively. System precision is a measure that determines system's capability in diagnosing and classifying epileptic patients (true patients) correctly. Accuracy is but another index for evaluating such systems. It includes a more generalized perspective and domain of patient's classification systems. It is equal to the ratio of all correctly diagnosed cases, whether healthy or unhealthy, to all correctly or incorrectly classified cases [22], [25-28]. Sensitivity, Specificity, and Accuracy are defined as follows [10], [29, 30].

III. Results

The following confusion matrix is obtained from applying the neural network on the test data. This set was a new one for the network and it was not trained by those data. Results show that the neural network worked correctly since healthy people and patients were correctly diagnosed. Predicting patients' condition based on the result in the training phase are shown in Table 3. Predicting patients' condition based on the result in the test phase are available in Table 4.

TABLE III
Predicting Patients' Condition based on the Result in the Training Phase

Total	Epileptic	Convulsive	Healthy	Predicting
60	0	0	60	healthy
90	0	90	0	convulsive
90	90	0	0	epileptic
240	90	90	60	Total

TABLE IV
Predicting Patients' Condition based on the Result in the Test Phase (20 Percent of the Samples, that is 60 Cases)

Total	Epileptic	Convulsive	Healthy	Predicting
8	0	0	8	healthy
26	2	23	1	convulsive
26	24	1	1	epileptic
60	26	24	10	Total

For a better understanding, it is necessary to calculate the sensitivity and specificity of the proposed method. According to confusion matrix and Equations (2), (3), and (4), sensitivity, specificity, and precision of the neural network are as follows. The proposed classification system's sensitivity is 100%, which means the proposed system can diagnose all epileptic cases correctly. System's specificity was 97.1%, which is significant. It means that the proposed system could diagnose 98.33% and even a higher number of the convulsive cases correctly. Results of confusion matrix for classification of test data are shown in Table 5.

$$Sensitivity = \frac{TP}{TP+FN} \times 100 \quad (2)$$

$$Specificity = \frac{TN}{FP+TN} \times 100 \quad (3)$$

$$Accuracy = \frac{TP+TN}{TP+TN+FP+FN} \times 100 \quad (4)$$

TABLE V
Confusion Matrix (Accuracy, Sensitivity and Specificity) for Classification (Data Size: 240 Training Samples and 60 Testing Samples)

Accuracy	Sensitivity	Specificity
98.33%	100%	97.1%

A. Comparison of the Proposed Method with other Methods

Results from implementing the proposed MLP artificial neural network yield the highest sensitivity and precision. Many researchers have used wavelet transform in diagnosing epilepsy. Shoeb et al. used wavelet decomposition for generating feature vector [31]. Meier et al. exploited the combination of wavelet and time for extracting features as the input data for support vector machine (SVM) [32]. Abibullaevet all identified and presented various wavelet function for diagnosing convulsion and epilepsy, including (bior1,3, Db5, Db2) [33]. Adeli et al. analyzed EEG signals for detecting EEG changes based on correlation function; frequency domain features, frequency time analysis, entropy, and wavelet transform [14]. Using chaos analysis, they divided the wavelets obtained from EEG signals into healthy and epileptic categories. Some other linear and non-linear methods were also used in predicting epileptic attacks [32], [34-38]. Results from various studies carried out using wavelet transform are shown in Table 6 [39]. Another disadvantage of existing solutions is their low precision and high dispersion which leads into a weak diagnosis. It is due to the high number of effective variables in physiological systems [6]. The aim of this study was to improve prediction results. Therefore, some changes were made to input and output variables. The type of selected wavelet function and variables were the reasons for a higher sensitivity and precision. Due to the limitation facing diagnosis systems, MLP structure was selected as the most appropriate artificial neural network structure with respect to the repetition of various conditions. The combination of artificial intelligence methods in classifying patterns, including artificial neural networks with wavelet transform resulted in an improved efficiency, agility, and diagnosis in the proposed method.

TABLE VI
Comparition Accuracy from previous Research Work [28].

Studies	Accuracy (%)
Our Accuracy	98.33
Guler and Ubeyli(2005)	97
Kannathal et al.(2005)	90
Subasi(2007)	95
Chua et al(2008)	88.78
Ubeyli et al(2009)	92.9
Oweis and abdulahy(2011)	94
Orhan et al(2011)	96.67
Yuan et al(2011)	96.5

IV. Conclusion

This paper aimed at proposing a new method for improving the precision of prediction and classifying different states of EEG signals into healthy, convulsive, and epileptic states. Using wavelet transform and MLP, sensitivity, specificity, and precision indexes were improved significantly.

References

[1] Litt B Echauz, J. Prediction of epileptic seizures. The Lancet Neurology 2002;1: 22-30.

[2] Subasi A, Erçelebi E. Classification of EEG signals using neural network and logistic regression. Computer methods and programs in biomedicine 2005;78:87-99.

[3] Stein A.G, Eder H. G, Blum D. E, Drachev A, Fisher R. S. An automated drug delivery system for focal epilepsy. Epilepsy research 2000;39: 103-114.

[4] Osorio I, Frei M. G. Real-time detection, quantification, warning, and control of epileptic seizures: The foundations for a scientific epileptology. Epilepsy &Behavior 2009;16: 391-396.

[5] Mormann F, Kreuz T, Andrzejak R. G, David P,Lehnertz K, Elger C. E. Epileptic seizures are preceded by a decrease in synchronization. Epilepsy research 2003;53: 173-185.

[6] Iasemidis L. D. Epileptic seizure prediction and control. In: IEEE 2003 Biomedical Engineering ; pp. 549-558.

[7] Tong S, Thakor N. V. Quantitative EEG analysis methods and clinical applications. Artech House, 2009.

[8] Deburchgraeve W,Cherian P. J, De Vos M, Swarte R. M, Blok J. H, Visser G. H, Van Huffel S. Automated neonatal seizure detection mimicking a human observer reading EEG. Clinical Neurophysiology 2008;119: 2447-2454.

[9] Andrzejak R. G, Lehnertz K, Mormann F, Rieke C, David P, Elger C. E. Indications of nonlinear deterministic and finite-dimensional structures in time series of brain electrical activity: Dependence on recording region and brain state. Physical Review E 2001;64: 061907.

[10] Kumari, Pinki, and AbhishekVaish. "Brainwave based user identification system: A pilot study in robotics environment." *Robotics and Autonomous Systems* 65 (2015): 15-23.

[11] Kumari, Pinki, and AbhishekVaish. "Feature-level fusion of mental task's brain signal for an efficient identification system." *Neural Computing and Applications*: 1-11.

[12] Durka P. J. Adaptive time-frequency parametrization of epileptic spikes. Physical Review E 2004;69:051914.

[13] Sörnmo L, Laguna P. Bioelectrical signal processing in cardiac and neurological applications. Academic Press 2005.

[14] Adeli H, Ghosh-Dastidar S, Dadmehr N. A wavelet-chaos methodology for analysis of EEGs and EEG subbands to detect seizure and epilepsy.In: IEEE 2007 Biomedical Engineering; 54: 205-211.

[15] Guo L, Rivero D, Dorado J, Rabunal J. R, Pazos A. Automatic epileptic seizure detection in EEGs based on line length feature and artificial neural networks. . Journal of neuroscience methods 2010; 191: 101-109.

[16] Yuan Q, Zhou W, Li S, Cai D. Epileptic EEG classification based on extreme learning machine and nonlinear features. Epilepsy research 2011; 96: 29-38.

[17] Subasi A. Epileptic seizure detection using dynamic wavelet network. Expert Systems with Applications 2005;29: 343-355.

[18] Khan Y. U, Farooq O, Sharma P. Automatic detection of seizure onset in pediatric EEG. International Joural of Embeded Systems and Applications 2012; 2: 81-89.

[19] Livingstone D. J. Artificial Neural Networks: Methods and Applications (Methods in Molecular Biology). Humana Press, 2008.

[20] Dreiseitl S, Ohno-Machado L. Logistic regression and artificial neural network classification models: a methodology review. Journal of biomedical informatics 2002;35: 352-359.

[21] Zini G, d'Onofrio G. Neural network in hematopoietic malignancies. Clinica chimica acta 2003; 333:195-201.

[22] Ramchoun H, Amine M, Idrissi J, Ghanou Y, Ettaouil M. Multilayer Perceptron: Architecture Optimization and Training. International Journal of Interactive Multimedia and Artificial Inteligence. 2016;4(Special Issue on Artificial Intelligence Underpinning).

[23] Semwal, Vijay Bhaskar, Manish Raj, and Gora Chand Nandi. "Biometric gait identification based on a multilayer perceptron." *Robotics and Autonomous Systems* 65 (2015): 65-75.

[24] Abhinav-Vishwa MK, Lal SD, Vardwaj P. Clasification of arrhythmic ECG data using machine learning techniques. International Journal of Interactive Multimedia and Artificial Intelligence. 2011 Dec;1(4).

[25] Vaish, Abhishek, and PinkiKumari. "A Comparative Study on Machine Learning Algorithms in Emotion State Recognition Using ECG." *Proceedings of the Second International Conference on Soft Computing for Problem Solving (SocProS 2012), December 28-30, 2012*. Springer India, 2014.

[26] Semwal, Vijay Bhaskar, KaushikMondal, and G. C. Nandi. "Robust and accurate feature selection for humanoid push recovery and classification: deep learning approach." *Neural Computing and Applications*: 1-10.

[27] Singha, Joyeeta, and RabulHussainLaskar. "Self co-articulation detection and trajectory guided recognition for dynamic hand gestures." *IET Computer Vision* (2015).

[28] Singha, Joyeeta, and RabulHussainLaskar,"Hand gesture recognition using two-level speed normalization, feature selection and classifier fusion", Multimedia Systems, 2016.

[29] Kumari, Pinki, and AbhishekVaish. "Information-Theoretic Measures on Intrinsic Mode Function for the Individual Identification Using EEG Sensors."*Sensors Journal, IEEE* 15.9 (2015): 4950-4960.

[30] Singha, Joyeeta, and RabulHussainLaskar, "Recognition of global hand gestures using self co-articulation information and classifier fusion", Journal on Multimodal User Interfaces, Volume 10, Issue 1, pp 77-93.

[31] Shoeb A, Edwards H , Connolly J, Bourgeois B, Treves S. T, Guttag J. Patient-specific seizure onset detection. Epilepsy & Behavior 2004; 5:483-498.

[32] Meier R, Dittrich H, Schulze-Bonhage A, Aertsen A. Detecting epileptic seizures in long-term human EEG: a new approach to automatic online and real-time detection and classification of polymorphic seizure patterns. Journal of Clinical Neurophysiology 2008; 25: 119-131.

[33] Abibullaev B, Kim M. S, Seo H. D. Seizure detection in temporal lobe epileptic EEGs using the best basis wavelet functions. Journal of medical systems 2010; 34:755-765.

[34] Kannathal N, Choo M. L, Acharya U. R, Sadasivan P. K. Entropies for detection of epilepsy in EEG. Computer methods and programs in biomedicine 2005; 80: 187-194.

[35] Polat K, Güneş S. Classification of epileptiform EEG using a hybrid system based on decision tree classifier and fast Fourier transform. Applied Mathematics and Computation 2007;187: 1017-1026.

[36] Chan A. M, Sun F. T, Boto E. H, Wingeier B. M. Automated seizure onset detection for accurate onset time determination in intracranial EEG. Clinical Neurophysiology 2008; 119:2687-2696.

[37] Aarabi A, Fazel-Rezai R, Aghakhani Y.A fuzzy rule-based system for epileptic seizure detection in intracranial EEG. Clinical Neurophysiology 2009; 120: 1648-1657.

[38] Niederhauser J. J, Esteller R, Echauz J, Vachtsevanos G, Litt B. Detection of seizure precursors from depth-EEG using a sign periodogram transform .In: IEEE 2003 Biomedical Engineering; 50: 449-458.

[39] Orosco L,Correa A.G,Laciar E.Review:Asurvey of Performance and Techniques for Automatic Eplilepsy Detection. Journal of Medical and Biological Engineering 2013;33:526-537.

Mansour Esmaeilpour

Mansour Esmaeilpour, received the B.S. and M.S. degrees in Computer Engineering-Software Engineering in Iran, in 2002 and 2004, respectively. He also received the Ph.D. degree in Computer Engineering from The National University of Malaysia, in 2012. Currently, he is an assistant professor in Computer Engineering Department at Islamic Azad University, Hamedan Branch, Hamedan, Iran. As well as, he worked from 2013 to 2014 as Postdoctoral Researcher at National University of Malaysia. His research interests include Data mining, Process Mining, Learning Systems and Machine Learning.

Rezvan Abbasi

Rezvan Abbasi received her B.S in Computer Software Engineering and M.S in Computer System Architecture Engineering from Islamic Azad University, Arak Branch, Arak and she is PhD student in Computer System Architecture Engineering in Islamic Azad University, Kerman branch now. Her main research interest is in computer arithmetic, signal processing and Nano-technology Design.

Brain Computer Interface for Micro-controller Driven Robot Based on Emotiv Sensors

Parth Gargava[1], Krishna Asawa[2] *

[1]Centre for Development of Advanced Computing (India)
[2]Jaypee Institute of Information Technology (India)

Received 31 August 2016 | Accepted 1 November 2016 | Published 23 December 2016

Abstract

A Brain Computer Interface (BCI) is developed to navigate a micro-controller based robot using Emotiv sensors. The BCI system has a pipeline of 5 stages- signal acquisition, pre-processing, feature extraction, classification and CUDA inter- facing. It shall aid in serving a prototype for physical movement of neurological patients who are unable to control or operate on their muscular movements. All stages of the pipeline are designed to process bodily actions like eye blinks to command navigation of the robot. This prototype works on features learning and classification centric techniques using support vector machine. The suggested pipeline, ensures successful navigation of a robot in four directions in real time with accuracy of 93 percent.

Keywords

Emotiv, Brain Computer Interface, Support Vector Machine, Robot, Microcontroller.

DOI: 10.9781/ijimai.2017.457

I. Introduction

Brain computer interfaces are systems which act as a communication channel between the human brain and an external device. In the first international meeting on Brain Computer Interface (BCI) technology, BCIs have been de- fined as an aid to users' communication and also control channels which do not vary on the brain's normal output of peripheral nerves and muscles [1]. Brain Computer Interfaces is a growing field which has added a new dimension to Human Computer Interaction. BCI development comes mainly from the concern of creating a novel interaction channel between users, especially those who are unable to control or operate on their muscular movements. The motivation for this proposal is to work for people who have neurological disorder such as Amyotrophic Lateral Sclerosis (ALS) [2], referred to as Lou Gehrig's disease, Dystonia and Ataxia. Patients suffering from such severe disorders are unable to perform any muscular movement and in order to help them, we have devised this prototype which shall help the patients in physical movements in the form of a wheel chair [3]. Brain Computer Interface systems acquire signals in the form of energy potential (electroencephalogram signals) which are processed and sent to an external device. Previously, non-invasive brain computer interfaces' systems have significantly reduced labor and cost, such as in BCI2000 which facilitates applications for various domains such as biomedical engineers, computer scientists, environment and investigators [4]. Another system has been developed which is a software controller that is matched with the individual's residual motor abilities [5]. It was a rehabilitation program carried out in a house-like simulation. In current progress, F.Gallan, M. Nuttin and E. Lew have developed an asynchronous and non-invasive which tested patients through experiments to work on brain computer interface in an environment which is complex and aids sound analysis [6]. In a recent developed system of brain computer interface in the University of Bremen, the makers of the project made a human machine interface (HMI)semi-autonomous robot by the name of FRIEND II which was executed and compiled by the MASSiVE control architecture [7]. Learning from these projects, this paper present a brain computer interface system where we are applying machine learning technique, support vector machine to the visual patterns of the signals to navigate a robot using an Arduino Duemilanove microcontroller [8]. In order to extract signals for the brain computer interface, we use an Emotive Headset which captures neuro-signals [9]. After fetching signals from the brain, we de-noise or filter the noise and unwanted signal interruptions from the input signals. Later we apply Support Vector Machine algorithm to classify signals to intents of our choice in order to navigate a robot. We used an Arduino Duemilanove micro-controller to transfer the output signals in order to control the robot using imagined movements.

* Corresponding author.
E-mail addresses: parthstein@gmail.com (Parth Gargava), krishna.asawa@jiit.ac.in (Krishna Asawa).

II. Related Work

A brief overview of the work and research done on brain computer interface systems helps us gauge the current development.

It has been used in 2003 as a clinical application to study patients with motor impairment [10]. Their objective was to see whether a patient with a severe cerebral palsy was able to control a brain computer interface system. The research concluded with the patients being able to produce distinct EEG patterns with an accuracy of 70 percent. This technique based on EEG biofeedback helped improve actual levels of communication ability for patients with physical disorders. This application with the use of 'tele monitoring- assisted' BCI facilities served as a motivation to complete this project. In 2000, University of California, San Diego conducted a research which explored imagination on mu rhythms and readiness potentials which yielded to major classification using pattern recognition techniques [11].The authors of the research concluded that mu rhythm can not

only be changed or modulated by self-generated movement but by virtually imagining the movement. The study also concludes that self-generated limb actions have distinct properties from single limb movements. Such kind of practical BCI systems use identification and its classifying with pattern recognition techniques.

In the initial days of brain computer interface, volunteers were asked in 2004 to navigate through a 2 dimensional maze using their thought processes which was further aided using high field MRI scanner [12]. The authors understood real time fMRI to construe the spatial distribution of brain functions as commands of brain computer interface. With a high field MRI scanner, activities of the brain were segregated into 4 distinct functional tasks which were translated into commands for four directional cursors. This work helped us in understanding how to divide signals in four patterns.

In 2003, Georgia State university brainLab validated brain computer interface interactions with respect to real life ap- plications such as in communication, creative expression and environment [13]. The authors used methods of Human Com- puter Interaction to train brain computer interface systems to real world scenarios wherein they also discuss challenges of having cumulative BCI outputs with human computer interface paradigms to achieve best interaction. This research used and tested various domains to validate interactions completed by BCI systems. This paper motivated us to improve and enhance the quality of life for those with neurological disorders such as ALS.

BCI2000 was a system developed in 2004 which could conduct multiple applications using one system [4]. Such an application varies on comparisons of different brain signals, algorithms and its output formats. BCI2000 can successfully aid biomedical engineers, computer scientists and people from various professions in the practical usage of an online operation of brain computer interface. Its documentation helped us understand the multi-domain features of existing brain computer interface.

Initially, two macaque monkeys were trained to perform movements related to limbs [14]. Using bilateral electromyography, the authors concluded the presence of a neural representation which can be successfully out in a brain-machine interface. Monkeys have been used in other projects too where they have completed tasks successfully using Brain computer interface systems [15].

In the review of the first international meeting on brain computer interface technology, the members discussed that the pivotal element in every brain computer interface system is the algorithm which converts or translates electro physiological input from a given set of users to control external devices. Existing BCI systems work on the transformation rate of 10- 25 b/min [1] and such achievement can be enhanced using only improved signal processing, user training and more efficient algorithms.

III. Tools and Technology Used

1. Emotiv headset [16]: A sensor headset by Emotiv is used for practical and commercial usage in research applications for brain computer interface. Emotiv heaset in our project is used to detect libraries such as mental commands, and facial expressions. The 14 EEG channel locations are AF3, F7, F3, FC5, T7, P7, O1, O2, P8, T8, FC6, F4, F8, AF4. In our project we used Emotiv headset to measure facial expression in the form of eye blinks.
2. Emotiv control panel: The Headset Setup panel is dis- played by default when starting Emotiv Control Panel. The main function of this panel is to display contact quality feedback for the neuroheadsets EEG sensors and provide guidance to the user in fitting the neuroheadset correctly. It is extremely important for the user to achieve the best possible contact quality before proceeding to the other Emotiv Control Panel tabs. Poor contact quality will result in poor quality EEG signals
3. Emotiv test bench: Real-time display of the Emotiv head- set data stream, including EEG, contact quality, FFT, gyro (if fitted custom option), wireless packet acquisition/loss display, marker events, headset battery level Record and replay files in binary EEGLAB format. Command line file converter included to produce .csv format. Define and insert timed markers into the data stream, including on- screen buttons and defined serial port events. Markers are stored in EEG data file. It is used to check EEG quality by verifying eye blinks and alpha rhythms.
4. Open ViBe [17]: The signals acquired from the sensors are then filtered in Open ViBe scenarios which helps in processing of the input. Open ViBe acts as a base for signal processing of the fetched input.
5. MATLAB [18]: After processing signals we used support vector machine algorithm using LIBSVM library to pro- cess the input signals to intents of our choice. The intents were classified to numerals which help in providing input to Arduino micr-controller.
6. LIBSVM [19]: LIBSVM is an open source machine learning library which is written in C++, and it implements SMO algorithm for kernelised support vector machines for use of classification and regression. An SVM also uses a discriminant hyperplane to identify classes. However, concerning SVM, the selected hyperplane is the one that maximizes the margins, i.e., the distance from the nearest training points (see Figure 1). Maximizing the margins is known to increase the generalization capabilities. As RFLDA, an SVM uses a regularization parameter C that enables accommodation to outliers and allows errors on the training set. Such an SVM enables classification using linear decision boundaries, and is known as linear SVM. This classifier has been applied, always with success, to a relatively large number of synchronous BCI problems. However, it is possible to create nonlinear decision boundaries, with only a low increase of the classifiers complexity, by using the kernel trick. It consists in implicitly mapping the data to another space, generally of much higher dimensionality, using a kernel function K(x, y). The kernel generally used in BCI research is the Gaussian or Radial Basis Function (RBF) kernel.

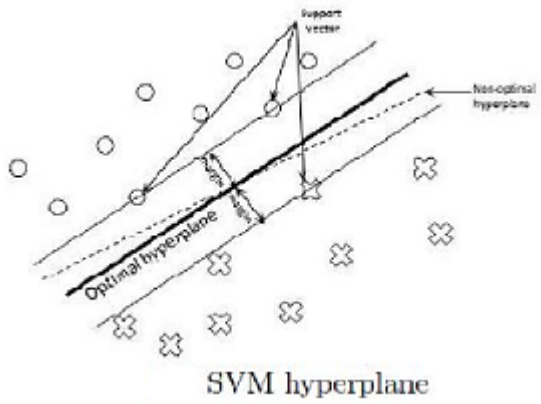

Fig. 1. Support Vector Machine Hyperplane.

7. Arduino Duemilanove [8]: The Arduino Duemilanove is a micro-controller which is powered by any USB connection or with external supply. These kits help in developing digital devices for the physical world. In our project we have developed the micro-controller to build a robot for its navigation using imagined movements.

Fig. 2. Arduino micro-controller.

8. CUDA (Compute Unified Device Architecture)[20]: We used a dll file of CUDA where the code was imported. The CUDA platform was used to enhance the efficacy of the system while using in real time and remove time lag. Our project of a BCI system followed the given chronology for execution:
   - Fetching of signals from Emotiv Epoch sensors:

     Here we use sensors to acquire brain signals (in the form of EEG) which also includes articulates, noise and unwanted elements [21].
   - Filtering and signal processing:

     In order to utilise data received from brain, it is imperative that we remove all noise from the signals which may have come possibly due to sweat, heart beats or hair on the scalp. This achieved using filters in the Open ViBe platform [22].
   - Extraction of significant features:

     This allows significant parts of signals acquired to be discriminated and differentiated from others as features in our Brain Computer Interface system [23].
   - Classification of signals:

     In this process a set of features are assigned classes which can be in correspondence to the navigation required from brain signals.
   - CUDA processing and interfacing:

     In this step we interface all platforms to get the application working, and enhance the speed of the application by interfacing the final end user application on a CUDA platform [20].

Various challenges were faced by us in developing an application based on Brain Computer Interface system such as:

- Acquisition of brain signals from the sensor device Emotiv Epoch requires an expert who has used such sensors before. A key challenge for us was to set up the device in order to get valuable output [9].
- The delay in transmission of messages after classifying was more than 2 seconds (before applying CUDA) which made it difficult for us to read the final output since they were not corresponding to the input we were giving in a real time scenario [24].

IV. Brain Computer Interface System Processing Steps to End User Application

In this section, the paper discusses various steps of a brain computer interface pipeline.

We discuss fetching and acquisition of brain signals in sub-section IV-A, followed by de-noising methods in sub- section IV-B, extraction of valuable features and its classification in sub-section IV-C, subsequent classification of signals in sub-section IV-D.

A. EEG Signal Acquisition Paradigm

Signals are fetched by an Emotiv EPOC [25] which is a wireless and multiple channeled neuro-head-gear which has 14 sensors to detect electric signals detected from brain. It is used to acquire EEG signals. The Emotiv headset follows International10-20 locations: AF3, F7, F3, FC5, T7, P7, O1, O2, P8, T8, FC6, F4, F8, AF4 [26]. A BCI simulator is configured to present the visual stimulus to the user while the EEG data is being collected. The simulator specified the number classes and trials for each class, along with the limits for the duration of trials. For training the classifier, eye movements were defined as the classes and 30 trials were conducted for each class in a random sequence, with each trial lasting from 1.5-3.5 seconds. For collecting labelled EEG data Graz motor Imagery BCI simulator is used which displays certain arrows according to the number of classes defined and on each arrow an intent has to be performed. The acquisition client collected the EEG data while the stimulus was presented to the user using the simulator. Event markers indicate the time instants to mark the beginning and end of trials. The data acquired was passed to a visualizer and also written into a generic stream writer module that dumped the OpenVibe stream to a binary file, with markers indicating the start and end of a trial, the appearance of the arrow and the fixation cross.

B. Pre-processing

For de-noising of data, the emotiv provides software which completes basic signal processing at a threshold frequency of 85Hz, which is then continued by applying a high pass filter with a threshold value of 0.15 Hz. For pre- processing the EEG signals, the Emotiv headset provides basic signal processing which includes low pass filtering of the EEG data with a cut-off frequency at 85 Hz, followed by a high pass filter with a cut-off at 0.16 Hz. Finally, a notch filter is applied at 50-60 Hz is applied to remove the noise due to supply lines interference. Further, our application involves identification of the following intents: eye blinks, right eye wink and left eye wink. These intents are identified by EEG activity in the alpha frequency band, hence we perform band-pass filtering of the EEG signals in the range of 1 to 4 Hz.

In our application, butterworth filter is used for band- passing the signals generated.

A Butterworth filter of order n at threshold frequency D0 has the frequency as depicted in Equation 1.

$$H(u,v) = \frac{1}{1 + \left(\frac{D(u,v)}{D_o}\right)^{2n}} \tag{1}$$

C. Feature Extraction and Classification

This section discusses our feature extraction techniques where we use band power of signals to differentiate signals from each other. The reason why we used band power features and visual patterns against traditional features is given in [27].

Logarithmic value of band power features is taken to derive the EEG signals as X, the feature matrix vector as FV of a size of [channelsX1] is calculated as given in Equation 2.

$$FV[i] = \log(BP_{X^i}) \tag{2}$$

The band-power of the EEG signal is used as a fea- ture, which is simple to compute and computationally inexpensive. Computation of band-power as a feature has been previously used in BCI systems. We compute the band-power features from EEG signals of a trial, represented as a matrix X of size [channelsXsamples] (where channels represent the number of channels of the recorded EEG data and samples is determined by the sampling rate of the EEG acquisition device multiplied by the length of the time window in which the trial data is taken) After obtaining features we used LIBSVM for classification

which is an open-source implementation of Support Vector Machine [28]. There is comparison of classification accuracies using two classifiers: LDA and SVM. In case of multi-class LDA the accuracy is low and so to improve multi-class classification accuracy SVM is used. The trained classifier is used to identify eye blinks in an online session for the subject.

D. Transferring Signals to a Robot

Once we fetched the signals from an acquisition device, and process it on MATLAB, we interface it on a CUDA platform to remove data lag and then navigate a simple robot using Arduino, an open source development plat- form [29]. We accelerated our C++ code by moving the computationally intensive portions of code to an NVIDIA GPU. In addition to providing drop-in library acceleration, we were able to efficiently access the massive parallel power of a GPU with a some syntactic elements and calling functions from the CUDA Runtime API such as global kernel function. In this step we also assigned the final output of the classifier to control an external device. We sent the output to an Arduino which is used to control the movement of a servo motor. After obtaining processed signals from Matlab (with the use of OpenViBe), we use the data to move a simple robot with the help of arduino, an open source development platform . In this project, an Arduino Due Milanove was used with two motors, wheels and wires. The robot followed the output which was fed through MATLAB into the Arduino once a connection was built using a USB cable.

The results and test cases are shown in Table I.

TABLE I
RESULTS AND ACCURACY

TESTs	MODULE	SUCCESS (in %)
0	Acquisition of signals from device	98
1	De-noising and filtering data	100
2	Feature extraction and classification	91
3	Output on Arduino platform through MATLAB	93
5	Overall system	93

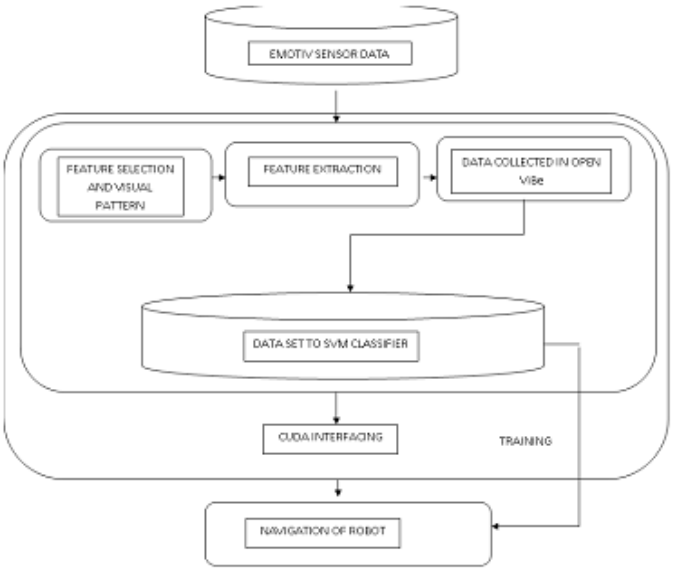

Fig. 3. Process implementation and framework.

V. Result and Accuracy

In this section, we discuss the tests undertaken at each step of the BCI pipeline and detailed summary of test cases:

- Acquisition of signals from device- The input signals were fetched from Emotiv Epoch sensor by 10 users where each one of them took 20 readings each of every intent (left eye blink, right eye blink, both eyes blink, neutral state). Out of the 800 recordings, we were successfully able to catch 785 recordings, which gives us the accuracy of 98 percent.
- De-noising and filtering of data- In this step, we took all 800 signals received by multiple users and converted into meaningful data by applying band pass filter. All signals were successfully de-noised giving us an accuracy of 100 percent.
- Feature extraction and classification- Using band power features, we applied support vector machine algorithm using LIBSVM to classify intents. out of the 800 signals, we were successfully able to classify 730 input signals which gives us an accuracy of 91 percent.
- Output on Arduino platform through MATLAB- After processing and classification, out of the 730 signals which were given as input to the Arduino Due Milanove micro-controller, only 681 signals were converted into successful actions by the robot for navigation. The basic challenge in this step was the interfacing with a considerable time lag (6 seconds) of MATLAB, Arduino platform and Open ViBe in a real time system. This challenge was met by integrating on a CUDA platform which using parallel processing made the system faster by reducing the time lag to 0.5 seconds. The accuracy achieved in this step is 93 percent.
- Over all accuracy of the system is the sum average of all above mentioned accuracies ie. 95 percent. This result is discussed in Table 1.

VI. Conclusion and Future Work

This project provides a real-time, easy to use imple- mentation of a Brain Computer Interface system which can identify multiple states without a time lag of more than 0.5 seconds. This system does not require individual training, and has high accuracies in achieving classifica- tion. Its future work involves development of medical aid for those with neurological diseases based on EEG signals for different intents.

Acknowledgment

This work would not have been possible without the support of Centre for Development of Advanced Computing, Noida for their help in the usage of Emotiv headset.

References

[1] Jonathan R Wolpaw, Niels Birbaumer, William J Heetderks, Dennis J McFarland, P Hunter Peckham, Gerwin Schalk, Emanuel Donchin, Louis A Quatrano, Charles J Robinson, Theresa M Vaughan, et al.Brain-computer interface technology: a review of the first international meeting. IEEE transactions on rehabilitation engineering, 8(2):164–173, 2000.

[2] Amyotrophic Lateral Sclerosis ALS. Amyotrophic lateral sclero- sis (als). 2007.

[3] John T Dimos, Kit T Rodolfa, Kathy K Niakan, Laurin M Weisenthal, Hiroshi Mitsumoto, Wendy Chung, Gist F Croft, Genevieve Saphier, Rudy Leibel, Robin Goland, et al. Induced pluripotent stem cells generated from patients with als can be differentiated into motor neurons. science,321(5893):1218–1221, 2008.

[4] Gerwin Schalk, Dennis J McFarland, Thilo Hinterberger, Niels Birbaumer, and Jonathan R Wolpaw. Bci2000: a general-purposebrain-computer interface (bci) system. Biomedical Engineering, IEEE Transactions on, 51(6):1034–1043, 2004.

[5] Febo Cincotti, Donatella Mattia, Fabio Aloise, Simona Bufalari, Gerwin Schalk, Giuseppe Oriolo, Andrea Cherubini, Maria Grazia Marciani, and

Fabio Babiloni. Non-invasive brain–computer interface system: towards its application as assistive technology. Brain research bulletin, 75(6):796–803, 2008.

[6] Ferran Galan,´ Marnix Nuttin, Eileen Lew, Pierre W Ferrez, Gerolf Vanacker, Johan Philips, and J del R Millan´. Abrain-actuated wheelchair: asynchronous and non-invasivebrain–computer inter- faces for continuous control of robots. Clinical Neurophysiology, 119(9):2159–2169, 2008.

[7] Diana Valbuena, Marco Cyriacks, Ola Friman, Ivan Volosyak, and Axel Graser. Brain-computer interface forhigh-level control of rehabilitation robotic systems. In Rehabilitation Robotics, 2007. ICORR 2007. IEEE 10th International Conference on, pages 619– 625. IEEE, 2007.

[8] Alicia M Gibb. New media art, design, and the Arduino micro- controller: A malleable tool. PhD thesis, Pratt Institute, 2010.

[9] Matthieu Duvinage, Thierry Castermans, Mathieu Petieau, Thomas Hoellinger, Guy Cheron, and Thierry Dutoit. Perfor- mance of the emotiv epoc headset for p300-based applications. Biomed Eng Online, 12:56, 2013.

[10] C Neuper, GR Muller,¨ A Kubler,¨ N Birbaumer, and G Pfurtscheller. Clinical application of an eeg-based brain– computer interface: a case study in a patient with severe motor impairment. Clinical neurophysiology, 114(3):399–409, 2003.

[11] Jaime A Pineda, BZ Allison, and A Vankov. The effects of self- movement, observation, and imagination on rhythms and readi- ness potentials (rp's): toward a brain-computer interface (bci). Rehabilitation Engineering, IEEE Transactions on,8(2):219–222, 2000.

[12] Seung-Schik Yoo, Ty Fairneny, Nan-Kuei Chen, Seh-Eun Choo, Lawrence P Panych, HyunWook Park, Soo-Young Lee, and Ferenc A Jolesz. Brain–computer interface using fmri: spatial navigation by thoughts. Neuroreport, 15(10):1591–1595, 2004.

[13] Melody M Moore. Real-world applications for brain-computerinterface technology. Neural Systems and Rehabilitation Engi- neering, IEEE Transactions on, 11(2):162–165, 2003.

[14] Karunesh Ganguly, Lavi Secundo, Gireeja Ranade, Amy Ors- born, Edward F Chang, Dragan F Dimitrov, Jonathan D Wallis, Nicholas M Barbaro, Robert T Knight, and Jose M Carmena. Cortical representation of ipsilateral arm movements in monkey and man. The Journal of Neuroscience, 29(41):12948–12956, 2009.

[15] Michele Baum. Monkey uses brain power to feed itself with robotic arm. Pitt Chronicle. http://www. chronicle. pitt. edu, 2008.

[16] Matthieu Duvinage, Thierry Castermans, Thierry Dutoit, M Petieau, T Hoellinger, C De Saedeleer, K Seetharaman, and G Cheron. A p300-based quantitative comparison between a medical eeg device and emotive headset.

[17] Yann Renard, Fabien Lotte, Guillaume Gibert, Marco Congedo, Emmanuel Maby, Vincent Delannoy, Olivier Bertrand, and Ana- tole Lecuyer´. Openvibe: an open-sourcesoftware platform to design, test, and use brain-computerinterfaces in real and virtual environments. Presence: teleoperators and virtual environments, 19(1):35–53, 2010.

[18] Duane Hanselman and Bruce C Littlefield. Mastering MATLAB 5: A comprehensive tutorial and reference. Prentice Hall PTR, 1997.

[19] C Chang and C Lin. fLIBSVMg: a library for support vector machines (version 2.3). 2001.

[20] CUDA Nvidia. Compute unified device architecture programming guide. 2007.

[21] Benjamin Blankertz, Guido Dornhege, Matthias Krauledat, Klaus- Robert Muller,¨ and Gabriel Curio. The non-invasive berlin brain– computer interface: fast acquisition of effective performance in untrained subjects. NeuroImage, 37(2):539–550, 2007.

[22] Ali Bashashati, Mehrdad Fatourechi, Rabab K Ward, and Gary E Birch. A survey of signal processing algorithms in brain– computer interfaces based on electrical brain signals. Journal of Neural engineering, 4(2):R32, 2007.

[23] Vladimir Bostanov. Bci competition 2003-data sets ib and iib: feature extraction from event-related brain potentials with the con- tinuous wavelet transform and the t-value scalogram. Biomedical Engineering, IEEE Transactions on, 51(6):1057–1061, 2004.

[24] Gopal Santhanam, Stephen I Ryu, M Yu Byron, Afsheen Afshar, and Krishna V Shenoy. A high-performancebrain–computer interface. nature, 442(7099):195–198, 2006.

[25] Robert Lievesley, Martin Wozencroft, and David Ewins. The emotiv epoc neuroheadset: an inexpensive method of controlling assistive technologies using facial expressions and thoughts?Journal of Assistive Technologies, 5(2):67–82, 2011.

[26] Richard W Homan, John Herman, and Phillip Purdy. Cerebral location of international 10–20 system electrode placement. Elec- troencephalography and clinical neurophysiology, 66(4):376–382, 1987.

[27] George Townsend, Bernhard Graimann, and Gert Pfurtscheller. A comparison of common spatial patterns with complex band power features in a four-class bci experiment. Biomedical Engineering, IEEE Transactions on, 53(4):642–651, 2006.

[28] Chih-Chung Chang and Chih-Jen Lin. Libsvm: a library for support vector machines. ACM Transactions on Intelligent Systems and Technology (TIST), 2(3):27, 2011.

[29] Michael Margolis. Make an Arduino-controlled robot. " O'Reilly Media, Inc.", 2012.

Parth Gargava

Parth Gargava is Research and Development Engineer at Centre for development of Advanced Computing. He is also Vice President from Jaypee Institute of Inormation Technology, Student Council. He got is bachelor degree in Technologi at Jaypee institute of information technology. He is currently working in his doctoral thesis.

Dr. Krishna Asawa

Dr. Krishna Asawa working with Jaypee Institute of Information Technology, Noida, India since 2003. During her teaching career of about 16 years, she pursued and experienced teaching subjects like Data Structures, Algorithm Analysis and Design, Artificial Intelligence, Soft Computing, Distributed Databases, Computer Architecture and Organization, Logic Programming, Theory of Computation, Database System, Human Computer Interaction, Cryptography, Management Information System. Apart from teaching, she is an active researcher and currently advisor of 4 research scholars. She is also a member of technical program committee of referred Journals and Conference Proceedings. She is actively involved in curriculum planning, syllabus design, editing and reviewing text books at an engineering graduate level. She has been an organizing member of workshops and conferences, organized by the CSE department of JIIT. She has also served as an external examiner and adjunct instructor at the other Universities.

Diagnosis of Malignant Melanoma of Skin Cancer Types

Abbas H. Hassin Alasadi, Baidaa M. Alsafy *

Department of Computer Science at Basra University, Basra (Iraq)
Computer Science Department, Science College, ThiQar University, ThiQar (Iraq)

Received 26 June 2016| Accepted 1 November 2016 | Published 23 December 2016

Abstract

Malignant melanoma is a kind of skin cancer that begins in melanocytes. It can influence on the skin only, or it may expand to the bones and organs. It is less common, but more serious and aggressive than other types of skin cancer. Malignant Melanoma can happen anywhere on the skin, but it is widespread in certain locations such as the legs in women, the back and chest in men, the face, the neck, mouth, eyes, and genitals. In this paper, a proposed algorithm is designed for diagnosing malignant melanoma types by using digital image processing techniques. The algorithm consists of four steps: preprocessing, separation, features extraction, and diagnosis. A neural network (NN) used to diagnosis malignant melanoma types. The total accuracy of the neural network was 100% for training and 93% for testing. The evaluation of the algorithm is done by using sensitivity, specificity, and accuracy. The sensitivity of NN in diagnosing malignant melanoma types was 95.6%, while the specificity was 92.2% and the accuracy was 93.9%. The experimental results are acceptable.

Keywords

Malignant Melanoma; Preprocessing; Separation; Feature Extraction; Diagnosis.

DOI: 10.9781/ijimai.2017.458

I. Introduction

The abnormal growths of melanocytes cause malignant melanoma skin cancer, which invades or spreads to other parts of the body without normal controls; malignant melanoma divided into four types, which are classified by their histologic features and are listed according to their frequency of occurrence [1, 2]:

A. Superficial Spreading Melanoma

SSMM is the most popular kind of malignant melanoma, which effects on all ages. It may occur on any part of the body and it is usually found on the legs of women and the trunk of men, it is usually greater than 0.5cm in diameter. It usually develops as an asymmetric plague with variation in color such as black, red, brown, blue, and white as pigment pattern and irregularity (notching of borders), see Fig.1(a).

B. Nodular Malignant Melanoma

NMM typically presents as dome-shaped dark brown or black nodule that ulcerates and bleeds, it is less common but more malignant. It is most commonly found on the trunk, although anybody site can be affected, including covered areas such as the axillae and buttocks. Recognition may be delayed because an irregular edge and multiple colors are often absent. The outline of the lesion may be irregular and its color varied. Often, it will have a well-defined border and symmetry in contract to other melanoma, see Fig.1 (b).

* Corresponding author.
E-mail addresses: abbashh2002@gmail.com, abbas.hassin@uobasrah.edu.iq (Abbas H. Hassin Alasadi), baidaalsafi@yahoo.com (Baidaa M.Alsafy).

C. Lentigo Malignant Melanoma

LMM is a specific type of malignant melanoma that develops in chronically sun-exposed areas, particularly the face, in the elderly; varying admixtures of pink, gray, blue, and white represent it. The borders are frequently highly irregular and notched. The overall size may range from 1.0 to 20.0 cm or larger. Begins as a macule with tan color that spreads peripherally with gradual mixed darkening and become palpable, as a papule, nodule or plaque and transformed into LM melanoma darken [3], see Fig.1 (c).

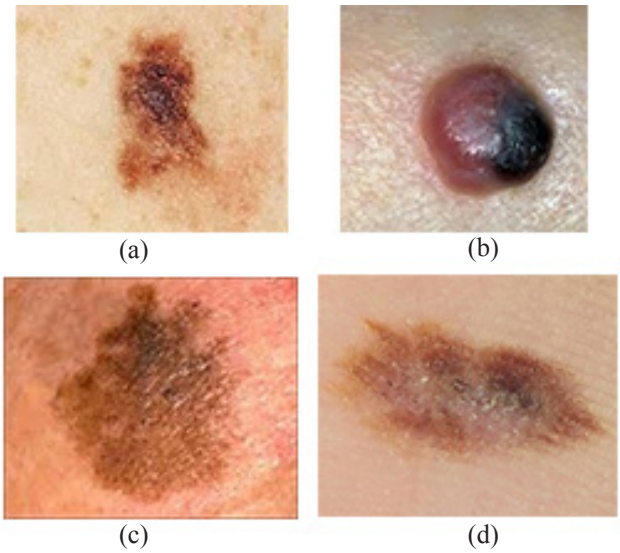

Fig. 1. Malignant Melanoma Types. (a) Superficial Spreading Melanoma. (b) Nodular Melanoma (c) Lentigo malignant Melanoma. (d) Acral Lentiginous Melanoma.

D. Acral Lentiginous Melanoma

Acral and nail malignant melanoma is a very rare lesion. It usually arises in an acral location or on a mucous membrane and is initially flat and irregular, but soon becomes raised and subsequently nodular, borders may show marked irregularity and notching. The size ranges from 0.9 to 12 cm or greater. Advanced lesions exhibit raised papules or nodules that are blue, black or amelanotic and often ulcerated. It usually starting under the cuticle and producing pigmented streak in the nail plate2, see Fig.1 (d).

II. The Proposed Algorithm

This section gives a general view of the proposed algorithm for diagnosis malignant melanoma skin cancer. The structure of the proposed algorithm is shown in Fig. 2.

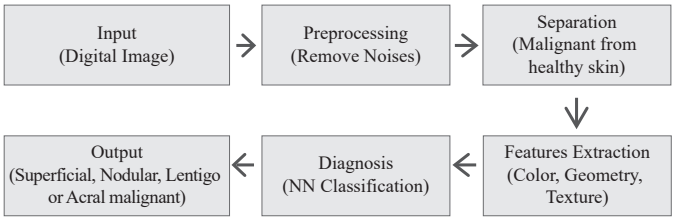

Fig. 2. The essential steps of the proposed algorithm.

Logically, the first step of the classification of malignant melanoma of skin cancer system is the input image. Image in digital format is given as an input to the system. Next step, is the preprocessing which includes noises removal. Median [4] and Gaussian Filtering [5] remove the noises. After filtering, the image is subjected to separation step that separates the malignant lesion from normal skin. Some unique features distinguish the malignant melanoma of skin cancer types. The feature extraction techniques used here are color features; texture features and shape features. The selected features are given as the input to Neural Network classifier (NN) which classifies the given datasets into malignant melanoma types.

A. Preprocessing

In this paper, the images databases of melanoma skin cancer are obtained from the Lloyd Dermatology and Laser Center6. This database contains about 200 color images for malignant melanoma of skin cancer. Images are captured in the JPEG format, with maximum resolution size 481x734 pixels, which were later resized to 256 x 512 pixels. The aim of the preprocessing step is to enhance the images and remove noises using Median and Gaussian Filtering, then apply contrast enhancement which sharpen the image border and improve the accuracy for separation. A Gaussian filter was used on the image to reduce the noise; Gaussian filter is a low pass filter that suppresses high frequency detail while preserving the low frequency components of the image. A sigma value of 0.5 was chosen to enable noise filtering while still keeping the edge components of the image.

Median Filtering is an image filtering method that makes the skin cancer image smoother. In which each pixel value in an image is exchanged with the median value of its neighboring pixels including itself. To reduce the noise while keeping the edges, the median filter is applied. It is used for decreasing the effect of small structures such as thin hair and separated unwanted pixels such as air bubbles. In order to have preferable performance and get high contrast for the image .We use image adjustment that removes the unwanted part of the image that came from some noises. The result improved the shape and edges of image. Additionally, contrast enhancement can sharpen the border of image and raise the accuracy for separation see Fig. 3.

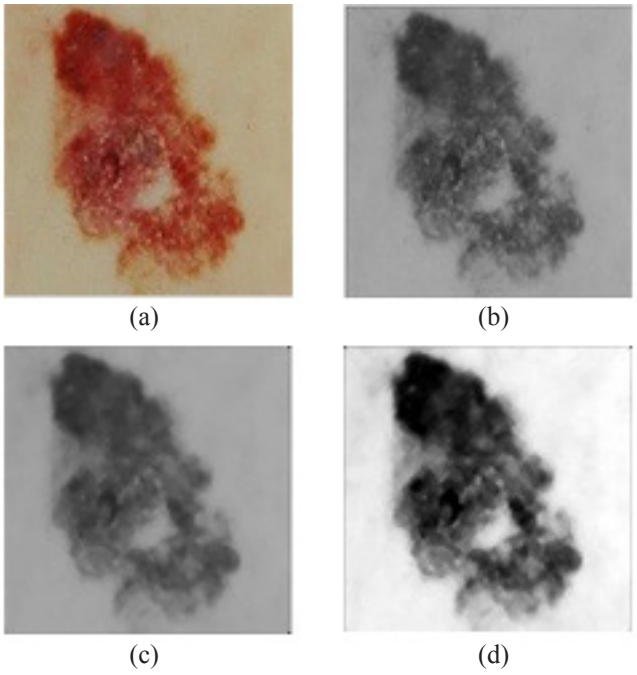

Fig.3. Sample of malignant melanoma images after applying the preprocessing steps. (a) Original image. (b) Applying Gaussian filter. (c) Applying median filter. (d) After image adjustment.

B. Skin Lesion Separation

In this paper, we must separate skin lesion in color images to extract color features, and gray level images to extract texture features so skin lesion separation stage pass into two stages:

C. Skin Lesion Separation for Color Images

The main steps for lesion separation can be categorized into four sections: (1) Thresholding and converting to binary image (2) Finding of initial point (3) Traced boundary (4) Detected skin lesion shows the results separation step. Fig. 4. shows example of all steps the results separation. Algorithm (1) describes the steps of lesion separation algorithm.

Algorithm (1): Lesion Separation for color image.

Input: Color image after preprocessing step.

Output: Color image with detecting lesion.

Step1: Converting color image into gray level image with increasing the contrast of the output image using image adjustment.

Step2: Using gray thresholding, which computes a global threshold that can be used to convert an intensity image to a binary image.

Step3: Detect the size of binary images, which returns the sizes of each dimension.

Step4: Returns an array of 1s that is the same size as image using ones which returns an n-by-n matrix of 1s.

Step5: Inverting between binary image and the result of step4.

Step6: Finding of initial point by detecting the point between row and column (detect the point in row and detect the point in column) in binary image.

Step7: Trace boundary of image by applies bwtraceboundary, which traces the outline of an object in binary image, then display traced boundary to color image to detect lesion.

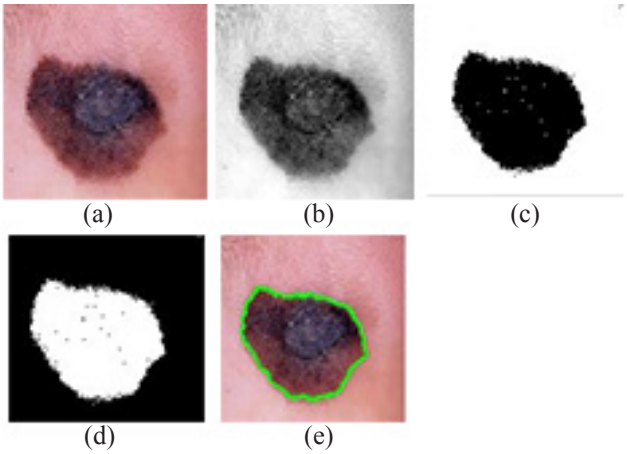

Fig. 4. Example of the main lesion separation steps. (a) Original image. (b) Converting into gray level with increasing the contrast. (c) Applying Thresholding and converting to binary image. (d) Inverting binary image. (e) Traced boundary and detected lesion.

D. Skin Lesion Separation for Gray Level Images

The main steps for lesion separation can be categorized into four sections (1) thresholding (2) morphological operation (3) border detection (4) lesion extraction. Fig. 5 shows the results separation step. Algorithm (2) describes the steps of lesion separation algorithm.

***Algorithm** (2): Lesion Separation for Gray Level Image.*

Input: Gray level image after preprocessing step.

Output: Gray level image contain lesion only.

*Step1: The gray level image is of the size (256*512).*

Step2: Thresholding was used, the pixels of image (C) less than 100 equals to Zero (C(C<100) =0).

Step3: Create Binary image with some unwanted pixels.

Step4: Remove unwanted pixels from binary image that have fewer than (400) unwanted pixels, producing another binary image without unwanted pixels.

Step5: Clear the image border, which suppresses structures that are lighter than their surroundings and that are connected to the image border.

Step6: Filling the holes in the binary image.

Step7: Remove unwanted pixels from binary image that have fewer than (200) unwanted pixels, producing another binary image without unwanted pixels.

Step8: Perform closing morphological with the structuring element as a disk shape of size=1 on the binary image.

Step9: Filling the holes in the binary image.

Step10: Convert the input gray level image into unsigned 8-bit integers.

Step11: Convert the image that results of the step10 into unsigned 8-bit integers.

Step12: Multiplies each element in array (image result from step 10) by the corresponding element in array (image result from step 11) and regains the result in the corresponding element of the output array.

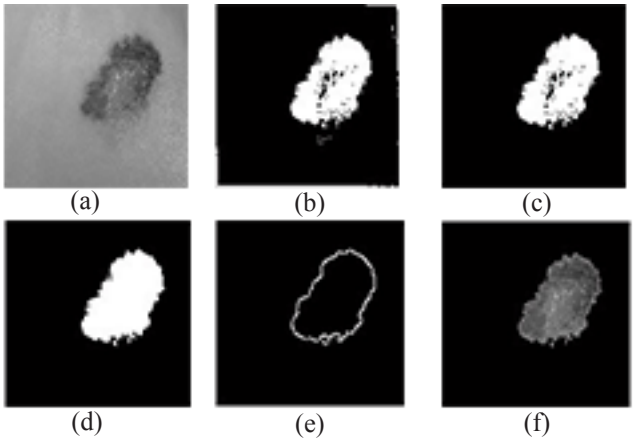

Fig. 5. Example of the main lesion separation steps. (a) Image after preprocessing. (b) Applying Thresholding and converting to binary image. (c) Remove unwanted pixels. (d) Apply morphological operation. (e) Detect border. (f) Lesion separation.

E. Feature Extraction

These features are selected for distinguish malignant melanoma types. Three feature extraction types are proposed here; color, geometry and texture features see Fig. 6.

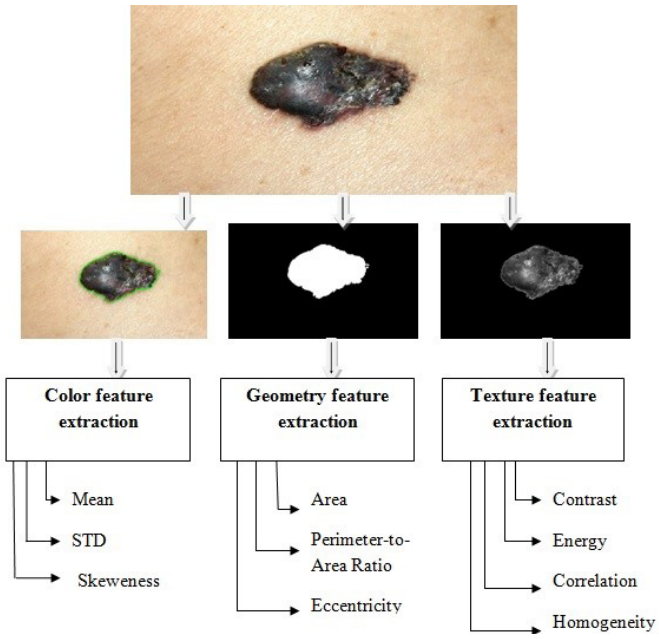

Fig. 6. Feature extraction to classification malignant melanoma types.

F. Color Features

The color features include; mean, skewness, and standard derivation. These features extract the Color Moment (CM) descriptor proposed in [7]. The common moments are mean, standard deviation, and skewness; the corresponding calculation can be defined as follows respectively:

$$\mu_i = \frac{1}{N}\sum_{j=1}^{N} f_j \tag{1}$$

$$\sigma_i = \left(\frac{1}{N}\sum_{j=1}^{N}\left(f_j - \mu_i\right)^2\right)^{\frac{1}{2}} \tag{2}$$

$$\gamma_i = \left(\frac{1}{N} \sum_{j=1}^{N} \left(f_j - \mu_i \right)^3 \right)^{\frac{1}{3}} \quad (3)$$

Where f_{ij} is the color value of the i[th] color component of the jth image pixel and N is the total number of pixels in the image. $\mu_i, \sigma_i, \gamma_i$ (i=1,2,3) denote the mean, standard deviation, and skewness of each channel of an image respectively. Algorithm (3) describes the steps of color features extraction algorithm.

Algorithm (3): Color features extraction

Input: Color image for malignant melanoma.

Output: Color features vector.

Step1: Convert the RGB color map into an HSV color map. The column of the output matrix represents Hue, Saturation, and Value respectively.

Step2: Compute mean for each H, S, and V channel as in (1).

Step3: Compute standard derivation for each H, S, and V channel as in (2).

Step4: Compute skewness for each H, S, and V channel as in the (3).

G. Geometry Features

The geometry features include Area of the lesion, Perimeter-to-Area Ratio of the lesion and, Eccentricity. We divide the perimeter by area using the hypothesis that a lesion with a large perimeter-to-area ratio will likely have a jagged boundary, while a pigmented lesion with a small perimeter-to-area ratio will likely have smoothed edge. Eccentricity is defined as the ratio of the Eigen values of the covariance matrix that corresponds to a binary image of the shape. To calculate eccentricity we have to computes the ratio of the distance between the foci of the ellipse fitted to the shape and its major axis length. The output is between 0 and 1, with 0 representing a circle and 1 a line. Algorithm (4) describes the steps of geometry features algorithm.

Algorithm (4): Compute Geometry Features.

Input: Binary image which results from separation step after apply morphological operation.

Output: Geometry features vector.

Step1: Compute the area of the lesion.

Step2: Compute the perimeter of the lesion using compute the distance around the boundary of the region.

Step3: Compute the perimeter-to-area ratio by divided the perimeter to area.

Step4: Compute the eccentricity, which is the ratio of the distance between the foci of the ellipse and its major axis length.

H. Texture Features

The texture features consist of contrast, correlation, energy, and homogeneity. All are computed from GLCM proposed in [8] for the four directions (0, 45, 90, and135) to gray level image of malignant melanoma. These features are described as below:

Contrast measures the amount of local variations in an image.

$$\text{Contrast} = \sum_i \sum_j (\text{i - j})^2 P(i, j) \quad (4)$$

Correlation is a measurement of gray tone linear dependencies in the image.

$$\text{Correlation} = \frac{\left(\sum_i \sum_j (\text{i - j})^2 P(i, j) \right) - \mu_x \mu_y}{\sigma_x \sigma_y} \quad (5)$$

Energy is a measurement of texture uniformity of an image, the more homogeneous the image, the larger the value.

$$\text{Energy} = \sum_i \sum_j P(i, j)^2 \quad (6)$$

Homogeneity is a measurement of the amount of local uniformity present in the image.

$$\text{Homogeneity} = \sum_i \sum_j \frac{P(i, j)}{1 + |i - j'|} \quad (7)$$

Algorithm (5) used to extract texture feature from gray level Co-occurrence matrix for gray level image.

Algorithm (5): Compute Texture Feature

Input: Gray level image, which results from the last step of lesion segmentation.

Output: Texture features vector.

Step1: Resize the entire image to size 128 * 128.

Step2: Compute the size of gray level image.

Step3: Compute GLCM to the gray level image with four off set (0, 45, 90, and 135). The GLCM creates by calculating how predominating a pixel with gray level (grayscale intensity) value i occurs horizontally adjacent to a pixel with the value j. (You can allocate other pixel spatial relationships using the 'Offsets' parameter (0, 45, 90, and 135). Each element (i , j) in GLCM assigns the number of times that the pixel with value i occurred horizontally adjacent to a pixel with value j.

Step4: Initialize Matrices at each edge (0, 45, 90, 135) to zero G0= G1= G2= G3= zeros.

Step5: Compute the texture feature to GLCM contrast, correlation, energy, and homogeneity for each angle as in (4), (5), (6), and (7) respectively.

After extract the three types of features malignant melanoma images, combine in one vector to use in the diagnosis step to recognize among malignant melanoma types, you must refer that features extraction step make in training and testing phases.

I. Diagnosis

The last step of the proposed algorithm is diagnosis malignant melanoma types, after obtained features vector and store it, the diagnosis step is followed, in this paper, we use neural network to diagnoses among malignant melanoma types.

Algorithm (6): NN Classification

Input: A vector of features (28 features).

Output: Total accuracy from the NN.

Step1: Create feed forward neural network with three hidden layers, number of neuron in each hidden layer 150, 160,170 respectively, these number of layers are chosen after experiment (try and error), input layer for creating neural network is identified by characteristics of inputs. We have twenty eight features vector. Therefore, the number of neuron in input layer is twenty eight, and out layer neuron determined by number of class, we have four classes (malignant melanoma types) therefore the number of neuron in output layer is four.

Step2: Determine the important parameter, learning rate equal to 0.00001, epochs equal to 1000, maximum number of iterations, training time infinity, data division function (divide rand), transfer function of i^{th} layer hyperbolic tangent sigmoid transfer function is used 'tansig', linear activation function is selected for output layer 'purelin' , performance function, default = 'mse

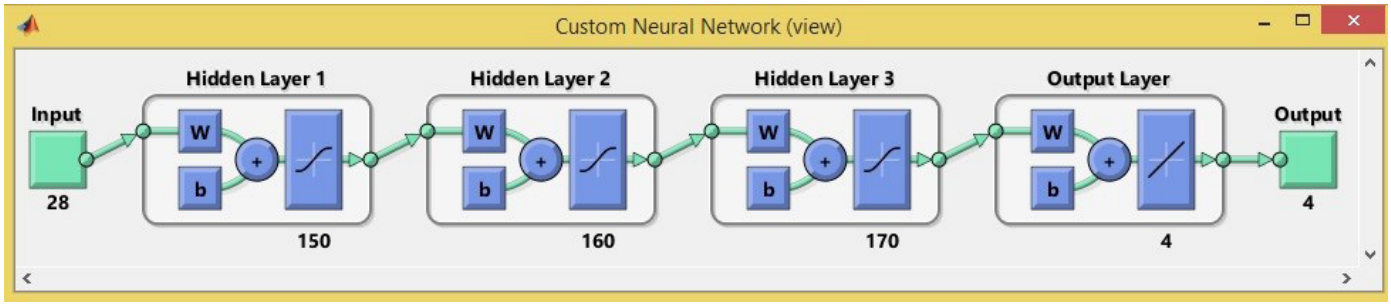

Fig. 7 Structure of neural network.

'and training function is back propagation function, weight and bias is generating randomly. These parameters are chosen in our work because it makes the NN gives effective results.

Step3: Training the network with train data and target matrix, target matrix is matrix with four row and four column, each row consists of vector of zero values except a 1 in element `i`, where `i` is the class they are to perform.

Step4: Simulates the neural network by taking the initialized net and network input matrix (train data), return the indices to the largest output as class predict.

Step5: Compute the network performance.

Step6: Compute the network accuracy using confusion matrix.

Step7: Simulates the neural network by taking the training net and test data with target, return the indices to the largest output as class predict.

Step8: Compute the network performance.

Step9: Compute the network accuracy.

Fig. 7. shows the network structure with one input layer, three hidden layers and four output layers. It is 28×150×160×170×4 network structure. The input vector is twenty eight. The output vector is four. This thesis uses the above ANN architecture, feed forward back propagation learning algorithm to generate, train and test the neural network for malignant melanoma type's diagnosis. MATLAB software with its neural network toolbox is used. Data sets are portioned into two subsets, training set and testing set. The network gives high accuracy when train equal to 100% and test equal to 93% with best training performance is 3.8831e-014 at epoch 60.

The obtained results from training NN on 100 cases are 100%. When we test the NN on 100 cases for malignant melanoma types (Twenty five for each type), we found that seven of these cases fail in testing. Therefore, the accuracy of the system is 93%.

Table I and Table II illustrate the classification results of NN for types of melanoma skin cancer in training and testing stages.

TABLE I
CLASSIFICATION RESULTS FROM NN FOR MALIGNANT MELANOMA LESIONS IN TRAINING STAGE

Malignant Melanoma lesions	Classification Result (%)
Superficial Malignant Melanoma	100
Lentigo malignant melanoma	100
Nodular Malignant Melanoma	100
Acral Malignant Melanoma	100

TABLE II
CLASSIFICATION RESULTS FROM NN FOR MALIGNANT MELANOMA LESIONS IN TESTING STAGE

Malignant Melanoma lesions	Classification Result (%)
Superficial Malignant Melanoma	92
Lentigo malignant melanoma	96
Nodular Malignant Melanoma	92
Acral Malignant Melanoma	92
The accuracy for all types	93

III. PERFORMANCE EVALUATION MEASURES

The proposed system performance is evaluation by expressions of sensitivity, specificity, and accuracy. The three expressions determined as follow [9]:

- *Sensitivity* is used to measure the ratio of positives that are correctly identified; the result denotes positively (disease). It is computed as the following equations:

$$Sen. = \frac{TP}{(TP + FN)} * 100\% \tag{8}$$

- *Specificity* is used to measure the ratio of negatives that are correctly identified; the result denotes negatively (non-disease). It is computed as the following equations:

$$Spec. = \frac{TN}{(TN + FP)} * 100\% \tag{9}$$

- *Accuracy* is used to measure the eventuality that the diagnostic test is performed correctly. It is computed as in the following equations:

$$Accur. = \frac{(TP + TN)}{TP + TN + FP + FN} * 100\% \tag{10}$$

Where TP is True Positives that correctly diagnosed positive cases; TN is True Negative that correctly diagnosed negative cases, FP is False Positives that incorrectly diagnosed negative cases, and FN is False Negative that is incorrectly diagnosed positive cases.

The performance measure to the diagnosis malignant melanoma types is done by the expressions of sensitivity, specificity, and accuracy that are computed for ANN classification using (8), (9), and (10) respectively.

Table III and Table IV show the performance evaluation results of all experiment to diagnosis malignant melanoma types in training and testing stages.

TABLE III
TRAINING PERFORMANCE MEASURE

Data Type	Sensitivity%	Specificity%	Accuracy %
Suprfical Malignant Melanoma	100	100	100
Lentigo Malignant Melanoma	100	100	100
Nodular Malignant Melanoma	100	100	100
Acral Malignant Melanoma	100	100	100

TABLE IV
TESTING PERFORMANCE MEASURE.

Data Type	Sensitivity%	Specificity%	Accuracy %
Superficial Malignant Melanoma	95.6	92.2	93.9
Lentigo Malignant Melanoma	89.6	95.6	92.4
Nodular Malignant Melanoma	92.0	92.0	92.0
Acral Malignant Melanoma	95.6	92.2	93.9

IV. CONCLUSIONS

The work in the field of melanoma of skin cancer detection is difficult because of the different circumstances in which the images were taken, the multiplicity of devices used in obtaining the images and the distortions that occur in the stage of obtaining the images. The proposed algorithm that used in this paper encouraging results in terms of time that taken in the recognition based on neural network to diagnose malignant melanoma types. Early melanoma skin cancer diagnostic system using computer-based techniques is more efficient than the conventional biopsy methods. The cost involved as well as the time taken for detection is less in this proposed methodology. This system will be a great help in early detection of malignant melanomas for faster, cheaper, more intuitive and efficient treatment. The proposed method has an accuracy of 93% for recognition malignant melanoma types, which is much higher than that of conventional methods.

REFERENCES

[1] J. William, T. Berger, and D. Elston, Andrews' diseases of the skin: clinical dermatology, Elsevier Health Sciences, 2015.

[2] National Comprehensive Cancer Network, Melanoma, NCCN Guidelines for Patients, Version 1, 2014.

[3] K. Cheung, "Image Processing for Skin Cancer Detection: Malignant Melanoma Recognition", M.Sc. Thesis, Graduate Department of Electrical and Computer Engineering University of Toronto, 1997.

[4] G. Gupta, "Algorithm for image processing using improved median filter and comparison of mean, median and improved median filter. "International Journal of Soft Computing and Engineering 1.5 (2011): 2231-2307.

[5] H. Zhou, J. Wu and J. Zhang, Digital Image Processing part II, Bookboon, 2010.

[6] Melanoma Database: http://www.lloydderm.com

[7] D. Ping Tian, ''A Review on Image Feature Extraction and Representation Techniques", International Journal of Multimedia and Ubiquitous Engineering8.4 (2013): 385-396.

[8] E. Alaa, and H. Demirel, "Co-occurrence matrix and its statistical features as a new approach for face recognition." Turkish Journal of Electrical Engineering & Computer Sciences 19.1 (2011): 97-107.

[9] S. Mariam, S. Mabrouk, and A. Sharawy, "Automatic detection of melanoma skin cancer using texture analysis." International Journal of Computer Applications 42.20 (2012): 22-26.

Abbas H. Hassin Alasadi

Abbas H. Hassin Alasadi is Assistant Professor and Postgraduate Program Coordinator of the Department of Computer Science at Basra University. He received his PhD degree from School of Engineering and Computer Science / Harbin Institute of Technology, China. He spent more than ten years as Assistant Professor at different Universities abroad the current position. His research interests include Medical Image processing, Biometrics, Information retrieval, and Human-computer interaction. His research work have published in various international journals and conferences.
Dr. Abbas is an active reviewer in many journals of the areas of computer science and software engineering. He is one of ACIT,UJCS, and IJPRAI members.

Baidaa M. Alsafy

Lecturer at the Computer Science Department, Science College, ThiQar University, ThiQar, Iraq. She received her BSc from ThiQar University in Computer Science major. In 2015, she finished her MSc from Basra University. Her research interests include Biometrics and image processing.

A Revision of Preventive Web-based Psychotherapies in Subjects at Risk of Mental Disorders

Teresa Sánchez-Gutiérrez, PhD[1,2]; Sara Barbeito, PhD[1]; and Ana Calvo, PhD[1] *

[1]Facultad de Ciencias de la Salud. Universidad Internacional de la Rioja (UNIR) (Spain)
[2]Department of Methodology and Behavioural Sciences. National Distance Education University (UNED) (Spain)

Received 21 December 2016 | Accepted 1 November 2016 | Published 23 December 2016

Abstract

For the last years, the impulse of new technologies has overcome the traditional pathways of face-to-face clinical intervention and web-based psychological methodologies for intervention have started to gain success. This study aims to review the state-of-art about the effectiveness studies on preventive web-based interventions accomplished in samples of subjects at high risk for depressive, anxiety, eating behavior, problematic substance use symptoms and promotion of psychological well-being. Results showed that web-based psychological interventions for the prevention of mental disorders seemed to be effective for at risk individuals. Online health promotion in the general population was also effective to avoid the onset of clinical psychological circumstances. Future research should focus on personalized online intervention and on the evaluation of web-based engagement.

Keywords

High-risk, Online Psychotherapy, Prevention, Web-based Intervention.

DOI: 10.9781/ijimai.2017.459

I. Introduction

Psychotherapeutic treatments are well established and have been recommended as the first option interventions, either independently or as pharmacological treatment coadyuvant, for the treatment of a wide range of mental disorders. This fact is included in recognized worldwide associations, protocols and guidelines such as APA [1] and NICE [36].

For the last years, the impulse of new technologies has overcome the traditional pathways of face-to-face clinical intervention and web-based psychological methodologies for intervention have started to gain success [31]. Neither are they a replacement of traditional psychotherapy, but indeed they has become a complementary intervention since online therapy could maximize the population scope [6]. Internet therapies can offer scalable approaches whereby large numbers of people can receive treatment and/or prevention, potentially bypassing barriers related to cost, location, lack of trained professionals, and stigma [3], [11]. However, despite the robust rationale and promising evidence, relatively few research has being conducted in healthy populations and in preventive health studies in individuals at risk of mental disorders.

This study aims to review the state-of-art about the effectiveness studies on preventive web-based interventions accomplished in samples of subjects at high risk for any mental disorder onset.

II. Method

A search was conducted in ProQuest, PubMed, Cochrane and Web of Science database for internet-based preventive psychological interventions that were published between 2010 and 2016.

Results showed that literature on this issue focuses in five domains: depressive symptoms, anxiety symptoms, eating behaviour disorder symptoms, problematic substance use and promotion of psychological well-being.

III. Effectiveness of Web-based Psychotherapy in Individuals at Risk for Depression Symptoms

Most of the reviewed studies on depression symptoms in high risk individuals showed positive effects of online interventions. Reyes-Portillo et al. 2014 published a systematic review on 25 articles including web-based treatment and prevention programs for depression, anxiety, and suicide prevention in children, adolescents, and youth adults. They concluded that, even though depression and anxiety symptoms got reduced, there was limited evidence for the effectiveness of these kinds of interventions mainly due to the methodological design variations [40].

Within traditional therapies used for the treatment of depression disorders, Cognitive Behavioral Treatment (CBT) has proven to be the most effective and it is widely used by clinicians [8]. Internet-based Cognitive Behavioural Therapy (iCBT) has also been implemented for the decrease of depressive symptoms. Buntrock et al. 2016 performed a study comparing two groups of online intervention for the prevention of depression in 406 adults with subthreshold depression symptoms. Groups were randomized to either a web-based guided self-help intervention (cognitive-behavioral and problem-solving therapy supported by an online trainer) or a web-based psychoeducation program. They concluded that the use of a web-based guided self-help intervention compared with enhanced usual care reduced the incidence

* Corresponding author.
E-mail address: anabelen.calvo@unir.net

of MDD over 12 months. However, further research was needed to understand whether the effects are generalizable to both first onset of depression and depression recurrence as well as efficacy without the use of an online trainer [7]. Another study also found that the iCBT group had a significantly lower incidence of major depressive episodes at the 12-month follow-up than the control group in a study examining the effects of iCBT program on decreasing the risk of major depressive episodes among 20.000 workers employed in a private corporate group in [20]. Another study with 120 participants with mild to moderate depression were recruited from the general population and randomized to either guided ICBT or to live group treatment. Measures were completed before and after the intervention to assess depression, anxiety, and quality of life. Follow-ups were conducted at one-year and three-year after the treatment had ended. Results showed that both treatments were equally effective within the boundaries of non-inferiority and long-term effects could be sustained up to 3 years after treatment [2]. Moreover, Guille et at. 2015 designed a study to assess the effectiveness of a web-based cognitive behavioral therapy for the prevention of suicide in a sample of medical physicians at the beginning of their internships. Results suggested that this intervention helped reduce the he development of suicidal ideation among this population [18].

Third generation psychotherapies like acceptance and commitment therapy (ACT) are considered as empirically supported treatments with modest effect on managing depression [38]. Lappaplainen et al. 2015 investigated the effectiveness of an internet based ACT intervention in participants with depression symptoms. Conclusions of the study showed a decrease on depression symptoms which maintained through 12-month follow-up compared to the waitlist group [24].

Regarding non-functional depression symptoms, patients may experiment them as a consequence of organic disease. Thompson et al. (2015) implemented a study (Project UPLIFT) on the prevention of the onset of depression symptoms in patients with epilepsy. They performed a mindfulness-based cognitive therapy (MBCT) online intervention in a sample of 62 patients and concluded that the intervention reduced the number of symptoms of depression and increased patient´s life satisfaction compared to the treatment as usual group [46].

Online interventions are also used in student populations who must cope with depression symptoms. A study analyzed whether an unguided Internet-based self-help intervention helped reduce symptoms of depression in a sample of at risk university students. Results showed that it was effective for the reduction of depression symptoms and negative thoughts [28]. Morgan et al. (2012) performed The Mood Memos study, a randomized controlled trial testing whether self-help behaviors for depression could be improved by promotional messages sent by email to 1326 participants. Authors concluded that these emails were found to reduce depression symptoms and psychological distress relative to control emails that provided information only [32].

Furthermore, current research conducted on this issue has already published protocols about future studies on the effectiveness of preventive internet-based psychotherapy in individuals at risk for depression [17], still with no evidence results.

IV. Effectiveness of Web-based Psychotherapy in Individuals at Risk for Anxiety Disorders

Use of technology in psychotherapy has been a cost-effective way to disseminate empirically validated treatments for a wide variety of psychological problems, including anxiety disorders [35]. Christensen et al. 2014 tried to evaluate the effectiveness of a web-based program in preventing General Anxiety Disorder symptoms in a sample of young adults but they did not find significant differences in symptom reduction [10]. Another study was performed to establish the efficacy of two Internet-based prevention programs to reduce anxiety and depressive symptoms in adolescents. They concluded that both interventions reduced the depression and anxiety symptoms, but results should be cautiously interpreted because of the great loss-to-follow-up [49]. In the same line, in order to evaluate the efficacy of a transdiagnostic personality-trait-focused web-based intervention, a study was developed to reduce symptoms of common mental disorders, such as depression, anxiety, alcohol use and eating disorders in university students with a high risk for development. Results showed a reduction in depression and anxiety symptoms in the intervention group [34].

However, research in anxiety prevention has focused on the presence of symptoms or the high risk to develop posttraumatic stress disorders (PTSD). Kenardy et al. (2015) conducted a study on a web-based intervention to prevent long-term children PTSD. They concluded that intervention diminished the occurrence of trauma symptoms. Furthermore, when initial distress was not elevated, no significant differences were noted between the intervention and control group. Therefore, these results indicate the efficacy of early online intervention in children presenting with the specific risk factor of high initial distress [21]. However, other study tried to determine whether an internet based intervention called Trauma TIPS was effective in preventing the onset of PTSD symptoms in injury patients. Results showed that the program was not significantly effective in the reduction of PTSD onset and proposed that future research should add gameplay, a blended care context, and targeting high-risk individuals who would be more likely to benefit from the intervention [33]. In the same line, Marsac et al. 2013 conducted a study which aimed to evaluate the efficacy of a web-based psychoeducational intervention for parents in promoting emotional recovery following pediatric injury. They found ambiguous results and concluded that this intervention was insufficient in the prevention of PTSD symptoms [30]. Moreover, a protocol of a study about the prevention of PTSD in individuals who had a level 1 traffic accident was developed [16]. Results have not been published yet.

V. Effectiveness of Web-based Psychotherapy in Individuals at Risk for Fresenting Symptoms of Eating Disorder

Body image has become an important and overvalued issue in the general population. It is usual that people present concerns about body image but, in some cases, this worry could become pathological. A distortional body image is frequently present in eating disorders and in body dysmorphic disorder. Intervention in people at risk for the presence of symptoms of these disorders is crucial to minimize their impact on well-being. A study compared two groups (internet-based cognitive therapy and waitlist group) with binge eating disorder. The main findings showed that the online intervention significantly reduced the number of objective binge-eating episodes over the last 28 days in the treatment groups compared with the waitlist group. Reductions in the number of binge-eating episodes could be maintained from posttreatment to 12-month follow-up. Furthermore, the intervention significantly reduced scores on all secondary eating psychopathology outcomes [48].

Moreover, internet-based interventions on obesity could be effective and positively influence the decrease of associated stress symptoms, mainly related to the problems derived from a disturbed body image. Lappalainen et al. 2014 published a study protocol to test whether different interventions (including a web-guided Cognitive Behavioral Therapy-based (CBT) intervention) were effective in the promotion of physical and psychological well-being of a sample of obese and stressed individuals. Outcomes from the study are being developed [25].

VI. Effectiveness of Web-based Psychotherapy in Individuals at Risk for Substance Use Disorders

One of the most developed body of research on the effectiveness of online psychotherapy is the one related to substance use, mainly alcohol misuse. A systematic review on mobile technology-based interventions for adult alcohol users showed positive results on alcohol use reduction after interventions. However, because of methodological issues, these are preliminary results that should widely be investigated in future studies [15]. Another study aimed to evaluate the effectiveness of a computer-based intervention for the reduction of alcohol use in a sample of adolescents. Conclusions suggested that it could be a suitable orientation tool used to reduce the alcohol intake and binge drinking in adolescents [13].

Arnaud et al. (2016) evaluated the effectiveness of a 3-month follow-up fully automatized web-based brief intervention based on the motivational interviewing for a sample of 1449, 16-18year-old substance-using adolescents compared to controls with only assessment measures. They found a reduction in alcohol drinking and less existing substance use service barriers for at-risk drinking adolescents [4]. On the contrary, another study found no strong evidence of effectiveness of their study (AMADEUS-2) where they implemented an online alcohol intervention among studies with risky drinking behavior [5]. In the same line, Kypri et al. (2014) designed a web-based alcohol screening and psychoeducational brief intervention on the risky alcohol drinking in 3422 university students who were followed up to six months. They found a small reduction in the amount of alcohol consumed but not in other alcohol consumption and problem measures [22].

Likewise, current protocols designed to analyze the effectiveness of an internet-based self-help intervention to reduce co-occurring alcohol misuse and depression symptoms in adults in comparison to a waitlist are still in progress [41].

Regarding the online prevention of tobacco use onset, studies are scarce. Cremers et al. 2015 found that a web-based prevention program for adolescents at risk of tobacco initiation was not effective in the reduction of children´s intention to smoke and smoking behavior after 12 and 25 months of follow-up compared to the no information group [9]. Moreover, Lana et al. 2013 conducted a study to assess the impact of a web-based intervention supplemented with text messages to reduce cancer risk linked with smoking, unhealthy diet, alcohol consumption, obesity, sedentary lifestyle and sun exposure. They concluded that the web-based intervention supplemented with text messages had a positive global impact, but it leads to only minimal changes in risky behaviors. This intervention appears useful in controlling overweight adolescents [23].

Other drugs internet-based prevention treatment has not been fully investigated yet. An online intervention (Can Reduce) with self-help intervention was achieved to reduce cannabis use comparing the inclusion or absence of chat counselling in a group of risky heavy-cannabis users. Conclusions suggested a reduction of the amount of cannabis use in those participants who also used the online chat [43]. This team also is currently analyzing the same online intervention in participants with cocaine use. They aim to investigate the effectiveness of the web-based self-help intervention, Snow Control 2.0 with tailored chat counseling, which is based on CBT, Motivational Enhancement Therapy (MET), Behavioral Self-Management (BSM), and social problem solving. The objective of this protocol is to observe a reduction in the amount of cocaine use in at risk patients. Results of this research are still in progress [42]

Concerning polyconsumption, Schwinn et al. (2015) focused their attention in the prevention of drug use among sexual-minority youths, who were at risk of developing high substance abuse. They applied a web-based 3-session prevention program and concluded that at 3-month follow-up, adolescents reported less stress and less peer drug use, as well as higher coping, problem solving, and drug-use refusal skills. Efficacy of this program has not been analyzed yet [45]. This team also conducted a study on internet-based drug prevention among adolescent girls. They observed that girls from the intervention group reported lower rates of substance use and achieved gains over girls in the control group on normative beliefs and self-efficacy at posttest and 6-month follow-up, respectively [44].

VII. Web-based Psychological Health Promotion in the General Population

Internet-based intervention not only provides new delivery media for mental health treatments, it also opens the possibility for developing health promotion in the general population. The effects of an online positive psychology program (Bite Back) for the improvement of the well-being and mental health in a sample of Australian youth have been examined. Conclusions showed that this program decreased symptoms of depression and stress and increased well-being in young people, especially for those who used the website for 30 minutes [29].

University students' health promotion has been another focus of interest. One study was conducted to evaluate the efficacy of an Acceptance and Commitment Therapy (ACT) web-based program (The Student Compass) in order to increase university students' wellbeing. Results revealed a reduction in symptoms of stress, anxiety and depression within the intervention group [39]. Another study with the same aim found a decrease on the frequency of depression and anxiety symptoms in the ACT group relative to the waitlist group [27].

VIII. Computational Techniques for the Analysis of Web-based Psychological Interventions

The online interventions previously described generate a secondary (but not for this reason useless) extremely large amount of data regarding different aspects of the people under online treatment, from personal preferences used for marketing purposes to the confirmation of the presence of symptoms or diseases that could be altogether glued as jigsaw pieces[50].

The term "Big data" is becoming frequent in the psychology field, as it could be useful for the selection of effective web-based psychotherapies that had proven to be effective in population samples analyzed by data mining tools. The use of data mining in psychotherapy is still scarce, although some studies have found interesting usages for the health promotion. As an example, in a study conducted with data collected from elderly people under self-care programs which was analyzed with web usage mining, results showed association relationships, interest and sequence-based representation schemes that could be used for research in medicine, public health, nursing and psychology and for policy-making in the health care domain[19].

Another application of big data deals with the designing of instruments for the assessment of knowledge and behaviors. Preventive web-based intervention assessment tools could develop from studies whose main objective was to elaborate algorithms for the optimal selection of available items in questionnaires related to psychology and education subjects [12][37].

IX. Discussion

Web-based psychological interventions for the prevention of mental disorders seem to be effective for at risk individuals. Online health promotion in the general population is also effective to avoid the onset of clinical psychological circumstances. Moreover, internet-

based psychological intervention works as a suitable way for the economization and optimization of results. It could reach a variety of population: from those who present difficulties for the access of health promotion and prevention (those with mobility troubles and geographical barriers, lack of economic resources, stigma, special personality traits…), symptomatic patients, but also at risk individuals or people just interested in the improvement of their quality of life. This psychotherapy format could work for non-clinic intervention, such as counselling or coaching [43].

Despite the abundant research that just recently started on this topic, more body of research is needed in order to unify and structure methodology designs and increase the number of participants. On this regarding, a deep understanding of the user needs and preferences is needed to increase the participation and adherence of people to internet interventions, together with an actively involving of users in designing processes from the outset [14]. Technologies such as data mining techniques would help maximize the processing of large volumes of research data and would result in more accurate population representations and worldwide conclusions of web-based psychotherapy studies [26].

Promising directions of research include a greater focus on user-centered approaches (including user-centered design, intervention individualization, and design of modularized programs), increased emphasis on engagement (including methods such as gaming, telepresence and persuasive technology, and measuring engagement), increased international and intersectorial collaboration, and rapid testing and implementation [14].

Acknowledgment

This work is partially funded by Universidad Internacional de La Rioja, UNIR (UNIR, http://www.unir.net), under the Research Support Strategy: Emergent Research Group (2016-2018).

References

[1] A. P. A. Presidential Task Force on Evidence-Based Practice, Evidence-based practice in psychology, Am Psychol, vol 61, no 4, 271-285, 2006.

[2] G. Andersson, H. Hesser, A. Veilord, L. Svedling, F. Andersson, O. Sleman, et al., Randomised controlled non-inferiority trial with 3-year follow-up of internet-delivered versus face-to-face group cognitive behavioural therapy for depression, J Affect Disord, vol 151, no 3, pp 986-994, 2013.

[3] L.H. Andrade, J. Alonso, Z. Mneimneh, J.E. Wells, A. Al-Hamzawi, G. Borges, et al., Barriers to mental health treatment: results from the WHO World Mental Health surveys, Psychol Med, vol 44, no 6, pp 1303-1317, 2014.

[4] N. Arnaud, C. Baldus, T.H. Elgan, N. De Paepe, H. Tonnesen, L. Csemy, L., et al., Effectiveness of a Web-Based Screening and Fully Automated Brief Motivational Intervention for Adolescent Substance Use: A Randomized Controlled Trial, J Med Internet Res, vol 18, no 5, e103, 2016.

[5] P. Bendtsen, M. Bendtsen, N. Karlsson, I.R. White and J. McCambridge, Online Alcohol Assessment and Feedback for Hazardous and Harmful Drinkers: Findings from the AMADEUS-2 Randomized Controlled Trial of Routine Practice in Swedish Universities, J Med Internet Res, vol 17, no 7, e170, 2015.

[6] E. Bunge, P. López, J. Mandil, M. Gomar, R. Borgialli, Actitudes de los terapeutas argentinos hacia la incorporación de nuevas tecnologías en psicoterapia, Revista Argentina de Clínica Psicológica, vol 18, no 3, pp 209-216, 2009.

[7] C. Buntrock, D.D. Ebert, D. Lehr, F. Smit, H. Riper, M. Berking and P. Cuijpers, Effect of a Web-Based Guided Self-help Intervention for Prevention of Major Depression in Adults with Subthreshold Depression: A Randomized Clinical Trial. JAMA, vol 315, no 17, pp 1854-1863, 2016.

[8] A.C. Butler, J. E. Chapman, E.M. Forman and A. T. Beck, The empirical status of cognitive-behavioral therapy: a review of meta-analyses. Clin Psychol Rev, vol 26, no 1, pp 17-31, 2006.

[9] H.P. Cremers, L. Mercken, M. Candel, H. de Vries and A. Oenema, A Web-based, computer-tailored smoking prevention program to prevent children from starting to smoke after transferring to secondary school: randomized controlled trial. J Med Internet Res, vol 17, no 3, e59, 2015.

[10] H. Christensen, P. Batterham, A. Mackinnon, k.M. Griffiths, K.J. Kalia Hehir, J. Kenardy, et al., Prevention of generalized anxiety disorder using a web intervention, iChill: randomized controlled trial. J Med Internet Res, vol 16, no 9, e199, 2014.

[11] H. Christensen and I.B. Hickie, E-mental health: a new era in delivery of mental health services, Med J Aust, vol 192, no 11 Suppl, S2-3, 2010.

[12] V. Crisp, C. Ward, The development of a formative scenario- based computer assisted assessment tool in psychopatology for teachers: The PeCPAA project. Computers and education, vol 50, 1509-1526, 2008.

[13] R. M. Drost, A.T. Paulus, A. F., Jander, L. Mercken, H. de Vries, D. Ruwaard and S. M. Evers. A Web-Based Computer-Tailored Alcohol Prevention Program for Adolescents: Cost-Effectiveness and Intersectoral Costs and Benefits, J Med Internet Res, vol 18, no 4, e93, 2016.

[14] T. M. Fleming, D. de Beurs,Y. Khazaal, A. Gaggioli, G. Riva, C. Botella et al., Maximizing the Impact of e-Therapy and Serious Gaming: Time for a Paradigm Shift, Front Psychiatry,vol 7, 65, 2016.

[15] L. A. Fowler, S.L. Holt, D. Joshi, Mobile technology-based interventions for adult users of alcohol: A systematic review of the literature. Addict Behav,vol 62, pp 25-34, 2016.

[16] S. A. Freedman, E. Dayan, Y.B. Kimelman, H. Weissman and R. Eitan, Early intervention for preventing posttraumatic stress disorder: an Internet-based virtual reality treatment. Eur J Psychotraumatol, vol 6, 2015.

[17] T.G. Gladstone, M. Marko-Holguin, P. Rothberg, J. Nidetz, A. Diehl, D. T. DeFrino, D. T. et al., An internet-based adolescent depression preventive intervention: study protocol for a randomized control trial. Trials, vol 16, pp 203, 2015.

[18] C. Guille, Z. Zhao, J. Krystal, B. Nichols, K. Brady and S. Sen, Web-Based Cognitive Behavioral Therapy Intervention for the Prevention of Suicidal Ideation in Medical Interns: A Randomized Clinical Trial, JAMA Psychiatry,vol 72, no 12,pp 1192-1198, 2015.

[19] Y-S, Hung, B. Kuei-Ling, Chen, C-T, Yang , G-F Deng, Web usage mining for analysing elder self-care behavior patterns. Reference Expert Systems with Applications, vol 40, 775–783, 2013.

[20] K. Imamura, N. Kawakami, T. A. Furukawa,Y. Matsuyama, A. Shimazu, R. Umanodan, et al., Does Internet-based cognitive behavioral therapy (iCBT) prevent major depressive episode for workers? A 12-month follow-up of a randomized controlled trial, Psychol Med, vol 45, no 9, pp 1907-1917, 2015.

[21] J. A. Kenardy, C. M. Cox and F.L. Brown, A Web-Based Early Intervention Can Prevent Long-Term PTS Reactions in Children with High Initial Distress Following Accidental Injury., J Trauma Stress, vol 28, no 4, pp 366-369, 2015.

[22] K. Kypri, T. Vater, S. J. Bowe, J. B. Saunders, J. A., Cunningham, N. J. Horton and J. McCambridge, Web-based alcohol screening and brief intervention for university students: a randomized trial, JAMA, vol 311, no 12, pp 1218-1224, 2014.

[23] A. Lana, G. Faya-Ornia and M. L. Lopez, Impact of a web-based intervention supplemented with text messages to improve cancer prevention behaviors among adolescents: results from a randomized controlled trial, Prev Med, vol 59, pp 54-59, 2014.

[24] P. Lappalainen, S. Langrial, H. Oinas-Kukkonen, A. Tolvanen and R. Lappalainen, Web-based acceptance and commitment therapy for depressive symptoms with minimal support: a randomized controlled trial, Behav Modif, vol 39, no 6, pp 805-834, 2015.

[25] R. Lappalainen, E. Sairanen, E. Jarvela, S. Rantala, R. Korpela, S. Puttonen et al., The effectiveness and applicability of different lifestyle interventions for enhancing wellbeing: the study design for a randomized controlled trial for persons with metabolic syndrome risk factors and psychological distress, BMC Public Health, vol 14, pp 310, 2014.

[26] S-H. Liao, P-H. Chu, P-Y. Hsiao, Data mining techniques and applications – A decade review from 2000 to 2011. Expert Systems with Applications, vol 39,11303–11311, 2012.

[27] M. E. Levin, J. Pistorello, J. R. Seeley and S.C. Hayes, Feasibility of a prototype web-based acceptance and commitment therapy prevention program for college students. J Am Coll Health,vol 62, no 1,pp 20-30, 2014.

[28] O. K. Lintvedt, K.M. Griffiths, K. Sorensen, A. R. Ostvik, C.E. Wang,

M. Eisemann, and K. Waterloo, Evaluating the effectiveness and efficacy of unguided internet-based self-help intervention for the prevention of depression: a randomized controlled trial, Clin Psychol Psychother, vol 20, no 1, pp 10-27, 2013.

[29] V. Manicavasagar, D. Horswood, R. Burckhardt, A. Lum, D. Hadzi-Pavlovic and G. Parker, Feasibility and effectiveness of a web-based positive psychology program for youth mental health: randomized controlled trial, J Med Internet Res, vol 16, no 6, e140, 2014.

[30] M. L. Marsac, A. K. Hildenbrand, K. L. Kohser, F. K., Winston, Y. Li and N. Kassam-Adams, Preventing posttraumatic stress following pediatric injury: a randomized controlled trial of a web-based psycho-educational intervention for parents. J Pediatr Psychol, vol 38, no 10, pp 1101-1111, 2013.

[31] D. C. Mohr, M.N. Burns, S. M. Schueller, G. Clarke and M. Klinkman, Behavioral intervention technologies: evidence review and recommendations for future research in mental health. Gen Hosp Psychiatry, vol 35, no 4, pp 332-338, 2013.

[32] A. J. Morgan, A. F, Jorm and A. J. Mackinnon, Email-based promotion of self-help for subthreshold depression: Mood Memos randomised controlled trial, Br J Psychiatry, vol 200, no 5, pp 412-418, 2012.

[33] J. Mouthaan, M. Sijbrandij, G. J. de Vries, J. B. Reitsma, R. van de Schoot, J. Goslings, et al., Internet-based early intervention to prevent posttraumatic stress disorder in injury patients: randomized controlled trial. J Med Internet Res, vol 15, no 8, e165, 2013.

[34] P. Musiat, P. Conrod, J. Treasure, A. Tylee, C. Williams, U, Schmidt, Targeted prevention of common mental health disorders in university students: randomised controlled trial of a transdiagnostic trait-focused web-based intervention. PLoS One, vol 9, no 4, e93621, 2014.

[35] M. G. Newman, L.E. Szkodny, S. J. Llera and A. Przeworski, A review of technology-assisted self-help and minimal contact therapies for anxiety and depression: is human contact necessary for therapeutic efficacy? Clin Psychol Rev, vol 31, no 1, pp 89-103, 2011.

[36] NICE guidelines, Common mental health disorders: identification and pathways to care, NICE guidelines [CG123], 2011.

[37] M. Pérez, Las Terapias de tercera generación como terapias contextuales. Madrid: Sintesis, 2014.

[38] J. Pereira, M. Vilâ, Variable neighborhood search heuristics for a test assembly design problema. Expert Systems with Applications vol 42, 4805–4817, 2015.

[39] P. Rasanen, P. Lappalainen, J. Muotka, A. Tolvanen and R. Lappalainen, R, An online guided ACT intervention for enhancing the psychological wellbeing of university students: A randomized controlled clinical trial, Behav Res Ther,vol 78, pp 30-42, 2016.

[40] J. A. Reyes-Portillo, L. Mufson, L.L. Greenhill, M. S. Gould, P. W. Fisher, N. Tarlow, N and M.A. Rynn, Web-based interventions for youth internalizing problems: a systematic review, J Am Acad Child Adolesc Psychiatry, vol 53, no 12, pp 1254-1270 e1255, 2014.

[41] M. P. Schaub, M. Blankers, D. Lehr, L. Boss, H. Riper, J. Dekker, J., et al., Efficacy of an internet-based self-help intervention to reduce co-occurring alcohol misuse and depression symptoms in adults: study protocol of a three-arm randomised controlled trial, BMJ Open, vol 6, no 5, e011457, 2016.

[42] M. P. Schaub, L. J. Maier, A. Wenger, L. Stark, O. Berg, T. Beck, et al., Evaluating the efficacy of a web-based self-help intervention with and without chat counseling in reducing the cocaine use of problematic cocaine users: the study protocol of a pragmatic three-arm randomized controlled trial, BMC Psychiatry, vol 15, pp 156, 2015.

[43] M. P. Schaub, A. Wenger, O. Berg, T. Beck, L. Stark, E. Buehler and S. Haug, A Web-Based Self-Help Intervention with and Without Chat Counseling to Reduce Cannabis Use in Problematic Cannabis Users: Three-Arm Randomized Controlled Trial, J Med Internet Res, vol 17, no 10, e232, 2015.

[44] T. M. Schwinn, J. E. Hopkins and S. P. Schinke, Developing a Web-Based Intervention to Prevent Drug Use among Adolescent Girls, Res Soc Work Pract, vol 26, no 1, pp 8-13, 2016.

[45] T.M. Schwinn, B. Thom, S. P. Schinke and J. Hopkins, Preventing drug use among sexual-minority youths: findings from a tailored, web-based intervention, J Adolesc Health,vol 56, no 5,pp 571-573, 2015.

[46] N. J. Thompson, A. H. Patel, L. M. Selwa, S. C. Stoll, C.E. Begley, E. K. Johnson and R. T. Fraser, Expanding the efficacy of Project UPLIFT: Distance delivery of mindfulness-based depression prevention to people with epilepsy, J Consult Clin Psychol, vol 83, no 2, pp 304-313, 2015.

[47] A. Trujillo, Nuevas tecnologías y Psicología. Una perspectiva actual, Apuntes de Psicología, vol 23, no 3, pp 321-335, 2005.

[48] B. Wagner, M. Nagl, R. Dolemeyer, G. Klinitzke, J. Steining, A. Hilbert, A. Kersting, Randomized Controlled Trial of an Internet-Based Cognitive-Behavioral Treatment Program for Binge-Eating Disorder, Behavior Therapy, vol 47, pp 500-514, 2016.

[49] N. Wong, L.Kady, L. Mewton, M. Sunderland, G. Andrews, Preventing Anxiety and Depression in Adolescents: A Randomised Controlled Trial of Two School Based Internet-Delivered Cognitive Behavioural Therapy Programmes, Internet Interventions, vol 1, pp 90-94, 2014.

[50] I.Yaqooba, I. Abaker Targio Hashema, A. Gania, S. Mokhtara,Ejaz Ahmeda, N. Badrul Anuara, A. V. Vasilakosb, Big data: From beginning to futureInternational Journal of Information Management, vol 36,1231–1247, 2016.

Teresa Sanchez-Gutiérrez

Teresa Sanchez-Gutiérrez was born in 1984. She received her PhD from the Complutense University in Madrid (Psychopharmacology and substance abuse) in 2014. She worked as a researcher and psychotherapist at the Child and Adolescent Psychiatry Department, Hospital General Universitario Gregorio Marañón from 2010 to 2015. Since 2015, she became Professor and tutor at the National Distance Education University (UNED) in Córdoba and since 2016 she is Professor at Universidad Internacional de la Rioja (UNIR). She has contributed to scientific research with several manuscripts, book chapters and lectures at international and national congresses.

Sara Barbeito

Sara Barbeito was born in 1981. She received her PhD from the Medicine University of Bask country (neuroscience) in 2014. From 2004 to 2015 she was a researcher in the Santiago Apostol Hospital of Vitoria (CIBERSAM 10 group). Since 2015 she is Professor in the Rioja International University (UNIR). She has numerous international articles and book´s chapters.

Ana Calvo

Ana Calvo PhD is full Professor and Director of The Master´s in General Health Psychology at Universidad Internacional de la Rioja (UNIR) since 2015. She received her PhD from the Complutense University in Madrid in 2013. She worked as a researcher and psychotherapist at the Child and Adolescent Psychiatry Department, Hospital General Universitario Gregorio Marañón from 2009 to 2016. In addition, she was working during her international pre-doctoral fellowship in different early psychosis services for young people at Orygen Youth Health Clinical and research Centre and Melbourne University in Melbourne, Australia. (2012-2013) and She was working as a Post-doctoral Researcher fellow at Royal College of Surgeons in Ireland and Trinity College of Dublin in Dublin, Ireland (2015). She has contributed to scientific research with several manuscripts, book chapters and lectures at international and national congresses.

Comparison of Feedforward Network and Radial Basis Function to Detect Leukemia

Pragya Bagwari[1], Bhavya Saxena, Meenu Balodhi[2],Vishwanath Bijalwan[1] *

[1]Gopeshwar (Uttarakhand Government Institute), Uttarakhand (India)
[2]Uttaranchal University Dehradun,Uttarakhand (India)

Received 3 September 2016 | Accepted 1 November 2016 | Published 23 December 2016

Abstract

Leukemia is a fast growing cancer also called as blood cancer. It normally originates near bone marrow. The need for automatic leukemia detection system rises ever since the existing working methods include labor-intensive inspection of the blood marking as the initial step in the direction of diagnosis. This is very time consuming and also the correctness of the technique rest on the worker's capability. This paper describes few image segmentation and feature extraction methods used for leukemia detection. Analyzing through images is very important as from images; diseases can be detected and diagnosed at earlier stage. From there, further actions like controlling, monitoring and prevention of diseases can be done. Images are used as they are cheap and do not require expensive testing and lab equipment. The system will focus on white blood cells disease, leukemia. Changes in features will be used as a classifier input.

Keywords

K-mean Clustering, Texture Features, Feed Forward and RBFNN.

DOI: 10.9781/ijimai.2017.4510

I. Introduction

Leukemia is one of the many types of cancers. Leukemia is caused in the white blood cells near the bone marrow region of our body. In this the white blood cells (WBCs) which get infected turns blue. Like any other cancer in this also the cell divides itself at the faster pace. Even when it is not required they multiply causing a tumor. Detected and treated at an early stage of leukemia saves a lot of lives. According to leukemia research foundation, every four minutes someone is diagnosed with leukemia. More than 176,000 are expected in U.S.

Leukemia helps in detecting blood cancer using two basic modules of image processing i.e. Image segmentation and feature extraction. After these two modules we use two techniques of neural network i.e. feed forward network and radial basis function network (RBFNN) for the detection purposes. We compare the accuracy percentage in both of them. The technique with best accuracy percentage is recorded as the more efficient technique.

II. Related Work

Athira Krishnan, Sreekumar K [2] prposed a system to detect acute myelogenous leukemia which is a type of blood cancer. In this they have used two modules i.e. segmentation and feature extraction. In feature extraction they have extracted features like fractal dimensions, local binary patterns, texture features, shape and color features. Subrajeet Mohapatra, Dipti Patra et al [5] proposed a system unsupervised microscopic blood images using the data clustering techniques . In feature extraction shape and size of the cell. Ruggero Donida Labati IEEE Member, Vincenzo Piuri IEEE Fellow et al [8] they proposed an open database for the new researchers so that they can avail the images easily. The images are segmented using basic techniques.

* Corresponding author.
E-mail addresses: vishwanath.bijalwan@gmail.com

III. Methods

The procedure for leukemia detection in the microscopic images consist of image segmentation and feature extraction. The working procedure is shown in the figure below (fig. 1). The leukemia consists of red blood cells (RBCs), WBCs and platelets. The method is based on image segmentation so that we can easily separate WBCs from rest of the blood contents from the background and finally separation of nucleus and cytoplasm. As cytoplasm is insufficient so we have considered only the nucleus as the region of interest and its essential features are extracted.

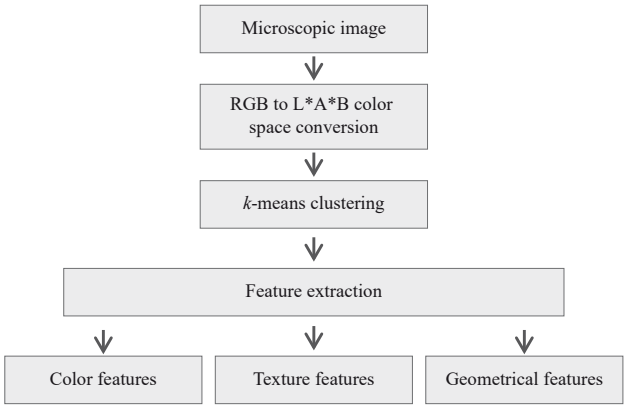

Fig. 1. Overview of the system.

IV. The Database

For the diagnosis of leukemia the visual analysis of peripheral blood samples is an important task. ALL-IDB i.e. the acute lymphoblastic leukemia image database for image processing is a public dataset of blood samples specifically designed for evaluation and the comparison of algorithm for segmentation and classification for each image in the dataset, the classification of cell is given and it is provided a specific set of figures of merits to be processed in order to fairly compare different algorithm when working with the proposed dataset. It contains about 39000 blood elements where the lymphocytes have been labeled by expert oncologists.

V. Image Segmentation

Image segmentation has drawn attention from many years in the field of research. There are many algorithms used in segmentation. So, algorithm that is developed for a particular set of images can't be used for another set of images.

The techniques used for image segmentation in this paper are K mean and clustering and Lab color space.

*A. L*A*B Color Space:*

Typically an image can be represented with the help of three color components. Images generated by the digital microscopes are usually in RGB color space which is visually difficult to segment. For better color based segmentation we map the RGB image into L*a* b* color space. This color space consists of a luminosity layer L*, chromaticity layers a* and b*. Since all the color information is in the a* and b* layers we use these two components for nucleus segmentation.

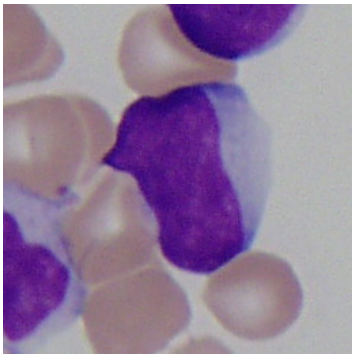

Fig. 2. Original Image.

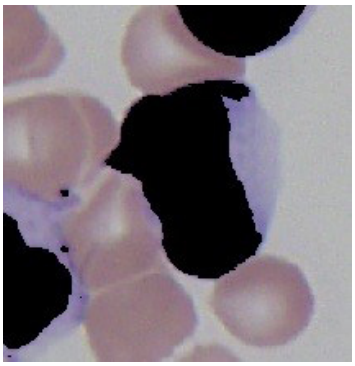

Fig. 3. Image after L*A*B.

B. K- means Clustering:

k-means clustering is a renowned subdividing method. In this substances are classified as belonging to one of k-groups. The consequences of partitioning method are a set of K clusters, each body of data set belonging to one cluster. In each cluster there may be a centroid or a cluster representative. In case where we reflect real-valued data, the arithmetic mean of the feature vectors for all objects within a cluster provides a suitable representative; alternative types of centroid may be mandatory in other cases. Clustering technique is used to create clusters from observations. It attempts to achieve partition such that objects within each cluster are as close to each other as possible, and as far from objects in other clusters as possible.

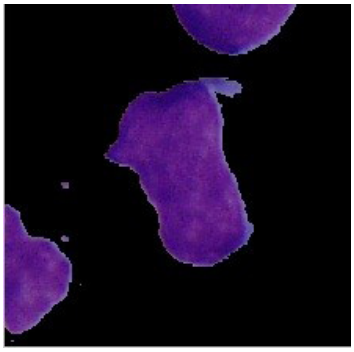

Fig. 4. Image after *k* mean technique.

VI. Feature Extraction

Feature extraction in image processing is a system of redefining a great set of dismissed data, into a set of features of reduced dimension by transforming the input data into the set of features is called feature extraction. In feature extraction color, shape and geometrical features are observed for nucleus and the cell separately. The two clusters are made through k-mean, cluster 2 is for detecting the infected cells whereas cluster 3 is for nucleus. The basic inbuilt functions of feature extraction used in MATLAB are used.

VII. Neural Networks

A neural network is an artificial system. In neural network the imitation of the activity of the brain is done. It imitates how the brain's neurons send messages through each other depending upon the work load some times. Several computing cells work in parallel to produce a result. This is usually seen as one of the possible ways artificial intelligence can work. Most neural networks can tolerate if one or more of the processing cells fail. A neural network is provided that has the capacity of "learning" to distinguish among patterns of data which may differ recognizably from idealized cases, and is able to perform pattern recognition faster while utilizing less memory and fewer clock cycles than neural networks implemented on sequential processors. This implementation is simpler and faster because of an inherent similarity between the flow of information in the brain and in data flow architecture. In this paper the comparison between two neural network techniques is done i.e. feedforward network and the radial basis function neural network (rbfnn).

A. Feed Forward Network:

Feed forward networks consist of a series of layers. The first layer has a connection from the network input. Each subsequent layer has a connection from the previous layer. The final layer produces the network's output. There are hidden layers in between the input and the output layer. This hidden layer contains the weight on each node. The more the weight is the more work the node will do Feed forward networks can be used for any kind of input to output mapping. A feed forward network with one hidden layer and enough neurons in the hidden layers, can fit any finite input-output mapping problem. Every pattern must have the same number of elements as the net has input nodes (excluding the bias unit), and every target the same number of elements as the net has output nodes.

Experiment results by feedforward network : The experiment results in feedforward are basically dependent on the neural nodes we are using. The more the weightage on the nodes the more work load it will take to give the output. It was experimented through different nodes, initially 50 nodes then 80 and then 100 nodes were used on classes A and B which represents the cell and the nucleus cluster respectively. Using 100 neural nodes made the system slow and inefficient so it is not suitable to use 100 nodes. Result for 50 and 80 nodes is below:

TABLE I
EXPERIMENTS DONE THROUGH DIFFERENT NEURONS

Classes	Using 50 neurons	Using 80 neurons
Class A	92%	94.7%
Class B	96%	94.8%

B. RBFNN:

Radial Basis Function Neural Network is a neural network system of good performance. It is efficient in finding the exact nonlinear system's mapping till we have the enough image samples. This neural network system uses the radial basis functions as activation functions. So, it is not dependent on the weights of the neurons. The output of the network is basically a linear combination of radial basis functions of the inputs and neuron parameters. The basic MATLAB technique for RBFNN is implemented for the experiment. Using RBFNN we have 100% accuracy in detecting the leukemia infected cells and nucleus.

VIII. CONCLUSION

The experiments were conducted using two neural network techniques that is feedforward network and the radial basis function. These two techniques were employed on the ALL-IDB images whose features were extracted after they were segmented using L*a*b color space technique and *k*-mean clustering. According to the experiments conducted above RBFNN is more efficient as it consumes less time and gives the 100% accuracy result. So, it's better to use RBFNN instead of feedforward network to detect the leukemia in the proposed system.

ACKNOWLEDGEMENT

This study was supported by Graphic Era Hill University, Dehradun, India. We also appreciate the cooperation of ALL-IDB for providing the database.

REFERENCES

[1] Azhari, Ed-Edily Mohd, et al. "Tumor Detection in Medical Imaging: A Survey."*International journal of Advanced Information Technology* 4 (2014).

[2] Athira Krishnan, Sreekumar K. "A Survey on Image Segmentation and Feature Extraction Methods for Acute Myelogenous Leukemia Detection in Blood Microscopic Images."

[3] Jagadeesh, S., E. Nagabhooshanam, and S. Venkatachalam. "Image processing based approach to cancer cell prediction in blood samples."*ME&HWDS Int. J. Technol. Eng. Sci* 1.1 (2013).

[4] Banzi, Jamali Firmat, and Xue Zhaojun. "Detecting Morphological Nature of Cancerous Cell Using Image Processing Algorithms." *International Journal of Scientific and Research Publications*: 11.

[5] Mohapatra, Subrajeet, Dipti Patra, and Sanghamitra Satpathy. "Unsupervised Blood Microscopic Image Segmentation and Leukemia Detection using Color based Clustering." *International Journal of Computer Information Systems and Industrial Management Applications* 4 (2012): 477-485.

[6] Mohapatra, Subrajeet, Dipti Patra, and Sanghamitra Satpathy. "Automated leukemia detection in blood microscopic images using statistical texture analysis." *Proceedings of the 2011 International Conference on Communication, Computing & Security*. ACM, 2011.

[7] Li, Yujie, et al. "An improved detection algorithm based on morphology methods for blood cancer cells detection." *Journal of Computational Information Systems* 7.13 (2011): 4724-4731.

[8] Labati, Ruggero Donida, Vincenzo Piuri, and Fabio Scotti. "All-IDB: The acute lymphoblastic leukemia image database for image processing." *Image processing (ICIP), 2011 18th IEEE international conference on*. IEEE, 2011.

[9] Alix-Panabières, Catherine, Sabine Riethdorf, and Klaus Pantel. "Circulating tumor cells and bone marrow micrometastasis." *Clinical Cancer Research*14.16 (2008): 5013-5021.

[10] Pullarkat, Vinod A., et al. "Mast cell disease associated with acute myeloid leukemia: detection of a new c-kit mutation Asp816His." *American journal of hematology* 65.4 (2000): 307-309.

[11] Kraeft, Stine-Kathrein, et al. "Detection and analysis of cancer cells in blood and bone marrow using a rare event imaging system." *Clinical cancer research*6.2 (2000): 434-442.

Pragya Bagwari

Pragya Bagwari is currently working as an Assistant Professor, department of CSE at IT Gopeshwar, Uttarakhand India. She has approx 2 years of Teaching and industrial experience. She done her B.Tech degree from UTU Dehradun and M.Tech degree from Graphic Era University Dehradun. Her area of Interest is Image processing , Wireless communication, Machine learning.

Bhavya Saxena

Bhavya Saxena is a research scholar. She obtained her B.Tech Degree from Rajasthan University and done her M.Tech from Graphic Era University. Her area of interest is Image processing and Wireless computing.

Meenu Balodhi

Meenu Balodhi obtained her Bachelors degree of Technology in Electronics & Communication and Masters Degree (M.Tech) from Graphic Era University Dehradun. She was outstanding and meritious student during her degree program. She has 4 Years of Teaching Experince as an Assistant Professor in Uttaranchal University Dehradun. Her area of Interest is OFC, image Processing , Machine learning. She has Worked as PC member in several IEEE conferences and national conferences. She is the renowned author of many reputed research papers of national and international Journals.

Vishwanath bijalwan

Vishwanath bijalwan obtained his B.Tech degree in ECE, from Dehradun Institute of Technology (UPTU) in 2009. He received his M.TECH degree from Uttarakhand Technical University in Digital Communication stream in 2012. Currently he is working as an Assistant Professor & head of the department ECE at IT, Gopeshwar (State Government Institute). Besides this he has been also serving some more academic duties of Examination controller, & Dean Student's welfare at IT Gopeshwar. He has total 5 years of teaching experience and 1 year industry experience. He has worked for various organizations, such as HCL Info system, Doon Institute of Engg. & Technology Rishikesh, Uttaranchal University Dehradun, and Institute of Technology, Gopeshwar. In Research domain he has published various research papers in international journals. His research area of interest is Wireless adhoc network, IEEE 802.15.4, & Machine learning. He has served as a PC member for many national & International conferences in the region; he is also serving as a reviewing board member for various international journals like OMICS group and various IEEE conferences like ICACCCA, ICACCA, CICN, ICACCE. He is also an active member of IAENG, UACEE. His teaching area of Interest is Digital Electronics & Design aspects, Electromagnetic field theory, Antenna & wave propagation & Digital signal processing.

Influence of Lymphocyte T CD4 Levels on the Neuropsychological Performance of Population Affected by HIV and with a Previous History of Substance Use

Enrique Vázquez-Justo [1,2] *; Amalia García-Torres [3,4]; Esperanza Vergara-Moragues[1,3,5]

[1] Portucalense Institute of Neuropsychology. Universidade Portucalense, Porto (Portugal)
[2] Policínico Êbam. Poio. Pontevedra (Spain)
[3] Clinic Unit of Infectious Diseases. Clinical Hospital of Puerto Real, Cádiz (Spain)
[4] Centro de Investigación Mente, Cerebro y Comportamiento (CIMCYC). University of Granada (UGR), Granada (Spain)
[5] Universidad Internacional de la Rioja (UNIR), Logroño (Spain)

Received 21 September 2016 | Accepted 1 November 2016 | Published 23 December 2016

Abstract

The immunological markers help to know if there is a good recovery of the immunological system in patients infected with HIV. Among them, the lymphocyte T CD4 rate is the main indicator of the patient's immunological state being used for staging HIV infection, evaluating the mortality or comorbidity risk and the vulnerability to certain oportunistic infections. However, its link with the presence of cognitive alterations is not clear. Therefore, the aim of this article is to study if lymphocyte T CD4 levels are connected with the neuropsychological performance of a group of people infected with HIV and with a previous history of substance use. The sample consisted of 80 seropositive males with a previous history of substance use. They were evaluated by means of a neuropsychological battery which assesses the most affected cognitive domains in HIV population. The results showed that the patients having a higher level of immunodeficiency (CD4 <200/mm3) have a poorer performance in terms of attention, visuomotor dexterity, visual memory, visual perception, auditory-verbal learning and inhibition. Therefore, our results show a realtion between the lymphocyte T CD4 rate and the neuropsychological performance in seropositive people with a previsous history of substance use.

Keywords

HIV, T CD4 Lymphocytes, Neuropsychological Evaluation.

DOI: 10.9781/ijimai.2017.4511

I. Introduction

Since the HIV primary infection the viral activity is continuous, and it produces the rise of a series of markers which will reflect the probability of HIV development at a certain speed. These markers show in a direct way (viral load, or lymphocytes T CD4) or in an indirect way (microglobulin ß-2, neopterin, or antigen p24) the action HIV takes on the immunological system of the patient, and they have been used independently or combined to identify the risk of progression to AIDS [9] (Table I).

All these markers have a high prognostic value. In the case of lymphocytes T CD4, their number is the main indicator of the patient's immunological state. Its count is used for staging HIV infection, evaluating the risk of comorbidity or mortality, and the vulnerability to certain oportunistic infections, the need for its prophylaxis and the occasional discontinuation [1] [15]. Nowadays, the universal indication of anti-retroviral treatment (ART) is recognised for all patients, regardless of the lymphocyte CD4 count. Thus, the absolute number and the percentage of lymphocytes CD4 must be periodically determined before initiating ART and, once it has been initiated, as a parameter of periodical monitoring of the immunological response to said treatment [15].

As far as the viral load is concerned, it must be determined during the initial assessment of the patient and before the beginning of ART, being the main parameter for the evaluation of ART's virological efficacy and to define the virological failure [7]. For all these reasons, we can conclude that the combination of these markers allows us to obtain a better overview of a patient's state, his/her prognosis and his/her response to treatment.

HIV may affect the cognitive development of these patients [10], these specific markers have been studied regarding the presence of neuropsychological affectation, although results are not very consistent. As far as immunological markers are concerned, the lymphocyte T CD4 rate of decrease is a good indicator to determine the probability of developing AIDS [2] [27] [36], however, its efficiency to predict neurological and neuropsychological affectation has not been confirmed. While some authors point out that the probability of developing neuropsychological affectation is higher among seropositive patients with low levels of lymphocytes CD4 [26] [28] [29] [15],

* Corresponding author.
E-mail address: enriquej@upt.pt

others, on the contrary, claim that there is no connection between the rate of lymphocytes T CD4 and neuropsychological functioning [14] [19] [21] [34]. In the end, immunological markers of HIV infection, specifically lymphocyte T CD4 count, have been associated to the presence of neuropsychological affectation in seropositive patients, though there does not seem to be an agreement about this in literature, which suggests the need for continuing research in order to clarify this subject.

For all these reasons, the objective of this article is to study the connection between lymphocytes T CD4 levels and the neuropsychological performance of former seropositive drug addicts.

TABLE I
MAIN BIOLOGICAL MARKERS OF HIV INFECTION
(ADAPTED FROM GARCÍA SORIANO & MIRÓ,1999)

Immunological markers	
Lymphocytes T CD4:	It is considered a severe immunodepression when the lymphocyte CD4 number, its percentage or the quotient CD4/CD8 is lower than 200/mm3, 15% or 0,3 respectively.
Microglobulin ß-2:	It is present in all the nucleated cells, including lymphocytes and macrofages. Its serum increase reflects the activation of these cells. In homosexuals infected with HIV it has been observed a progression of the infection when the plasmatic levels are higher than 5 g/ml. The results in drug addicts are contradictory.
Neopterin:	It is produced by monocytes and macrofages stimulated with interferon gamma produced by the activated lymphocytes T. In HIV-infected homosexuals it has been observed a progression of the infection with plasmatic levels higher than 20 nmol/l. The results in drug addicts are variable.
Virological markers	
Antigen p24:	It is detected at the beginning (acute infecction) and at the end (AIDS) of the infection. It is not detected when the patient has lymphocytes T CD4 higher than 500/mm3. Its apparition in an asymptomatic patient is a biological marker of progression. It is seldom used at present.
Viral load:	Measured through PCR (detection limit 200 copies/ml), bDNA (detection limit 500 copies/ml) y NASBA (detection limit 50 copies/ml) from plasma or serum. Viral load is the best prognostic and treatment-monitoring indicator.

II. METHODOLOGY

A. Subjects

This study is part of another one done on a wider population [32]. In order to conduct this research we have used a sample which comprised 80 males with a previous history of substance use, who voluntarily took part in the study, giving their informed consent. All the subjects for this study are former drug addicts with HIV infection. They were recruited at the Montecelo Hospital in Pontevedra, Xeral Cíes Hospital in Vigo, Xeral de Galicia Hospital in Santiago de Compostela and Juan Canalejo Hospital in A Coruña.

For the selection of the sample the professionals in the reference centres were informed of the requirements which the subjects for our study had to meet, and once selected, they were called at the centre, where the researcher informed them of the characteristics of the research, asking for their cooperation, and offering them the presentation of a report with all the results of the evaluation once it was complete. The subjects interested in taking part gave their informed consent and were called for the evaluation at the same centre where they had been selected, although some of them preferred taking the tests at the Faculty of Psychology in Santiago de Compostela.

We excluded from the study those subjects who showed, or had shown, neurological or medical pathologies that could affect the central nervous system, including dementia associated with HIV; psychiatric disorders; history of head trauma requiring hospitalization due to neurological complications; and antisocial personality disorder according to DSM-IV criteria (American Psychiatric Association, 1995). Also, we excluded subjects with moving or sensory defects, except in the case of visual ones corrected with lenses. Finally, based on the report from the professionals at the drug addict assistance units and the self-report from the subjects itself, we excluded those patients currently using psychotropic substances (illegal, medicine or alcohol) different from methadone.

Regarding the socio-demographic characteristics of the sample, 94% of the subjects presented right-hand dominance and 6% left-handed. 60% had primary studies, and the remaining 40% secondary or higher studies. 33% had a low socioeconomic level, and 67% a medium level. In terms of work situation, 40% were working when the study took place, and 60% were unemployed or retired (see Table II).

TABLE II.
SOCIO-DEMOGRAPHIC CHARACTERISTICS OF THE SAMPLE

		HIV+ N(%) 80 (100)	
Age*			34 (4.9)
Hand dominance	Right	94%	73 (91.2)
	Left	6%	7 (8.8)
Level of studies	Primary	60%	55 (68.7)
	Secondary or higher	40%	25 (31.3)
Job situation	Not working	60%	57 (71.2)
	Working	40%	23 (28.8)
Economical level	Low	33%	35 (43.8)
	Medium	67%	45 (56.3)

* Mean and standard deviation

Regarding the clinical characteristics of the sample, 39% of seropositive subjects were not having any antiretroviral treatment, unlike the remaining 61%; in terms of viral load, in 44% of the cases it was undetectable, whereas in 56% it was detectable. As far as lymphocyte T CD4 level is concerned, 25% of seropositive subjects had a count higher than 500, in 29% it was 200-499, and in 46% it was under 200 (see Table 3).

TABLE III.
CLINICAL CHARACTERISTICS OF THE SAMPLE

		HIV+ N(%)80 (100)
Antiretroviral treatment	Yes	61%
	No	39%
Viral load	Detectable	56%
	Undetectable	44%
Lymphocyte T CD4	>500	25%
	200-499	29%
	<200	46%

B. Tools for Neuropsychological Assessment

The tests included in the battery for neuropsychological exploration designed for this study were chosen because of their validity, and because they appeared to be sensitive to the neuropsychological deterioration in HIV-infected patients in other studies. We present below the list of tests used (Table 4) following the order of application, and clarifying the results collected with each test.

TABLE IV.
BATTERY OF NEUROPSYCHOLOGICAL EXPLORATION USED

• WAIS IV: Comprehension, Similarities, Digit Span, Vocabulary, Digit Symbol, Block Design and Object Assembly • Rey Auditory Verbal Learning Test • Visual Search and Attention Test • Trail-Making Test (parts A and B) • Verbal Fluency Test	• Benton's Visual Retention Test • Boston Naming Test • Stroop Test • Purdue's Pedgeboard Test • Rey-Osterrieth Complex Figure • Finger-Tapping Test • Wisconsin Card-Sorting Test

1. *Wechsler Adult Intelligence Scale* [35]. We used the following subtests from the Wechsler Adult Intelligence Scale (*WAIS IV*): Comprehension, Similarities, Digit Span, Vocabulary, Digit Symbol, Block Design and Object Assembly.

- *Comprehension* Subtest. It assesses the degree of appreciation of past experience applied to everyday situations, and of internalization of culture, especially of moral or ethical values. It consists of twelve open-ended questions, 14 common sense and practical reasoning questions, and 3 proverb questions that the subject must explain.
- *Similarities* Subtest. It is a test for verbal formation of concepts, which assesses the ability to assimilate and classify similarities and differences between objects, facts or ideas. It requires comprehension and associative thinking skills. The subject is asked to explain what a series of word pairs presented to him/her have in common.
- *Digit Span* Subtest. It consists of two parts: forward digit span, in which the subject must repeat some series of numbers in the same order, and backward digit span, in which the subject repeats other series of numbers in reverse order. It assesses immediate auditory memory (backward digit span), attention (forward digit span), and resistance to distraction.
- *Vocabulary* Subtest. The subject must tell the meaning of 40 words presented to him in order of increasing difficulty, which allows us to assess classification and conceptualization skills. The score obtained in this test was also used to calculate the cognitive reserve.
- *Digit Symbol* Subtest. It assesses the ability to learn an unfamiliar task, visuomotor skill, the degree of persistence when doing an unattractive task, and the information processing speed. It consists of a sheet which shows the subject some numbers, from 1 to 9, corresponding to a symbol, and a part where the numbers are, and in which the subject must draw the symbol corresponding to each number, as fast as possible in a limited time.
- *Block Design* Subtest. It assesses visuomotor integration, visuospatial organization, execution speed, and non-intellectual factors such as excessive care, impulsivity, and distraction. The task consists of having the subject perform a series of constructions according to a model using blocks and in a limited time.
- *Object Assembly* Subtest. It is a test for visuospatial organization speed and motor response, which assesses analysis skills and visual synthesis, visual and motor coordination. Sequential thinking also plays an important role in this test. The task consists of having the subject build figures from the pieces that he/she is given, in a limited time.

2. *Rey's Auditory Verbal Learning Test* [24]. It involves the reading, by the examiner, of a list of 15 words, which the subject must evoke immediately afterwards, in five different trials; and during a sixth evocation after an interference task (reading of 15 more words). It allows us to obtain seven scores, corresponding to the number of words evoked during the first five trials, a total score resulting from the addition of those, as well as the difference between the fifth and the sixth trials. This test allows us to asses immediate memory, it provides us with a learning curve, reveals inclinations towards patterns of retroactive and proactive interference, and measures the memory capacity after an interference.
3. *Visual Search and Attention Test* [31]. It is a test of visual cancellation which allows us to obtain a measurement of visual search skills and sustained attention. It comprises 4 sheets in which the subject must recognise and point out a certain letter or symbol among a series of distracting stimuli. With this test we obtain a score corresponding to the number of hits of the last two sheets.
4. *Trail-Making Test* [22]. It assesses skills of visual search and visuoconceptual and visuomotor exploration. It also assesses attention, mental flexibility, perceptive-motor skill and information processing speed. It consists of two tasks with separated scores, the score being the time that the subject needs to complete each task:

- *Trails A* , consisting of 25 circles numbered from 1 to 25 that the subject must join correlatively with a pencil stroke.
- *Trails B* , in which the 25 circles contain numbers from 1 to 13 and letters from A to L, the subject must join alternatively numbers and letters.

5. *Verbal Fluency Test* [6]. Its main objective is to assess verbal fluency. It consists of having the subject tell us as many words as possible starting with the letters F, A and S in three trials of one minute each. We get a score resulting from the addition of the number of words which the subject names with each letter.
6. *Benton Visual Retention Test* (Form C, Administration A) [5]. It assesses visuoconstructive skills, visual memory and visual perception, as well as spatial organization and visuospatial memory. It involves the presentation of ten sheets with printed figures for ten seconds each, asking the subject to reproduce them immediately once the stimulus sheet has been removed. This test gives us two scores: the number of sheets correctly reproduced, which measures the general efficiency of the execution, and the number of mistakes made.
7. *Boston Naming Test* [16]. It is a broad-spectrum figure-naming test, consisting of 60 sheets in which an object is represented, which the subject must name spontaneously, or with the help of a semantic or phonetic key. The score we obtain corresponds to the total number of figures named correctly.
8. *Stroop Test* [11]. It measures verbal fluency, cognitive efficiency, and the ability to inhibit stimuli which trigger automatic responses and, therefore, the ability to adapt perception and accommodate to new demands inhibiting a usual response in favour of an unusual one (cognitive flexibility). It consists of three sheets that the subject must read:

- In the first sheet, he/she must read the words red, green and blue printed in black ink, and randomly arranged in columns.
- In the second one, he/she must name the colour of ink with which some symbols "xxx" are printed.
- Finally, in the third sheet, the words red, green and blue appear printed with ink of those same colours. The subject must say the colour of the ink regardless of the written word.

A score is obtained for each sheet, consisting of the number of elements read in 45 seconds. We also calculate an interference score based on the score obtained in each sheet.

9. *Purdue Pegboard Test* [30]. It assesses manual dexterity (speed and precision) in activities involving wide hand, finger and arm movements, and psychomotor coordination. The test consists of having the subject place a series of pegs in the holes set in rows on a board, first with his/her non-dominant hand, then with his/her dominant hand, and finally with both hands. We get three scores from the number of pegs placed during each part of the task and we also get a score resulting from the addition of the three parts.
10. *Rey-Osterrieth Complex Figure Test* [25]. It assesses constructive ability and visual memory, and it also allows us to assess cognitive processing ability, taking into account problem-solving strategies and organization and planning abilities. The test consists of having the subject copy a figure and after three minutes, without previous warning, reproduce it by heart. We get a score from the accuracy of the copy and another one from the reproduction by heart, also valuing the time spent in each one of them, as well as the strategy followed to copy the figure.
11. *Finger-Tapping Test* [23]. It assesses control, and psychomotor speed. It involves a board with a button connected to a counter, and the subject must tap with his/her index finger for 10 seconds. The final score is the average number of hits during 5 trials. A score is obtained for each hand.
12. *Wisconsin Card-Sorting Test* [13]. It allows us to obtain an assessment of abstract thinking. It is considered a measurement of executive functions and cognitive flexibility, as it requires some abilities to develop and maintain the strategy which is most appropriate to solve a problem while the stimulation conditions are changing. This measurement is considered to be sensitive to the frontal function. It consists of four stimulus cards and 128 response cards containing diversely-shaped figures (circles, crosses, triangles, stars), colours (green, blue, red, yellow), and a varied number of figures (one, two, three, four). The subject must match the response cards with the stimulus cards, deducing the criteria to do so correctly from the information given by the examiner in each trial. With this test we get multiple performance scores connected to the different cognitive processes: number of categories completed, fails in maintaining the category (inability to maintain an appropriate strategy); percentage of perseverative responses (persistence in responding according to a wrong criterion); percentage of perseverative and non-perseverative mistakes; and percentage of responses at a conceptual level (conceptual efficiency).

C. Procedure

Once the subject had fulfilled the criteria for taking part in the study, after getting some good therapeutic adherence, and before performing the neuropsychological exploration, we collected, according to the information provided by the subject's self-report, information regarding the personal background and medical history of interest, as well as relevant information about their history of drug abuse. Then, if no reason was deduced from the information to exclude the subject from the study, we would initiate the neuropsychological exploration using the protocol described in the material section, following the instructions indicated by the corresponding application manuals. The characteristics of the tests application were constant for every subject, and they were performed individually, in two sessions with the examiner of approximately 45 minutes.

III. Results

A. Lymphocytes T CD4

In order to determine the level of immune compromise in the neuropsychological performance, we have divided the seropositive subjects in three groups, according to the lymphocyte T CD4 level (≥500, 499-200, <200) following the classification of the Centre for Disease Control (1992). The results are shown in Table 5, which presents the means and deviations typical from the groups in each one of the neuropsychological measures, and points out the relevant differences that have been observed, doing "post hoc" multiple comparison tests. In graphic 1 it is represented the performance of each group during the

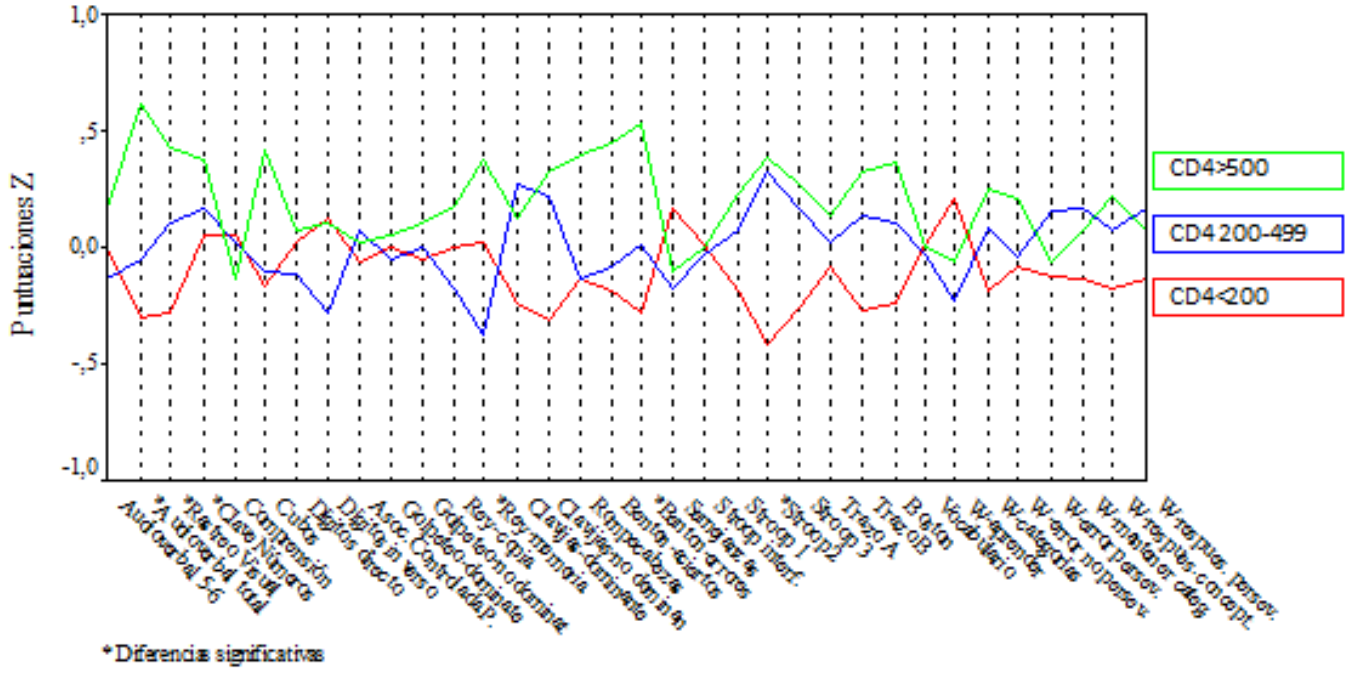

Fig. 1. Z scores from neuropsychological tests for seropositive drug addicts according to lymphocyte T CD4 level.

different neuropsychological tasks, once the direct scores have been transformed into Z scores, and its direction has been corrected.

B. Discussion

The relation of lymphocyte T CD4 levels, used as immunological markers of the progression of HIV infection, have also been studied in connection with the presence of neuropsychological affectation, although the results are not consistent. While some studies point out that the lower the level of lymphocyte T CD4 in seropositive subjects, the greater the neuropsychological deterioration [26] [29] [28], others, on the contrary, show that cognitive functioning is not connected at all with this immunological marker [14] [19] [21] [34].

As far as our research is concerned, we have noticed a selective effect of the level of immune compromise in some attention and memory tasks. Our findings show that seropositive subjects with higher immunodepression levels (CD4 <200/mm^3) obtain a poorer performance than those whose lymphocyte T CD4 levels are within the range of normality, in the Auditory Verbal Learning Test, Visual Search and Attention Test, WAIS Digit Symbol, Benton Visual Retention Test, and Stroop Test, which leads us to suggest that only the subjects with a high degree of immune compromise are neuropsychologically vulnerable.

Taking into account our findings and the fact that the immunodepression level did not show its effect in verbal and denominational tasks, concept formation and reasoning, visuoconstructive skills, manual dexterity and motor speed, and frontal functions, we can suggest that the deterioration of the immunological system does not affect the neuropsychological performance in a general way, it does so in a selective way in attention and memory tasks.

These results are in accordance with those obtained in other studies with drug addict subjects during the different stages of infection [8] [28], as well as those obtained with homosexual subjects [4] [18]

TABLE V
SCORES OBTAINED BY SEROPOSITIVE FORMER DRUG ADDICTS IN THE NEUROPSYCHOLOGUCAL TESTS ACCORDING TO LYMPHOCYTE T CD4 LEVELS [MEAN (STANDARD DEVIATION)]

	HIV+ Lymphocyte T CD4 level			
	> 500 n = 20	**499-200 n = 23**	**< 200 n = 37**	**F**
WAIS Comprehension	13.40 (4.15)	14.13 (4.00)	14.19 (4.05)	.26
WAIS Similarities	12.10 (6.08)	11.78 (4.58)	13.49 (4.87)	.94
WAIS Forward Digit Span	6.00 (1.12)	5.78 (1.28)	5.95 (1.18)	.20
WAIS Backward Digit Span	4.25 (1.07)	3.83 (1.23)	4.27 (0.90)	1.43
WAIS Vocabulary	42.30 (13.88)	41.91 (13.24)	42.32 (12.00)	.00
WAIS Digit Symbol a	48.45 (14.55)	45.52 (16.31)	38.34 (12.80)	3.77
WAIS Block Design	34.55 (8.38)	29.96 (9.78)	29.43 (7.90)	2.48
WAIS Object Assembly	31.80 (5.03)	27.13 (10.54)	27.11 (8.53)	2.28
AVLT , 5-6	1.65 (1.87)	2.26 (1.60)	1.97 (2.07)	.55
AVLT, total a	45.65 (6.41)	38.91 (8.07)	36.41 (10.08)	6.35
VSAT a	129.40 (25.92)	117.43 (39.55)	102.86 (36.19)	3.91
Trails A	43.20 (14.97)	45.61 (25.51)	48.38 (23.03)	.37
Trails B	89.60 (41.28)	101.04 (59.89)	128.65 (76.96)	2.72
Verbal Fluency Test	28.95 (10.60)	29.43 (11.08)	28.03 (9.44)	.14
BVRT, correct	7.25 (1.62)	6.13 (2.40)	5.95 (1.90)	2.92
BVRT, errors a	4.05 (2.95)	6.17 (4.10)	7.41 (4.17)	4.85
Boston Naming	54.63 (2.29)	53.23 (5.47)	51.30 (6.25)	2.63
Stroop 1	99.40 (19.12)	96.26 (22.44)	90.89 (17.33)	1.37
Stroop 2 a, c	68.75 (13.95)	67.57 (16.44)	55.54 (14.83)	6.92
Stroop 3	39.35 (10.40)	37.87 (14.61)	32.54 (11.78)	2.43
Stroop: interference	-1.33 (8.31)	-1.62 (8.29)	-1.28 (7.28)	.01
Purdue dominant	13.70 (2.36)	14.09 (2.33)	12.78 (2.72)	2.08
Purdue nondominant	13.30 (2.20)	13.09 (1.76)	11.81 (2.53)	3.76
ROCF: copy	31.30 (2.25)	29.89 (4.92)	30.55 (3.66)	.73
ROCF: Delay b	17.25 (4.74)	12.96 (7.49)	15.22 (4.83)	3.17
Finger Tapping: dominant	42.81 (8.85)	41.60 (10.65)	42.24 (12.73)	.06
Finger Tapping: nondominant	38.89 (7.95)	37.87 (8.87)	37.31 (10.47)	.17
WCST Categories	4.15 (1.90)	3.83 (2.08)	3.22 (2.11)	1.50
WCST Learning	-6.39 (12.36)	-8.00 (10.45)	-3.66 (7.54)	1.05
WCST % Perseveratice errors	20.39 (14.25)	19.16 (10.88)	22.94 (14.41)	.61
WCST % Nonperseverative errors	14.67 (8.40)	17.58 (13.67)	18.13 (10.98)	.64
WCST Maintain set	0.90 (1.17)	0.78 (0.95)	1.17 (1.50)	.69
WCST Conceptual response	54.06 (23.15)	50.29 (23.32)	44.68 (22.40)	1.17
WCST Perseverative response	23.49 (18.50)	21.81 (13.58)	27.22 (19.19)	.73

a) Differences between CD4 > 500 y CD4 < 200 ($p < .05$)

b) Differences between CD4 > 500 y CD4 499-200 ($p < .05$)

c) Differences between CD4 499-200 y CD4 < 200 ($p < .05$)

[29], which describe problems of attention, verbal fluency and manual dexterity.

However, in some of the studies carried out with seropositive homosexuals, both asymptomatic and symptomatic, no connection between immune deterioration and neuropsychological performance has been described [3] [19] [21] [34], and Heaton and collaborators do not describe it either (1995) [14] with seropositive heterosexual subjects during different stages of the infection, despite having used the same neuropsychological tasks as we did.

Our hypothesis is that the differences between the results obtained in these studies and ours can be due not only to the fact of using different risk groups, but also to the classification used to determine immunodepression levels. In this regard, some authors use as an immunodepression criterion values under 400 or 500 lymphocytes T CD4/mm3 [21], whereas we have grouped together the subjects according to the current classification of HIV infection (CDC, 1992) which provides three differencial levels of immunodepression. That is why when using levels of immune compromise with broader ranges the possibility of finding differences in the neuropsychological performance are reduced. On the other hand, we also must consider that some studies argue that lymphocytes T CD4 are the best immunological marker of neuropsychological deterioration in seropositive drug addicts [36], while in homosexuals the best predictor seems to be microglobulin ß-2 [17]

On balance, our results support a direct relation between the lymphocyte T CD4 rate and the neuropsychological performance in seropositive people with a previous history of substance use in attention and memory tasks, whereas we do not observe this relation in the rest of skills assessed, which allows us to confirm that the processes of attention and memory decline with the deterioration of the immune system. Therefore, we consider that the deterioration of the immune system can be regarded as a risk factor for neuropsychological manifestations in seropositive former drug addicts during the different stages of the infection. These results provide necessary advances in this field, and studies in this way will have to be conitnued in order to keep working towards the progress of knowledge in the affectation of the lymphocyte T CD4 rate on HIV+ patients.

References

[1] D. Asboe, C. Aitken , M. Boffito , C. Booth, P. Cane, A. Fakoya, et al. (2012). British HIV Association guidelines for the routine investigation and monitoring of adult HIV-1-infected individuals. *HIV Medicine. Volume 13, Issue 1, January, Pages 1-44.*

[2] A. Balagopal, D.M. Asmuth, W.T. Yang, T.B. Campbell, N. Gupte, N. and L. Smeaton (2015). Pre-cART Elevation of CRP and CD4+ T-Cell Immune Activation Associated With HIV Clinical Progression in a Multinational Case-Cohort Study. *Journal of Acquired Immune Deficiency Syndromes, Volume 70, Issue 2, October, Pages 166-71.*

[3] M. R. Basso and R.A. Bornstein (2000). Effects of inmunosuppression and disease severity upon neuropsychological function in HIV infection. *Journal of Clinical and Experimental Neuropsychology, Volume 22, Issue 1, February, Pages 104-114.*

[4] J. T. Becker, L. Kingsley, J. Mullen, B. Cohen, E. Martin, E.N. Miller, A. Ragin, N. Sacktor, O.A. Selnes, B.R. Visscher; Multicenter AIDS Cohort Study (2009). Vascular risk factors, HIV serostatus, and cognitive dysfunction in gay and bisexual men. *Neurology, Volume 73, Issue 16, October, Pages1292-1299.*

[5] A.L. Benton (1981). Test de retención visual de Benton. Madrid: TEA.

[6] A.L. Benton and K.S. Hamsher (1978). Multiligual Aphasia Examination. Iowa City: University of Iowa.

[7] Documento de consenso de Gesida/Plan Nacional sobre SIDA respecto al tratamiento antirretroviral en adultos infectados por VIH (2016). Recuperado de : http://www.gesida-seimc.org/guias_clinicas.php?mn_MP=406&mn_MS=407

[8] R. Farinpour, E. Martin, M. Seindenberg, D. Pitrak, K. Pursell, K. Mullane, R. Novak, and M. Harrow (2000). Verbal working memory in HIV-seropositive drug users. *Journal of International Neuropsychological Society, Volume 6, Issue 5, July, Pages 548-555.*

[9] F. García, A. Soriano and J. Miró (1999). Marcadores serológicos e inmunológicos de la infección por VIH. En V. Soriano and J. González-Lahoz (Eds.), Manual del SIDA, pages 640-653. Madrid: IDEPSA.

[10] A. García-Torres, E. Vergara-Moragues, A. Piñón-Blanco A y M. Pérez-García (2015). HIV-related neuropsychological impairment in patients with previous substance use: A preliminary study. *Revista Latinoamericana de Psicología, Volum 47, Issue 3, July, Pages 213-221.*

[11] C. J.Golden (1994). Test de colores y palabras Stroop. Madrid: TEA.

[12] Grupo, de, expertos, Gesida, y, Secretaría, del, Plan, Nacional, sobre, Sida. (2014). Documento de consenso sobre el manejo clínico de los trastornos neurocognitivos asociados a la infección por el virus de la inmunodeficiencia humana (enero 2013). *Enfermedades Infecciosas y Microbiología Clínica, Volume 32, Pages 37-47.*

[13] R. K.Heaton, G.J. Chelune, J. L. Talley, G. Kay, G and C. Curtis (1993). Wisconsin Card Sorting Test Manual: Revised and expanded. USA: Psychological Assesment Resources.

[14] R. Heaton, I. Grant, N. Butters, D. White, D. Kirson, D, J. Atkinson, J. McCutchan, M. Taylor, M. Kelly, R. Ellis, T. Wolsof, R. Velin, T. Marcotte, J. Hesselink, T.Jernigan, J. Chandler, M. Wallace, Y. Abrason and The HNRC Group. (1995). The HNRC 500-neuropsychology of HIV infection at different disease stages. *Journal of the International Neuropsychological Society,Volume 1,Issue 3, May, Pages 231-251.*

[15] Insight Start Study Group, J. Lundgren , A. Babiker, F.Gordin , S. Emery, B. Grund et al.(2015). Initiation of antiretroviral therapy in early asymptomatic HIV infection. *The New England Journal of Medicine, Volume 373, Issue 9, August, Pages 795-807.*

[16] E. Kaplan, H. Goodglass and S. Weintraub. (1986). Test de Vocabulario de Boston. Madrid: Panamericana.

[17] A. Lifson, N. Hessol and G. Rutherford (1992). Progression and clinical outcome of infection due to human immunodeficiency virus. *Clinical Infectious Disease, Volume 14, issue 4,April, Pages 966-972.*

[18] K. Marder, X. Liu, Y. Stern, R. Malouf, G. Dooneief, K. Bell, G. Todak, G. Joseph, S. Sorrell, W. El-sadr, J. Willians, A. Ehrhardt, Z. Stein and J. Gorman (1995). Risk of human immunodeficiency virus type 1-related neurologic disease in a cohort of intravenous drug users. *Archives of Neurology, Volume 52, Issue 12, December, Pages 1174-1182.*

[19] E. Miller, O. Selnes, J. McArthur, P. Satz, J. Becker, B. Cohen, K. Sheridan, A. Machado, W. Van Gorp and B. Visscher (1990). Neuropsychological performance in HIV-1 infected homosexual men: The Multicenter AIDS Cohort Study (MACS). *Neurology, Volume 40, Issue 2, February, Pages 197-203.*

[20] A.Olson, A. Walker, A. Suthar, C. Sabin, H. Bucher, I. Jarrin, S. Moreno, S. Perez-Hoyos, K. Porter and D. Ford (in press). Limiting Cumulative HIV Viremia Copy Years by Early Treatment Reduces Risk of AIDS and Death. *Journal of acquired immune deficiency syndromes.*

[21] R. Podraza, C. Bornstein, M. Whitacre, R. Para, R. Fass, R. Rice and H. Nasrallah (1994). Neuropsychological performance and CD4 levels in HIV-1 asymptomatic infection. *Journal of Clinical and Experimental Neuropsychology, Volume 6, Issue 5, October, 777-783.*

[22] R. Reitan (1992). Trail Making Test: Manual for administration and scoring. Tucson: Reitan Neuropsychology Laboratory.

[23] R. Reitan (1979). Finger Tapping Test. Arizona: Reitan Neuropsychology Laboratory.

[24] [24] A.Rey (1964). L´examen Clinique en Psychologie. París: Presses Universitaries.

[25] A. Rey (1987). Test de copia de una figura compleja. Madrid: TEA.

[26] R. Schrier, S. Hong, M. Crescini, R. Ellis, J. Pérez-Santiago, C. Spina, S. Letendre. HNRP Group (2015). Cerebrospinal fluid (CSF) CD8+ T-cells that express interferon-gamma contribute to HIV associated neurocognitive disorders (HAND). *Plos One, Volume 10, Issue 2, Frebruary, doi: 10.1371/journal.pone.0116526.*

[27] A. Schwartländer, B. Bek, H. Skarabis, J. Koch, J. Burkowitz and M. Koch, For The Multicentre Cohort Study Group. (1993). Improvement of the predictive value of CD4+ lymphocite count by β_2-microglobulin, immunoglobulin A and erythrocyte sedimentation rate. *AIDS, Volume 7, Issue 6, June, Pages 813-821.*

[28] R. Stern, S. Silva, N. Chaisson and D. Evans (1996). Influence of cognitive

reserve on neuropsychological functioning in asymptomatic human immunodeficiency virus-1 infection. *Archives of Neurology, Volume 53, Issue 2, Frebruary, Pages 148-153.*

[29] Y. Stern, K. Liu, K. Marder, G. Todak, M. Sano, A. Ehrhardt and J. Gorman (1995). Neuropsychological changes in a prospectively followed cohort of homosexual and bisexual men with and without HIV infection. *Neurology, Volume 45, Issue 3, March, Pages 467-472.*

[30] J. Tiffin (1948). Purdue Pegboard. Indiana: Lafayette Instrument.

[31] M. Trenerry, B. Crosson, J. Beboe, and W. Leber (1990). Visual search and attention test. Florida: Psychological Assesment Resources.

[32] E. Vázquez-Justo, E. Vergara-Moragues, A. Piñón-Blanco, C. Guillén-Gestoso and M. Pérez-García (in press). Neuropsychological functioning in methadone maintenance patients with HIV. *Revista Latinoamericana de Psicología.*

[33] E. Vázquez-Justo, E. Vergara-Moragues, A. Piñón-Blanco, C. Guillén-Gestoso and M. Pérez-García (2014). Cognitive reserve during neuropsychological performance in HIV intravenous drug users. *Applied Neuropsychology: Adult, Volume 21, Issue 4, November, Pages 288-296. doi: 10.1080/23279095.2013.813852.*

[34] G. Villa, A. Salida, E. Moro, M. Tovadozza, A. Antinori, A. De Luca, R. Murri and E. Tamburrini (1996). Cognitive impairment in asymptomatic stoges of HIV infection. A longitudinal study. *European Neurology, Volume 36, Issue 3, Pages 125-133.*

[35] A. Wechsler (1995). Escala de Inteligencia de Weschler para adultos. Madrid: TEA.

[36] J. Zabay, J. Sempere, J. Benito, B. Gonzalez, E. Obregón, J. Díez, J and E. Fernandez-Cruz (1995). Serum β_2-microglobulin and prediction of progresion to AIDS in HIV-infected injection drug users. *Journal of Acquired Immune Deficiency Syndromes and Human Retrovirology, Volume 8, Issue 3, March, Pages 266-272.*

Enrique Vázquez-Justo

He has a Ph.D. in Psychology. He is a professor in the Department of Psychology and Education and Director of Portucalense Institute of Neuropsychology and Cognitive and Behavioral Neuroscience at the Portucalense University of Oporto. He is also Director of Ebam Clinics (Pontevedra, Spain) where he works in neuropsychological intervention. Moreover, he has collaborated and currently collaborates in several national and international Postgraduate courses in Neuropsychology. He has published articles in journals of international and national renown. He also works as a reviewer for international journals in the field of Neuropsychology and Neuroscience.

Amalia García Torres

Amalia García Torres is a Psychologist by the University of Granada and Master's Degree in Psychology of Health and in Neuropsychology. She currently works as a psychologist in GERASA (Chiclana de la Frontera, Cadiz, Spain) with HIV patients with social exclusion. She is also working on her doctoral thesis about "Cognitive Rehabilitation in HIV patients" and she is member for the research group "Neuropsychology and Clinical Psychoneuroimmunology" (CTS-581) at the University of Granada. During the past few years, she has participated in several national and international conferences on drug addiction and HIV. Moreover, she has published several scientific papers related to neuropsychology, addictions and HIV.

Esperanza Vergara-Moragues

Esperanza Vergara-Moragues has a Ph.D. in Psychology and she is expert in Clinical Psychopathology and Neuropsychology. She works as associate professor at the Universidad Internacional de La Rioja (UNIR) and she is member of the research groups "UNIR Research" and "Neuropsychology and Clinical Psychoneuroimmunology" (CTS-581) at the University of Granada. She has collaborated in several postgraduate courses in national and international universities. Also she collaborates at the Portucalense University of Oporto. Moreover, she has published and collaborate as a reviewer a wide array of recognized articles (journal citation report) about Neuropsychology and Psychopathology.

Virtual Planning and Intraoperative Navigation in Craniomaxillofacial Surgery

J. Guiñales, J.L. Cebrian*, M. Burgueño

Servicio de Cirugía Oral y Maxilofacial, Hospital Universitario La Paz, Madrid (Spain)

Received 16 September 2016 | Accepted 1 November 2016 | Published 23 December 2016

Abstract

Surgery planning assisted by computer represents one important example of the collaboration between surgeons and engineers. Virtual planning allows surgeons to pre-do the surgery by working over a virtual 3D model of the patient obtained through a computer tomography. Through surgical navigation, surgeons are helped while working with deep structures and can check if they are following accurately the surgical plan. These assistive tools are crucial in the field of facial reconstructive surgery. This paper describes two cases, one related to orbital fractures and another one related to oncological patients, showing the advantages that these tools provide, specifically when used for craniomaxillofacial surgery.

Keywords

Craniomaxillofacial Surgery, Facial Reconstructive Surgery, Computer-assisted Surgery, Surgical Navigation, Surgical Planning.

DOI: 10.9781/ijimai.2017.4512

I. Introduction

The collaboration between engineers and surgeons during the last ten years has facilitated the development of several tools that have incredibly improved the predictability and the results of the surgeries.

Virtual planning or surgery planning assisted by computer allows us to pre do the surgery, reproducing our mental plan, by working over a virtual 3D model of the patient obtained through a CT (computer tomography). Once we have the CT of the patient, there are several different softwares that can create this 3D model and with different tools, depending on the software, enable us to a wide range of options: select the affected area, segmentation of the skeleton in the different bones, perform osteotomies, move the bones, make mirroring images of the unaffected side, import STL models of the prostheses or plates or pre simulate the soft tissue changes after the surgery. Virtual planning represents the main example of the collaboration between surgeons and engineers. During this step, both will work hand by hand designing the surgical plan with the common goal of achieving the highest precision.

However, surgical planning is just one of the examples of this collaboration. Once we have finished our virtual planning we can also impress stereolithographic models of the different anatomical structures, the plates and prostheses or guides for the osteotomies than will help us through the different steps of the surgery.

One of the last applications resulting from this engineer-surgeon collaborations is the surgical navigation. Surgical navigation was born as an evolution of the stereotactic surgery in the field of Neurosurgery due to the integration of both the intraoperative positioning and the imaging diagnostic systems. Thanks to this tool we can intraoperatively know our real position by placing a pointer on the patient that will shows us precisely the situation in the patient's CT. This will help us while we are working with deep structures and more importantly in those cases where important structures such as arteries and nerves are in the nearby of our surgical field and must be protected. But the surgical navigation also allows us to check if we are following accurately the surgical plan. For example if we have placed a prosthesis, during the virtual planning step, in an specific position, we can check during the surgery if the real position fits with the planned one, and if not, correct it.

Although all these tools have implemented all kind of surgical specialities, they have become indispensable in the field of reconstructive surgery and specially facial reconstructive surgery. In this field every millimetre counts and it can be the difference between a good result and a complete disaster. We, as craniomaxillofacial surgeons, work in a field with a complex spacial relationship between the different anatomical structures in which these new technologies have revolutioned the way we plan and treat our patients.

In this last article, we want to share with you two different cases in which we will be able to show the advantages of these new tools in the craniomaxillofacial surgery.

II. Cases

First of all we will go through a simple case that we can came across frequently in our daily practice. This is the case of orbital fractures. Patients often suffer these kind of fractures resulting from direct trauma to the eye globe. Usually the floor of the orbit is the most affected wall, followed by the medial wall, with combining fractures in up to 50% of the cases.

The orbital cavity has an inverted pyramid form, with the base of this pyramid located at the anterior part. This cavity accommodates the eye globe, ocular muscles, orbital fat, nerves and vessels. Any change in the position of the walls will have a direct impact in the orbital volume and so it will affect to the eye position with an aesthetic and functional result that can lead to diplopia (double vision), exofalmos (anterior eye displacement), enoftalmos (posterior displacement of the eye), dystopia (vertical displacement of the eye) and even vision impairment resulting from orbital nerve affection. In such cases, reconstruction of the affected wall must be accomplished in order to restore the normal position of the wall and the orbital volume.

* Corresponding author.
E-mail address: josel.cebrian@salud.madrid.org

Until virtual planning softwares and navigations systems appeared, these cases were treated having as the only guide the preoperative x-rays of the patient. In such situations the surgeon can only guess the theoretical situation in which the affected wall should be, without any intraoperative references except for the surrounding structures that in many cases are also affected. Today, virtual planning software allows us to perform previously this surgery on the computer working with a 3D model of the orbit and plan the exact position in which the affected wall should be. Thanks to mirror image tools, we can reconstruct the orbit based on the unaffected side. As we know, orbits usually are symmetric in form and volume in non-syndromic patients, so we can make a mirror image of the unaffected side as use it as a model for the reconstruction. As so, we can design the desired position of the new wall, we can measure the dimensions of the fracture and now in advance the size and form of the mesh we will need to reconstruct it, we can now the spacial relations with the adjacent structures such as the optical nerve, we can measure the orbital volume of the new orbit and compare it with the healthy side, we can use the STL models of the commercialised meshes and see how the fit into the defect or if we will need to customize them, and if so do it before going to the operating room and finally we can work with the engineers in designing an specific implant for every case (Fig.1 and 2).

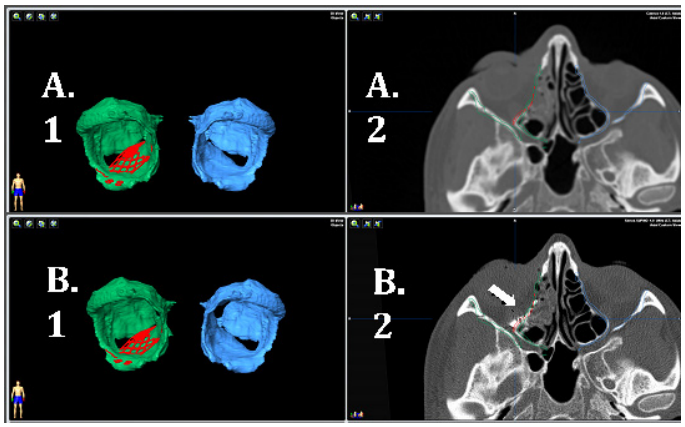

Fig. 1. A.1. 3D reconstruction of the normal orbital cavity. A.2. Medial orbital wall fracture (white arrow). Non-fractured medial orbital wall (red arrow). B.1. 3D orbital reconstruction (green). Mirroring from the healthy orbit (blue).

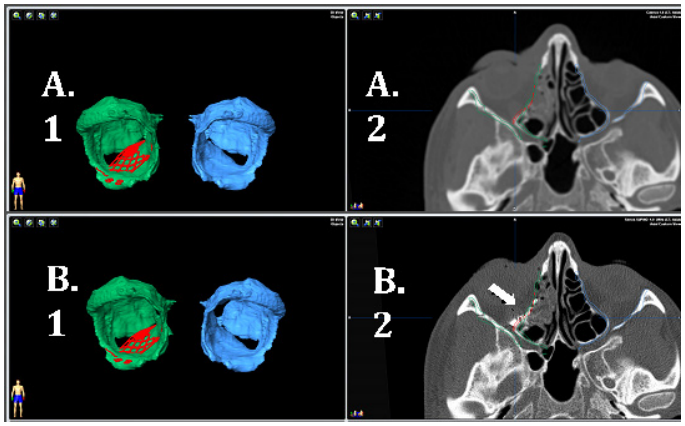

Fig. 2. A.1-2. Orbital reconstruction plate (red), obtained from STL archives of custom made plate, reconstructing orbital walls and placed in the right position using virtual surgery. B.1. Virtual surgical plan. B.2.Post-operative CT scan. Reconstruction plate placed in the right position (white arrow) using navigation

The next step in the orbital reconstruction planning is to use the intraoperative navigation to confirm our surgical planning. First of all we will use navigation to confirm the limits of the fracture and the correlation between the intraoperative findings and the scanner. We can also use it to know the exact point in which we are while we are performing the orbital dissection and to be sure of having a safety distance with the optical nerve. Once we have identified completely the fracture, we will place our orbital mesh and we will use the navigation to be sure that the final position fits with the desired plan. The navigation system incorporates a computer screen in which we can see not only the previous CT but also superimpose the surgical plan so we can in every moment be sure that we are following it faithfully.

The second case that we want to share with you is regarding about the utility of this tools in oncological patients. This is a case of a 64 years old man presenting at our office with a left zygomatic mass of three months of evolution with progressive growth. As the only previous disease, he suffered an adenoid cystic carcinoma 8 years before affecting the buccal mucosa of his left side. He went trough intervention with complete extirpation of the tumor and no risk factors associated. He remained out of clinical or radiological signs of recurrence until the moment he came to our office.

We perform a CT which showed a growing mass affecting to the left zygoma and extending into the maxillary bone and the orbital floor, with soft tissue extension up to the subcutaneous tissue. An intraoral biopsy confirmed the diagnosis of adenoid cystic carcinoma. A MRI (magnetic resonance imaging) was made for better study of the soft tissue affection.

For the virtual planning we use IPlan from Brainlab. We introduce both the CT and the MRI and thanks to the fusion tool, the software automatically fused both studies so we can work with both at the same time, having great definitions of the bone and the soft tissues. The next step is to define the tumor in the images and for so, the IPlan offers a special tool called Smartbrush that automatically outlines the tumor volume just by selecting the tumor, with a click of mouse, in two slices with different orientations (Figure 3). This tool recognises the selected structure, in this case the tumor, by choosing all the pixels with the same Hounsfield units. Once the tumor is automatically outlined, we can manually improve the selection contouring it with the mouse.

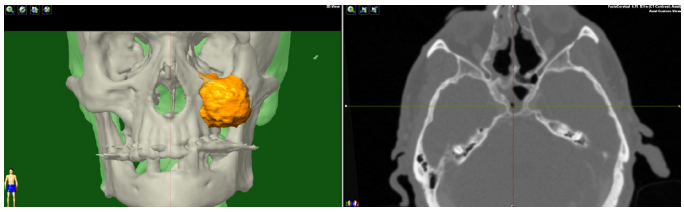

Fig. 3. Facial tumor outlined using smartbrush tool. Frontal view.

Adenoid cystic carcinoma is a malignant tumor that must be resected with free margins in order to ensure a complete resection and avoid recurrence. For that instance, we can easily defined the desired margin with the software just by selecting the amount it, and automatically a new object will be created which will include the tumor and the free selected volume around it (Figure 4). This new object will be our resection piece and the software will show us how it will affect to the adjacent structures. We can also subtract the resection from the 3D reconstruction and see how the final defect will be in order to plan the reconstruction. In our case, the resection will include the zygoma, the left maxilla including the alveolar process and the teeth up to the canine but preserving the nasal buttress, the orbital floor and infraorbital rim and the overlying skin.

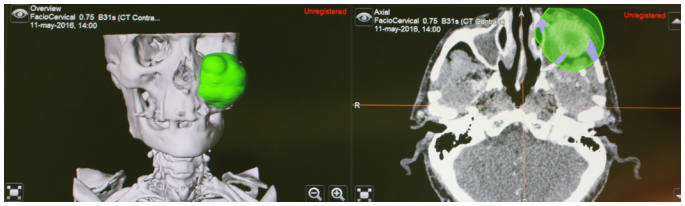

Fig. 4. Planned surgical resection with security margin (green).

After finishing the virtual planning we arrange an online appointment with the engineer of the brand that will provide us the surgical prosthesis. Previously we sent him the STL of the plan so he can have in advanced how our resection will be. In this case we worked with Johnson & Johnson which at the same time works with Materialise for all the stuff regarding the individualised implants and surgical guides. During this online appointment, we reviewed the surgical plan and we designed, the cutting guides with dental and bone anchorage that will marked the desire resection (Figure 5). Although we can navigate the resection following the plan without guides, these will help us to be more accurate and have a better fit of the prosthesis. After this, we designed the prosthesis, in this case a titanium customised implant that will reconstruct the orbital floor, the infraorbital rim, the zygoma and the anterior wall of the maxilla. Once again, we used a mirror image tool to superimpose the unaffected side over the affected side without the resection, so we will keep the symmetry during the reconstruction. We also planned the drilling holes in the prosthesis were we will place the screws to fix it and two guide lines over the orbital floor of the implant, in order to be able to navigate it and have a double check of correct position (Figure 6).

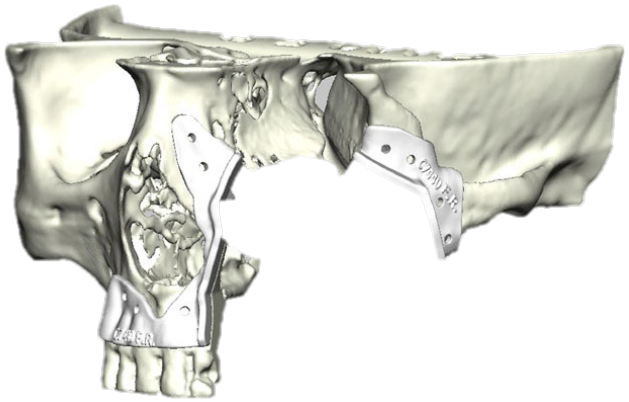

Fig. 5. Cutting guides (green arrow) and defect following resection (red arrow).

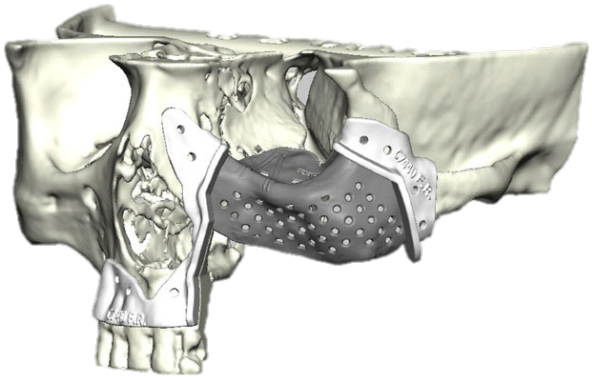

Fig. 6. Customized prostheses.

As you can see through the intraoperative pictures, thanks to the virtual planning, the surgical guides and the navigation system, in every moment we were sure that we were perfectly fitting the plan, with no option to fail, and achieving the greatest accuracy (Figure 7).

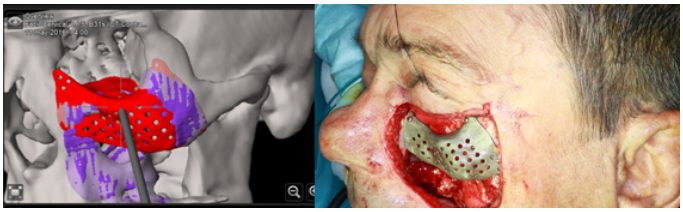

Fig. 7. Introperative navigation and surgical picture showing the accuracy of plate placement.

In conclusion, the new tools emerging from the collaboration between engineers and surgeons, make us no better surgeons but more predictable surgeons which at the end will help us to reach our final goal, offer to the patient the best treatment option.

Jorge Guiñales

Bachelor of Medicine and Surgery from the Autonomous University of Madrid. Resident of Oral & Maxillofacial Surgery at the University Hospital La Paz, Madrid. Dentistry student at the European University of Madrid. Vocal residents SECOM.

José Luis Cebrián Carretero

José Luis Cebrián Carretero got his Medical Degree Universidad Autónoma de Madrid (UAM) in 1993. He is PhD by the same university in 2005. He also studied Oral and Maxillofacial training H.U. La Paz from 1995 to 2000. He got is Dental Degree in the Universidad Europea de Madrid (UEM) in 2009. He is fellow of the European Board of Oral and Maxillofacial Surgery, Specialist in Oral and Maxillofacial Surgery, La Paz University Hospital, Madrid and Chief of Division in Oral and Maxillofacial Surgery, La Paz University Hospital, Madrid, and Director of Oral and Maxillofacial Surgery Departments at Quironsalud Hospital Sur de Madrid y Clínica La Luz. Finally he is Vice-President of the SECOM (Spanish Society of Oral and Maxillofacial Surgery). He is author of 2 books, 15 chapters and more than 50 scientific articles. His main research areas are Implantology, Head and Neck Oncologic Surgery and Orthognatic and Oral Surgery.

Miguel Burgueño García

Bachelor of Medicine and Surgery from the Complutense University of Madrid. Trained as a specialist in oral and maxillofacial surgery at the Hospital La Paz, where he served as deputy until 2005, when it becomes Chief. Degree of Doctor of Medicine from the Autonomous University of Madrid in 1995 and recognized career in facial surgery, in the following areas: reconstructive, microsurgical techniques, orthognathic surgery, deformities, facial fractures and facial cosmetic surgery. Associate professor in the Department of Surgery at the Autonomous University of Madrid. Director of numerous specialized training courses. He currently manage the course of Implantology at the Autonomous University of Madrid. European Board in Oral and Maxillofacial Surgery (certificate of excellence for professionals in the European Union). President of the Spanish Society of Oral and Maxillofacial Surgery between 2005-2007.

IJIMAI

http://ijimai.unir.net